

Structure and Dynamics of the H-mode Pedestal

T.H. Osborne¹, N. Asakura², T. Bolzonella³, E. Doyle¹³, J. Ferron¹, R.J. Groebner¹, Y. Igitkhanov⁴, K. Kamiya², J. Kinsey⁵, A. Kirk⁶, L.L. Lao¹, A.W. Leonard¹, A. Loarte⁷, J. Lonroth⁸, M.A. Mahdavi¹, D. Mossessian⁹, R. Moyer¹⁰, T. Onjun⁵, G. Pacher¹¹, T. Rognlien¹², S. Saarelma⁸, G. Saibene⁷, R. Sartori⁷, P.B. Snyder¹, G. Staebler¹, W. Suttrop⁴, A. Turnbull¹, H. Urano⁴, H.R. Wilson⁶, N.S. Wolf¹², X. Xu¹², H. Zohm⁴, ITPA Pedestal Topical Group

9th IAEA Technical Meeting on H-mode Physics and Transport Barriers

San Diego, CA USA, 24-26 September 2003

¹General Atomics, San Diego, ²JAERI, Naka, ³Consorzio RFX, Padova, ⁴Max-Planck-Institut für Plasmaphysik, Garching, ⁵LeHigh University, ⁶EURATOM/UKAEA Fusion Association, Culham, ⁷EFDA Close Support Unit, Garching, ⁸Helsinki University of Technology, ⁹Massachusetts Institute of Technology, ¹⁰University of California, San Diego, ¹¹Hydro Quebec (IREQ), ¹²Lawrence Livermore National Laboratory, ¹³University of California, Los Angeles



T. Osborne, HMWS03



Hydro Quebec (IREQ), Canada



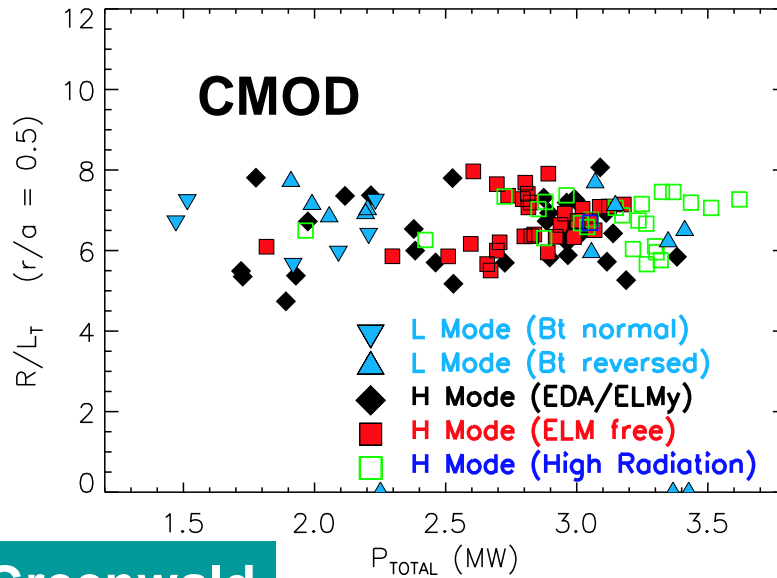
ASDEX Upgrade



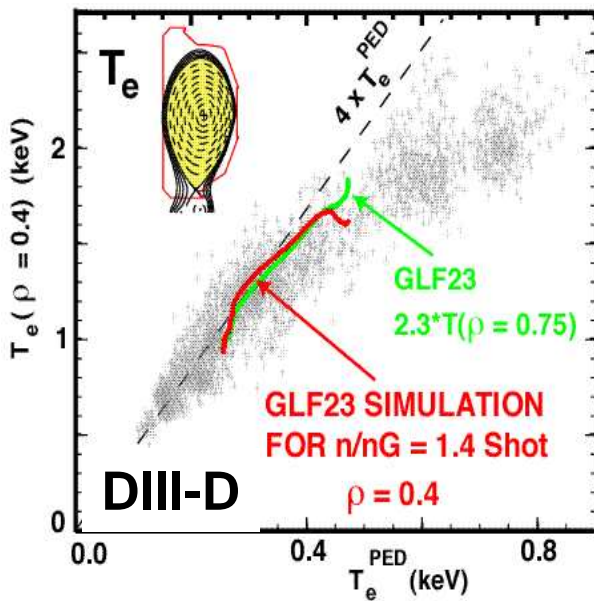
Outline

- Introduction: Importance of H-mode pedestal structure and dynamics
- Edge transport barrier, ETB, width results
- Edge stability
- Type I ELM effects
- Alternatives to the Type I ELM regime
 - Small ELM regimes
 - ELM free regimes

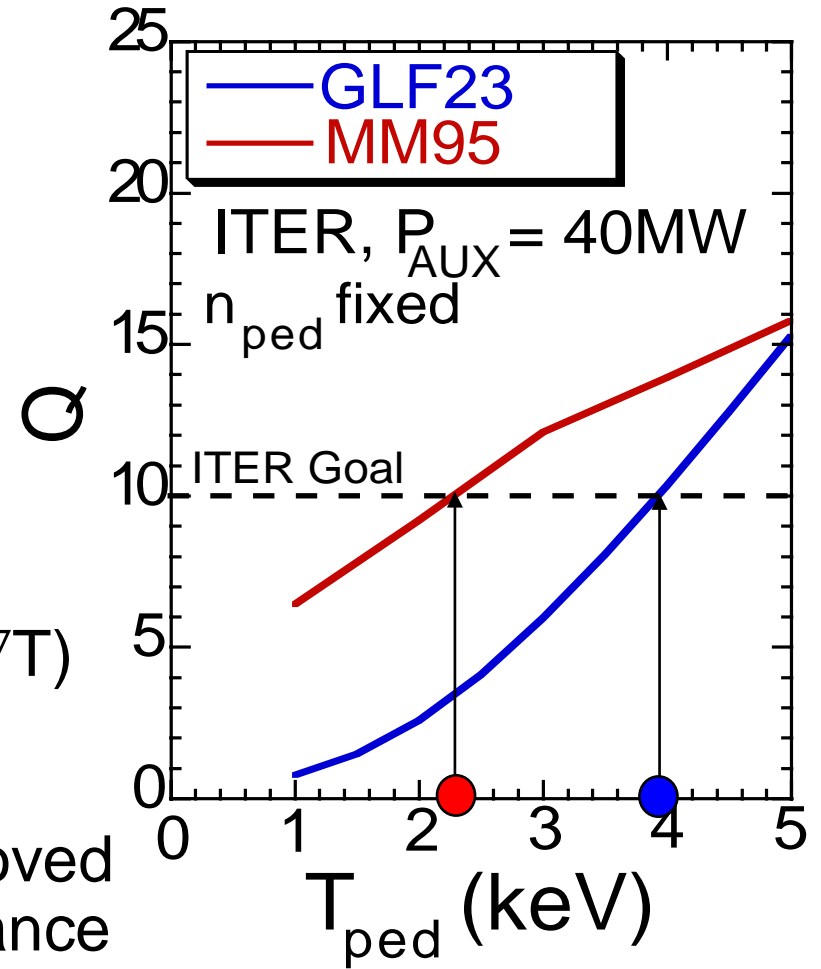
ETB structure is expected to strongly influence the performance of H-mode based BP Tokamak



M. Greenwald



● Stiff (fixed $T/\nabla T$) temperature profiles => strongly improved core performance with increasing pedestal energy.



J. Kinsey, IAEA 02

Type I ELM H-mode may not be compatible with BP Tokamak or ITB

- Type I ELM H-mode has high W_{PED} but ΔW_{ELM} can exceed divertor power handling capability or lead to ITB collapse.

- Physics of ΔW_{ELM}

- Alternatives to Type I regime

- Small ELM

- Type II ELM
 - Type III ELM
 - Grassy-ELM

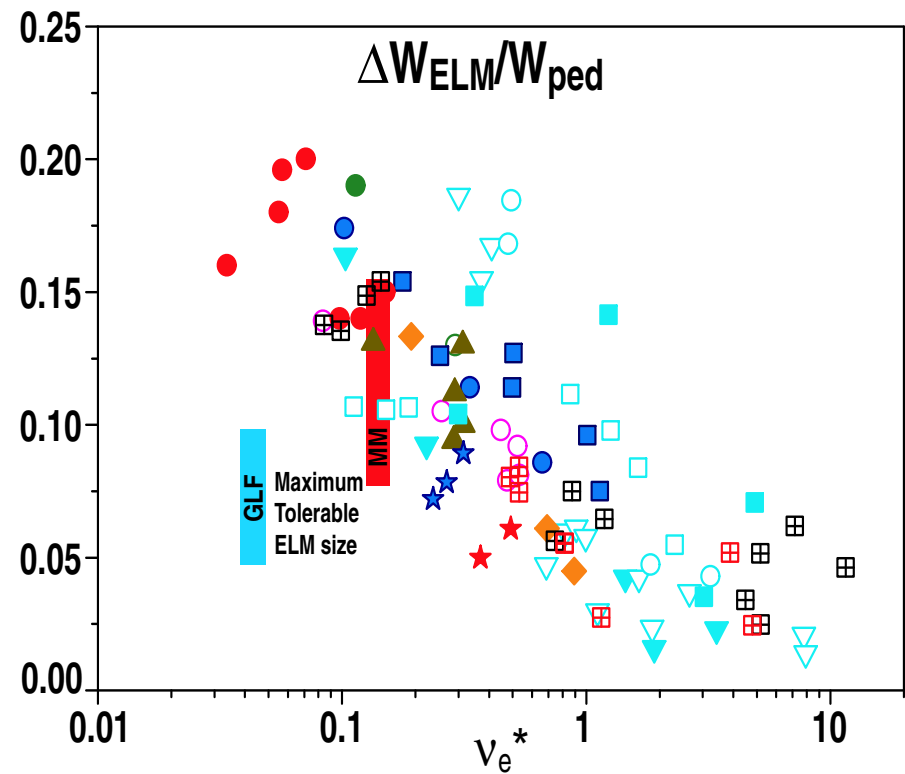
- ELM free but no impurity accumulation

- EDA-H-mode
 - QH-mode
 - HRS-H-mode

- ELM Control

- Ergodic boundary
 - Pellet injection

ITER-FEAT melting and ablation threshold requires $< 1 \text{ MJ/m}^2/\text{ELM}$ to divertor



A.Loarte, A.Leonard

Transport Barrier Width

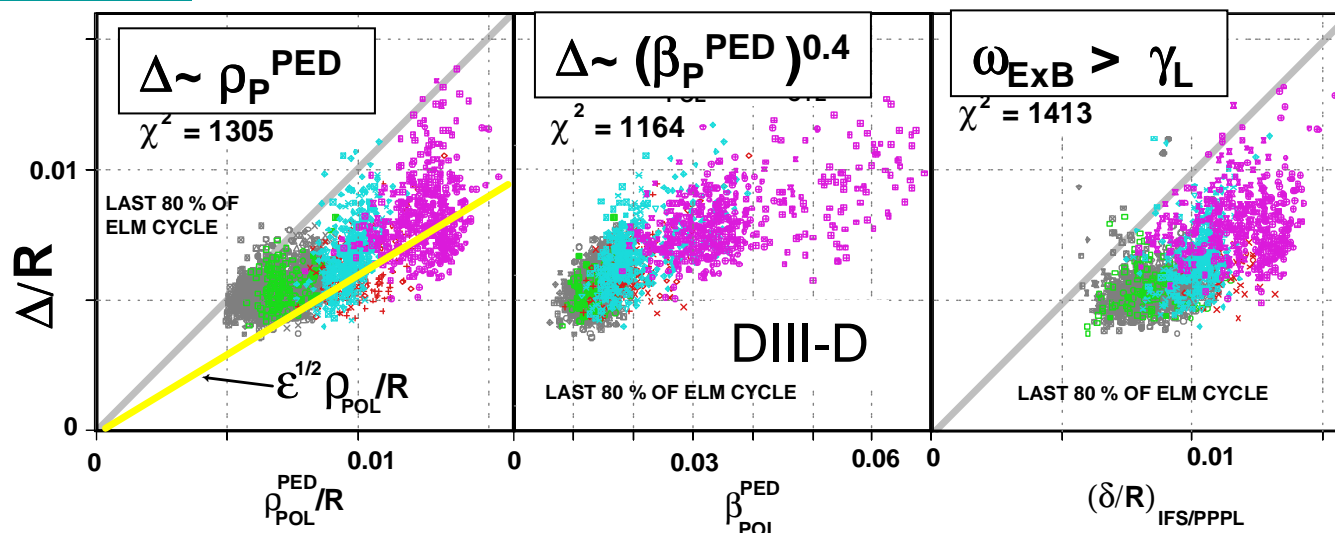
- Physics based empirical scalings.
- Role of neutrals in edge density profile and ETB width
- Dimensionless scaling experiments
- Turbulent transport modeling

Physics based empirical scaling of Δ have not yielded a statistically favored scaling that has held up to testing across experiments

| Scaling | Physics | σ (%) |
|--|---------------------------------------|--------------|
| $\Delta \propto \sqrt{\beta_\theta} R$ | Poloidal pressure | 32 |
| $\Delta \propto \rho S^2$ | Magnetic and flow shear stabilization | 65 |
| $\Delta \propto \sqrt{\rho R q}$ | Flow shear stabilization | 31 |
| $\Delta \propto \rho^{2/3} R^{1/3}$ | Diamagnetic stabilization | 26 |
| $\Delta \propto \sqrt{\epsilon} \rho_\theta$ | Ion orbit loss | 45 |
| $\Delta \propto 1/n_{ped}^{3/2}$ | Neutral penetration | 68 |

- Accurate measurement of barrier width difficult
- Databases made up of ELMing discharges highly constrained by stability
- Magnetic shear unmeasured until recently ([D.Thomas - F2](#))
- Neutral source profiles difficult to determine experimentally
- Expressions too simple

T. Onjin

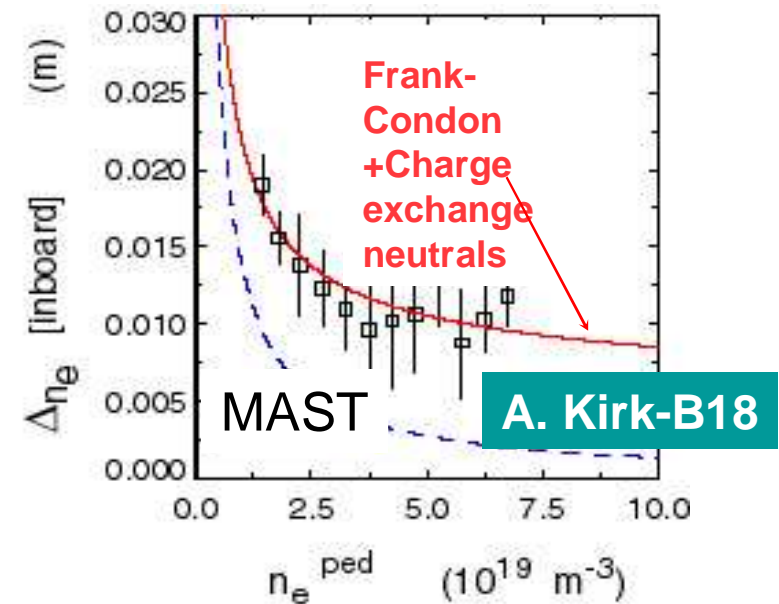
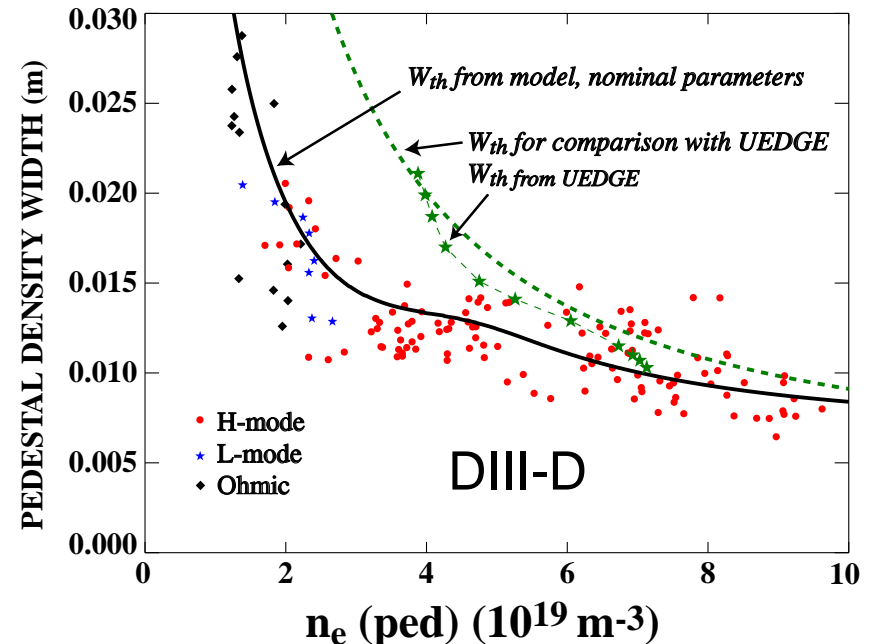
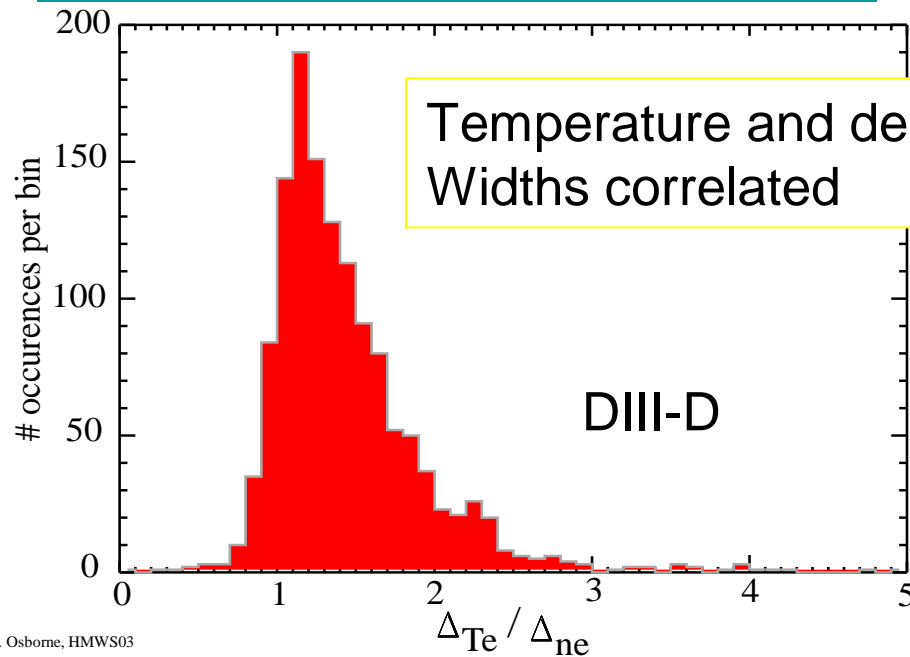


Does the edge particle source control the pedestal density profile and also perhaps the ETB width ?

- Analytic model for edge density profile: charge exchange and Franck-Condon neutrals

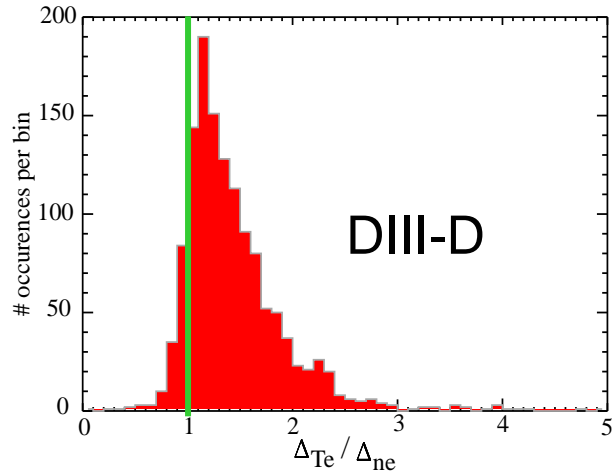
$$n_{ped}^2 \propto n_{sep} / f(\theta_0)$$
- $\nabla n_e \propto n_{ped}^2, \Delta_{ne} \propto 1/n_{ped}$
- Confirmed with 2-D UEDGE (fluid) modeling

M.A. Mahdavi, R. Groebner, N. Wolf

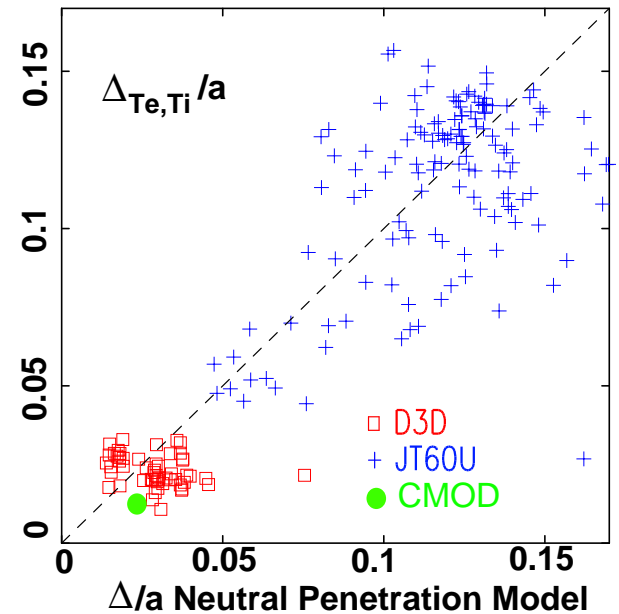
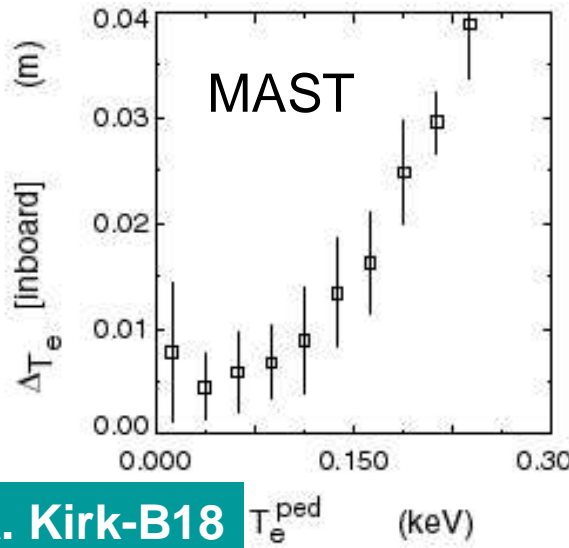
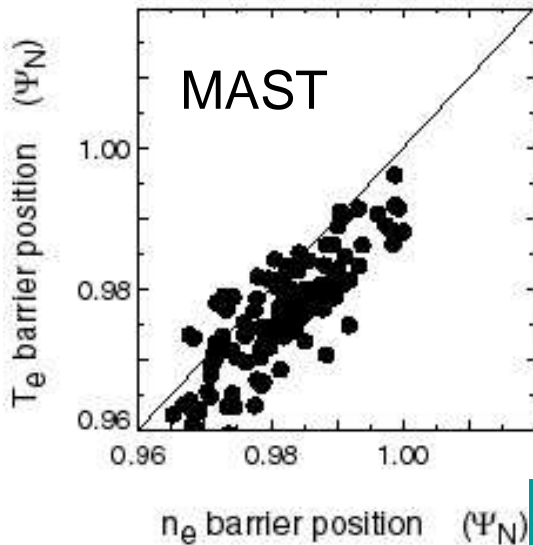


ETB width related to edge particle source ?

- Hinton, Staebler¹: Velocity shear can take on any value consistent with radial force balance \Rightarrow structure of particle and heat sources can control velocity shear and transport barrier width. $\Delta \approx [2\lambda L_n^{Sep} \ln(c\Gamma_{Sep} Q_{Sep})]^{1/2}$



- n_e and T_e widths correlated but spread is large
- T_e pedestal inboard of density pedestal
- T_e width increases with T_e^{PED}
- Neutral penetration model consistent with wide ETB on JT-60U
- Bad for ITER: $T_i^{SEP} = 5\text{KeV (GLF), } 1\text{KeV (MM)}$



A. Kirk-B18 T_e^{ped} (keV)

[1] Hinton, F.L., Staebler, G.M., Phys. Fluids B 5, (1993), 1281.

Pedestal dimensionless parameter scaling experiments to test role of neutrals and determine Δ scaling

- **Dimensionally identical experiments** match plasma shape and dimensionless parameters at top of pedestal in different size tokamaks: CMOD/DIII-D, CMOD/JET, JET/DIII-D, JET/JT-60U, AUG/DIII-D.

$$\beta \sim \frac{nT}{B^2}, \quad \rho_* \sim \frac{T^{1/2}}{aB}, \quad v_* \sim \frac{an}{T^2} A^{5/2} q, \quad q \sim \frac{aB}{AI}$$

$$\Rightarrow n \sim a^{-2}, \quad T \sim A^{5/4} a^{-1/2}, \quad B \sim A^{5/8} a^{-5/4}, \quad I \sim A^{-3/8} a^{-1/4}$$

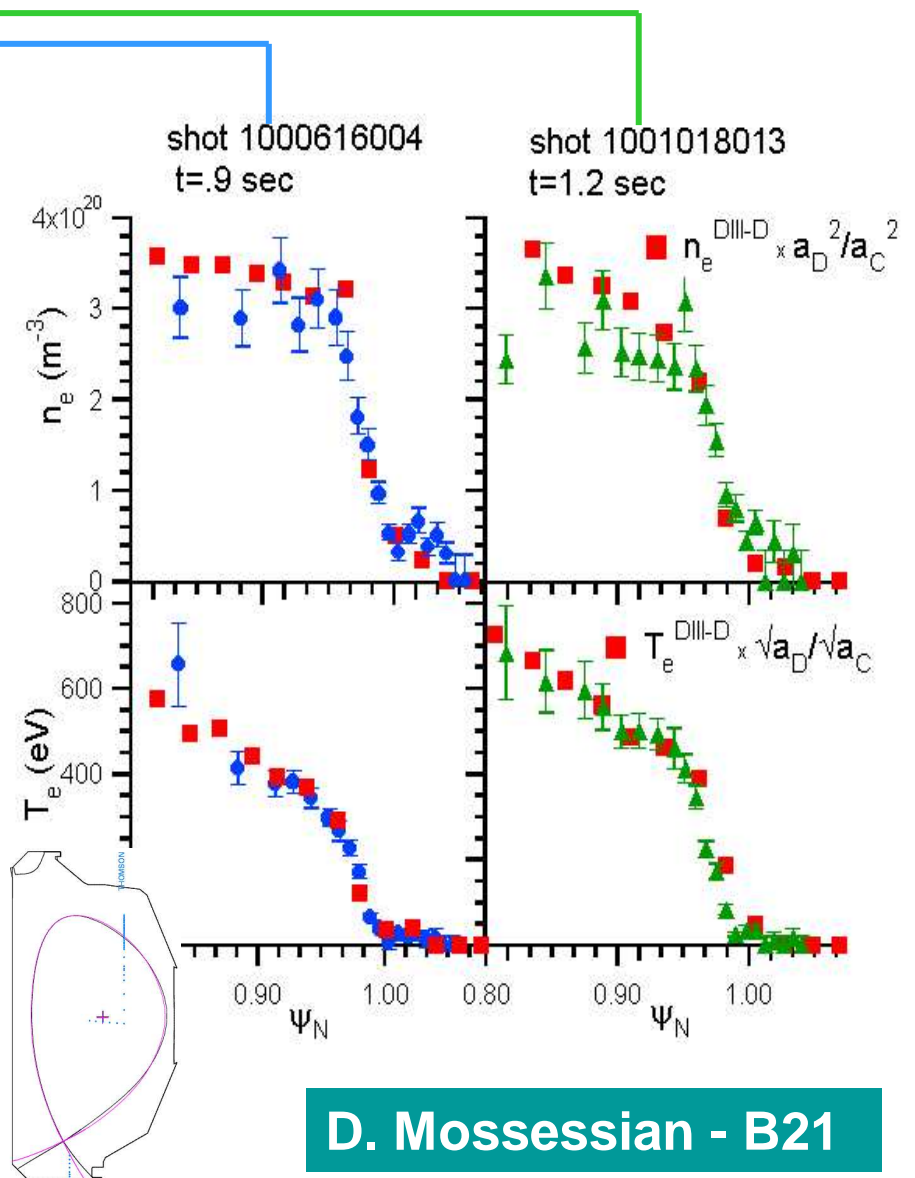
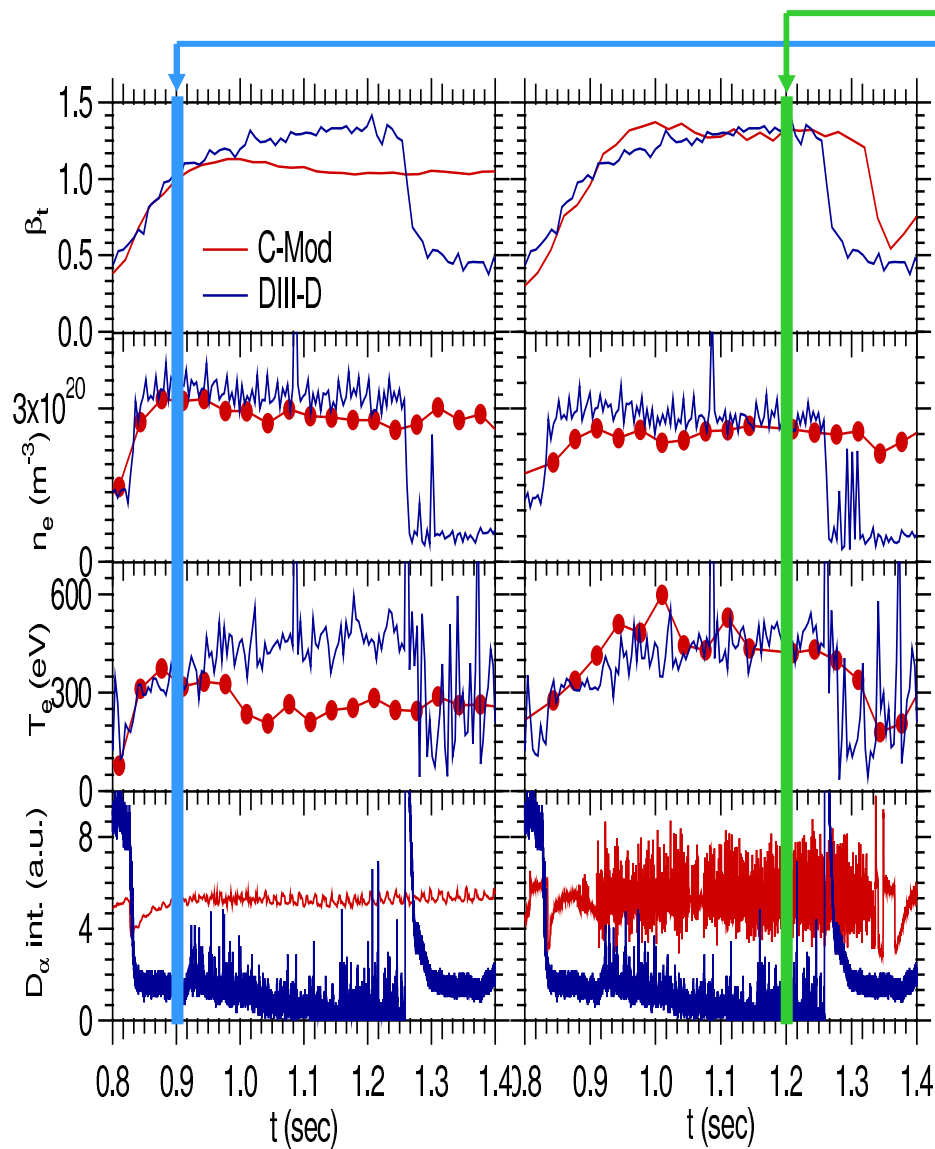
- Ionization mean free path with dimensionless parameters matched

$$\hat{\lambda}_N = \frac{\lambda_N}{a} \sim \frac{f(\theta)}{an} \sim af(\theta)$$

- Plasma physics control ETB width $\Rightarrow \Delta \sim a$; Neutrals control ETB width $\Rightarrow \Delta \sim a^2$

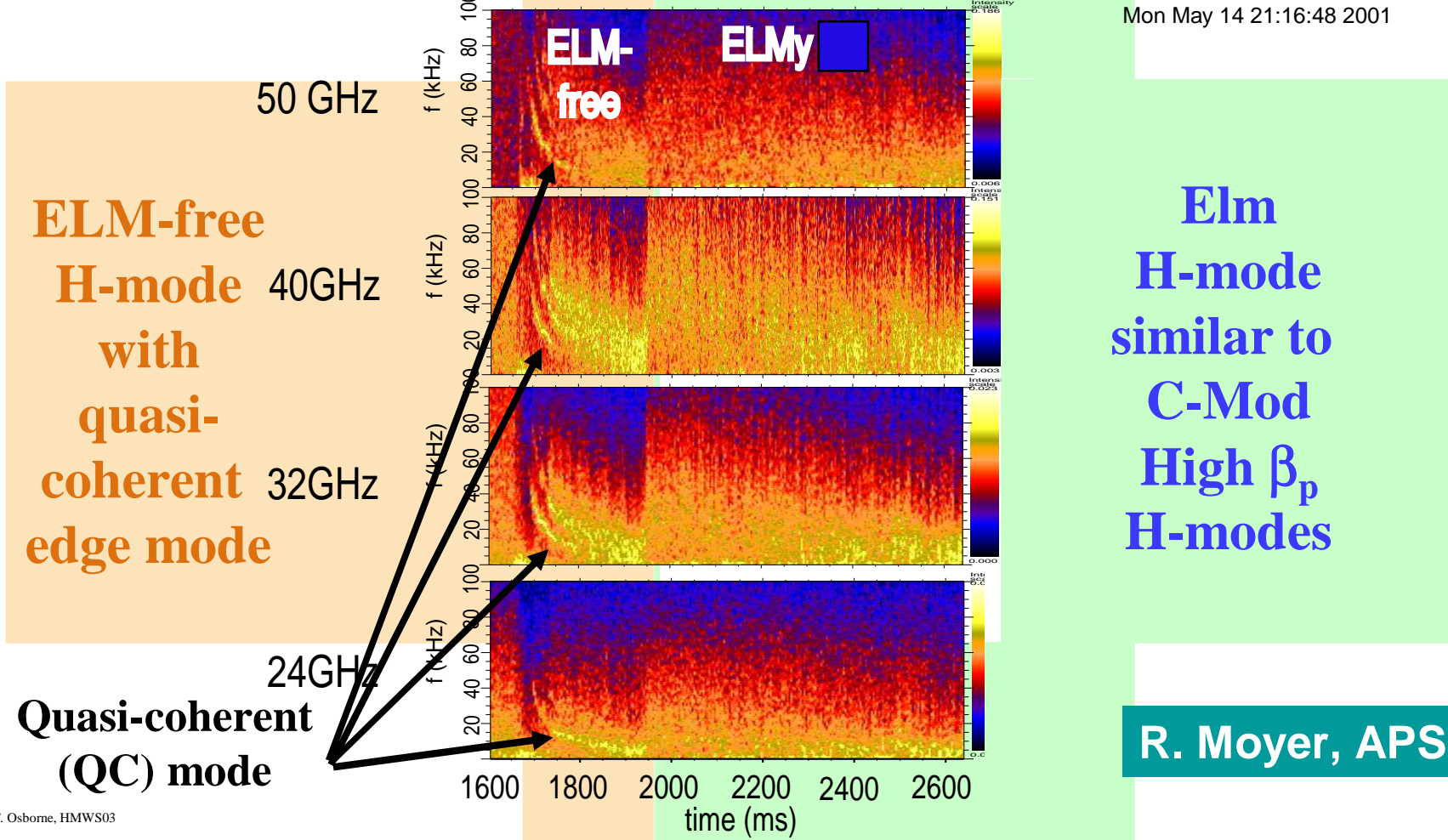
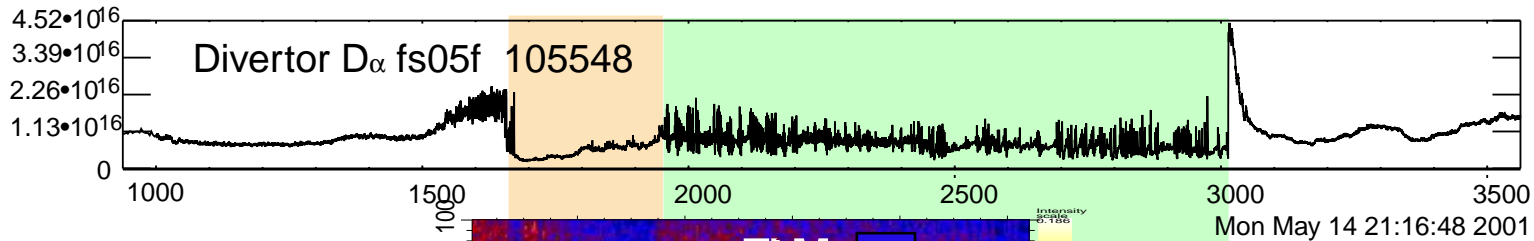
- Assuming dimensionless scaling and not neutral penetration applies carry out single dimensionless parameter scans to determine **dimensionless scaling**: JET/DIII-D $\Delta(\rho_*)$

Δ/a , β_T , ELM behavior all match under dimensionally identical pedestal conditions in CMOD/DIII-D comparison experiment



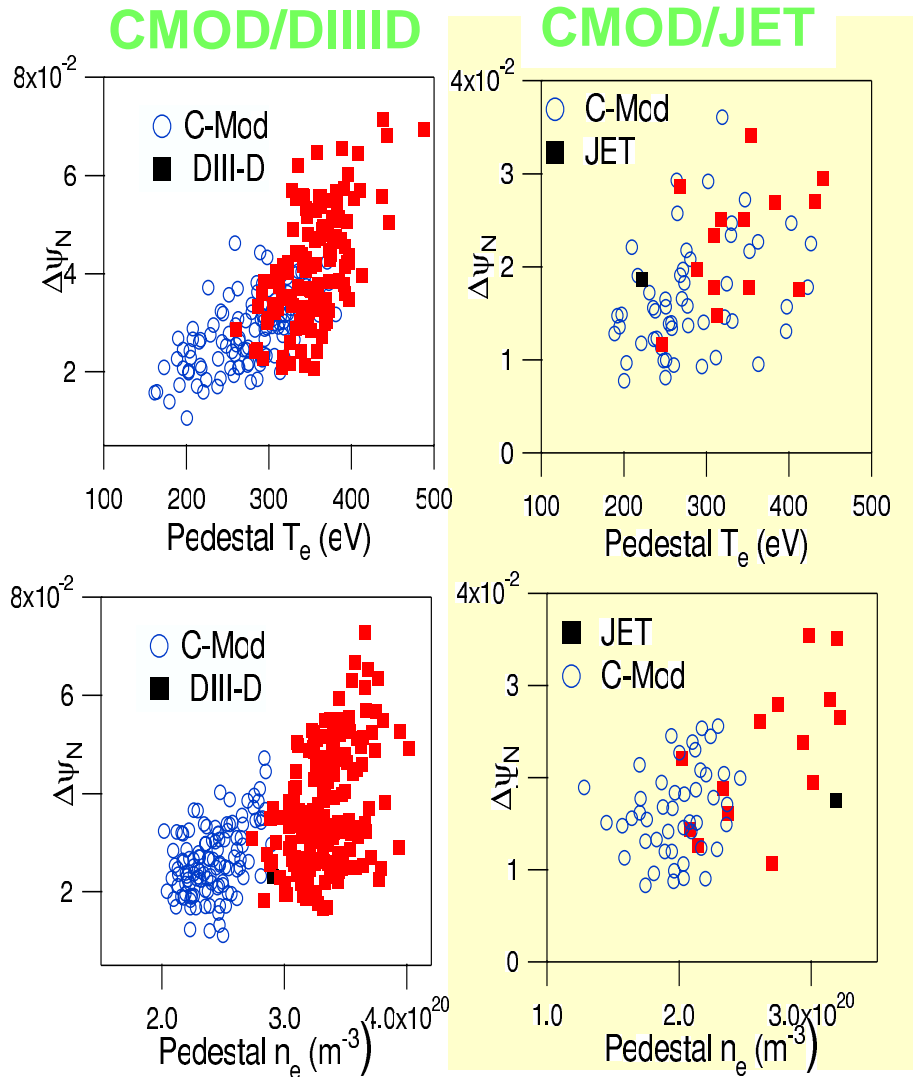
D. Mossessian - B21

Discharges with matched dimensionless pedestals have similar ELM behavior in CMOD/DIII-D comparison experiment

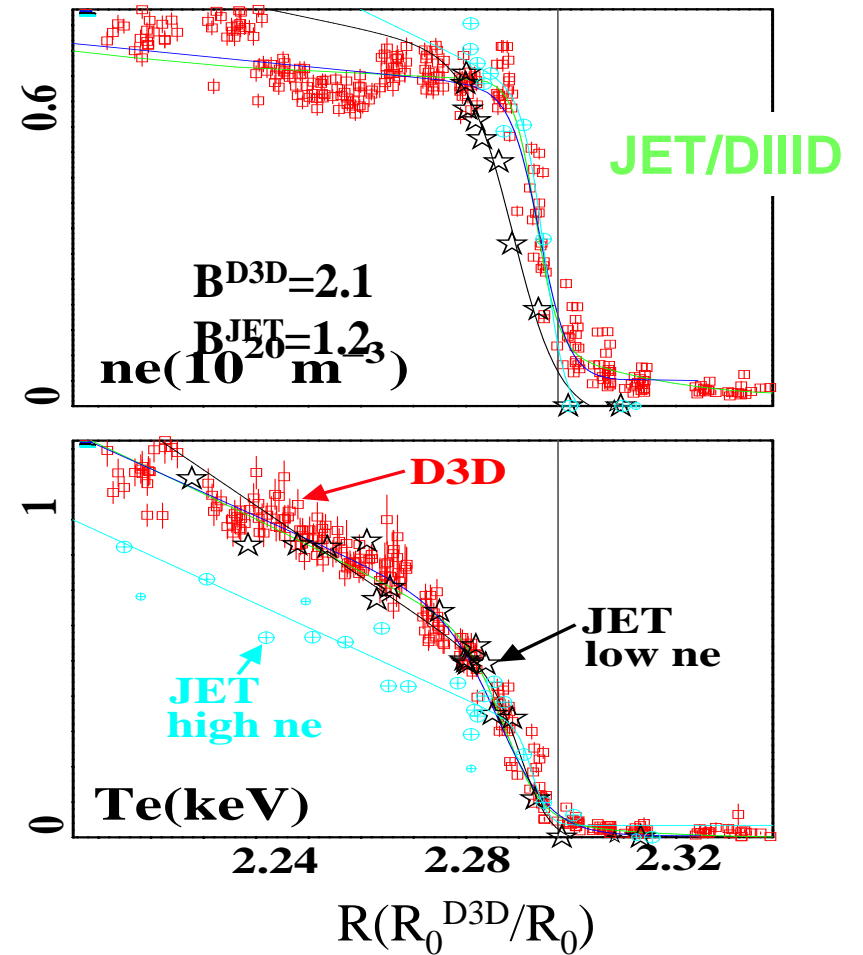


R. Moyer, APS01

CMOD/JET, JET/DIII-D pedestal dimensionally identical experiments also give $\Delta \sim a$



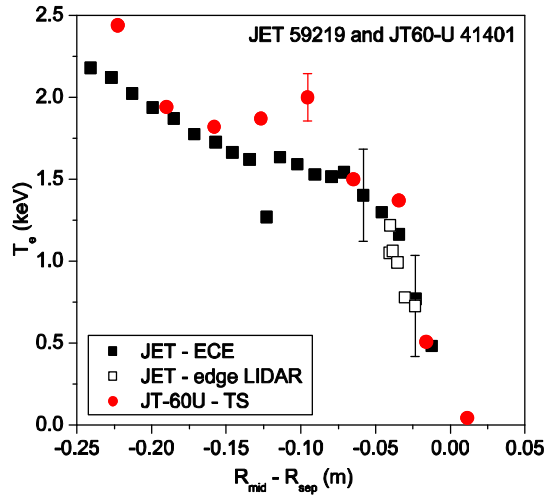
D. Mossessian – B21



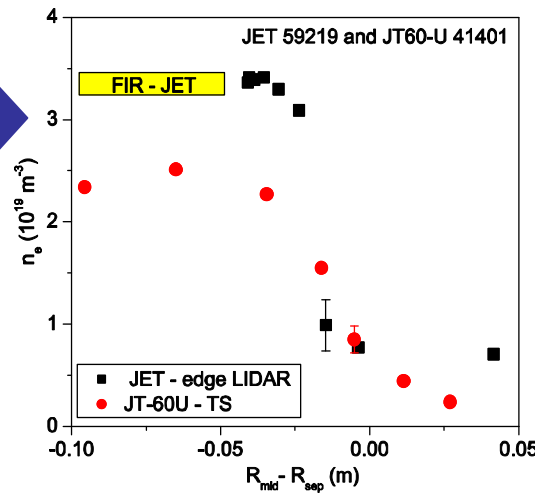
● $n_e T_e$ pedestal show less spatial separation on JET than DIII-D

A.Loarte, G.Saibene, T.Osborne

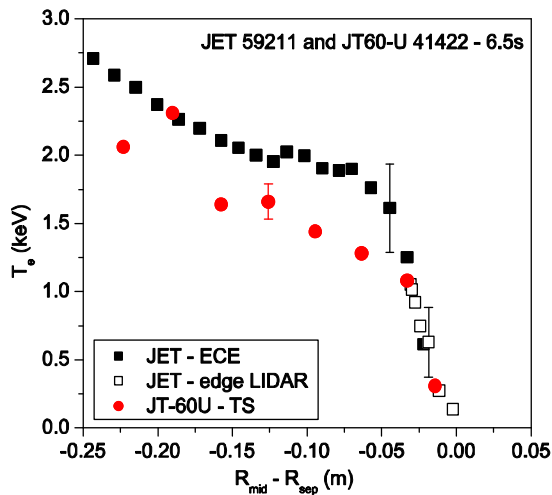
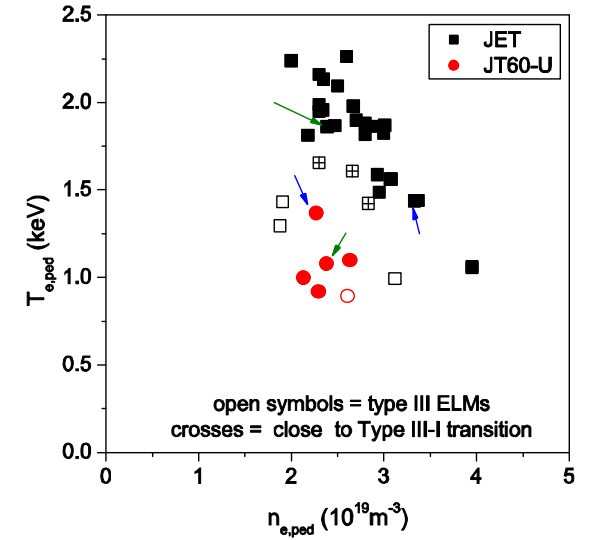
Dimensionally identical pedestals where not obtained in the JET/JT-60U exp possibly due to different rotation profiles



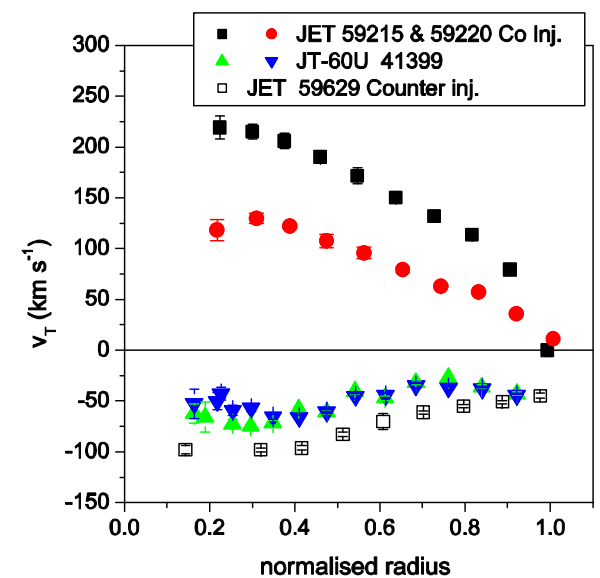
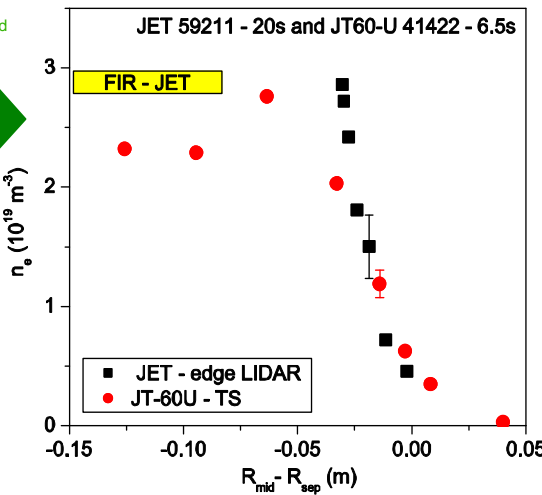
$=T_{ped} \neq n_{ped}$



At JT-60U β_{ped} JET is in Type III regime



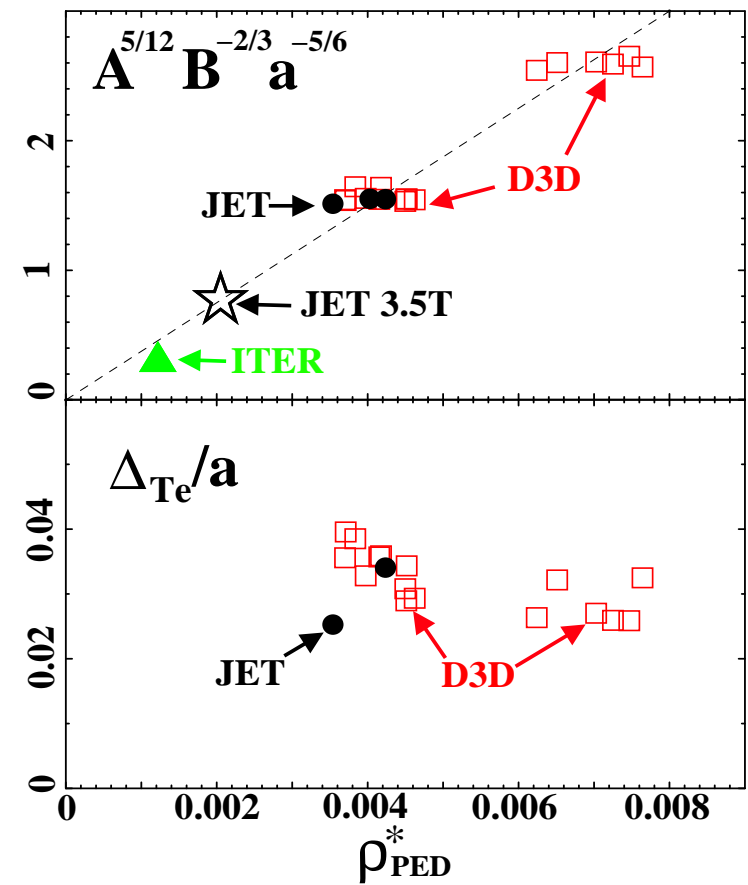
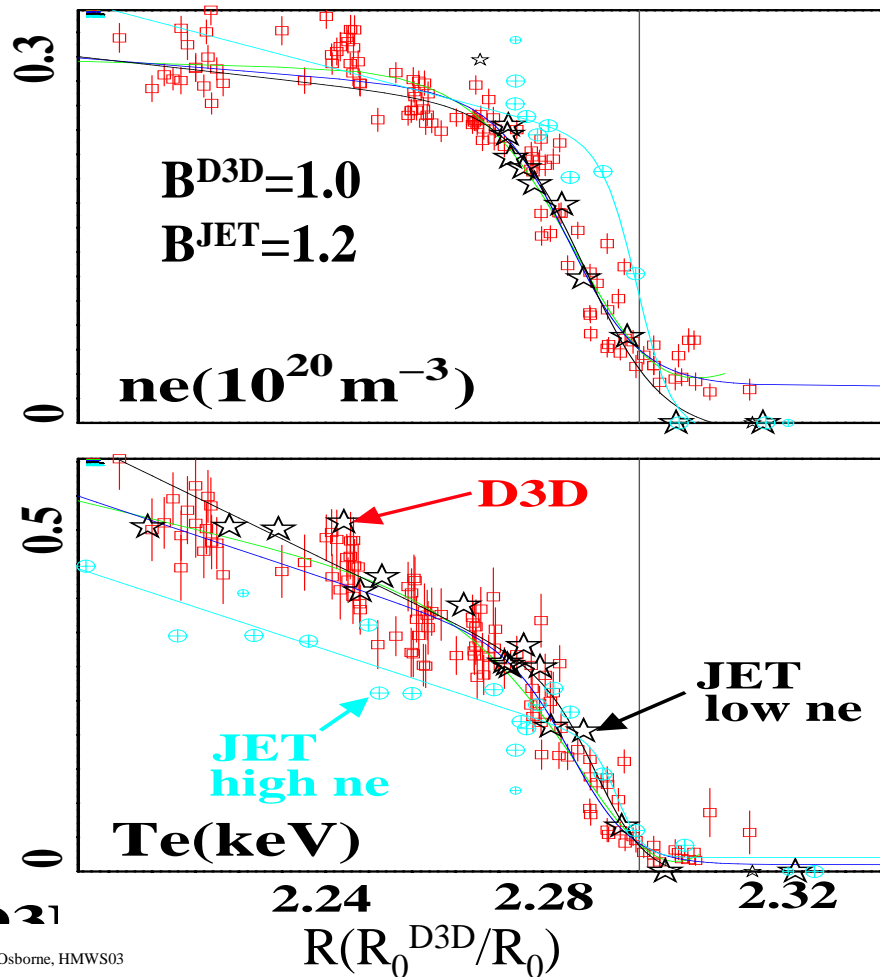
$=n_{ped} \neq T_{ped}$



G.Saibene – B22

No strong variation of Δ_T with ρ_* in JET/DIII-D pedestal dimensionless scaling experiment (no high B JET data)

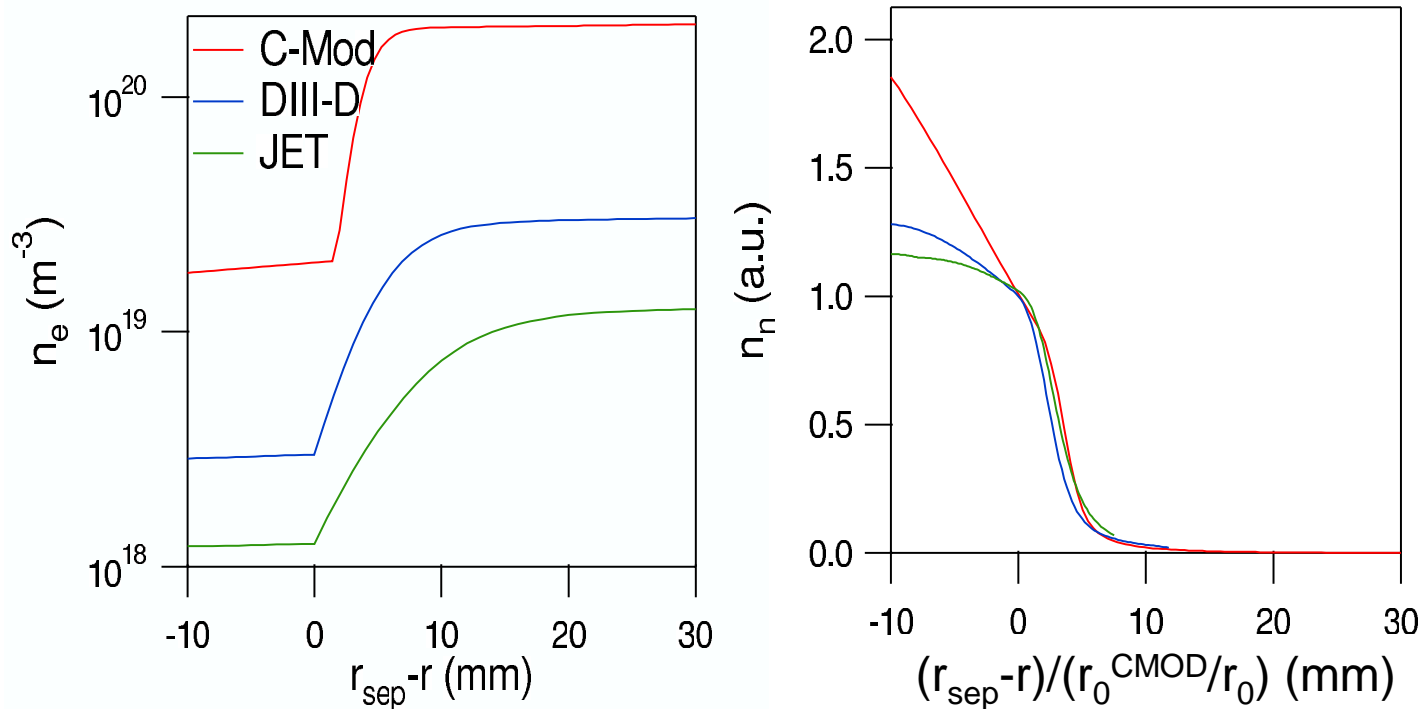
- β, v_*, q fixed as B is varied $\rho_* \sim A^{5/12} a^{-5/6} B^{-2/3}$
- Neutral penetration increases at low B $\hat{\lambda}_N \sim A^{5/6} a^{-2/3} B^{-4/3}$
- DIII-D density and temperature ped tops now same place



A.Loarte, G.Saibene, T.Osborne

Neutral particle transport simulations suggest control of ETB extent by neutral source may still be consistent with dimensionally identical expts

- KN1D 1-D kinetic neutral transport code predicts similar $\hat{\lambda}_N$ for JET/DIII-D/COM for dimensionless scaling values of n_e^{PED} rather than $\hat{\lambda}_N \sim a$
 - Since λ_N is comparable to Δ , density gradient has a strong effect on λ_N

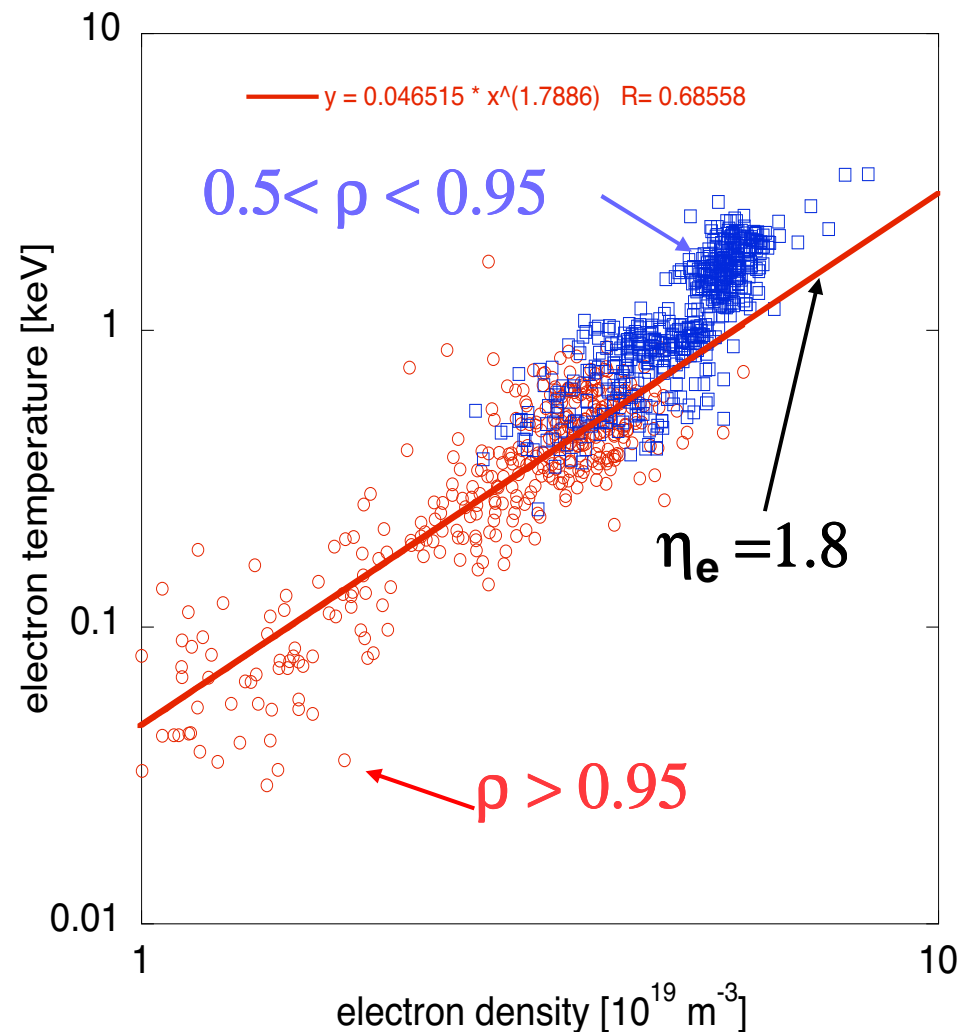


D. Mossessian – B21

Asdex-Upgrade results suggest edge T_e and n_e profiles may be tied together by edge turbulence constraint

- The AUG edge barrier satisfy $\eta_e \sim 2$, perhaps indicating that residual ETG turbulence is controlling transport across the barrier
- The profile deviates from $\eta_e \sim 2$ only in the plasma core.

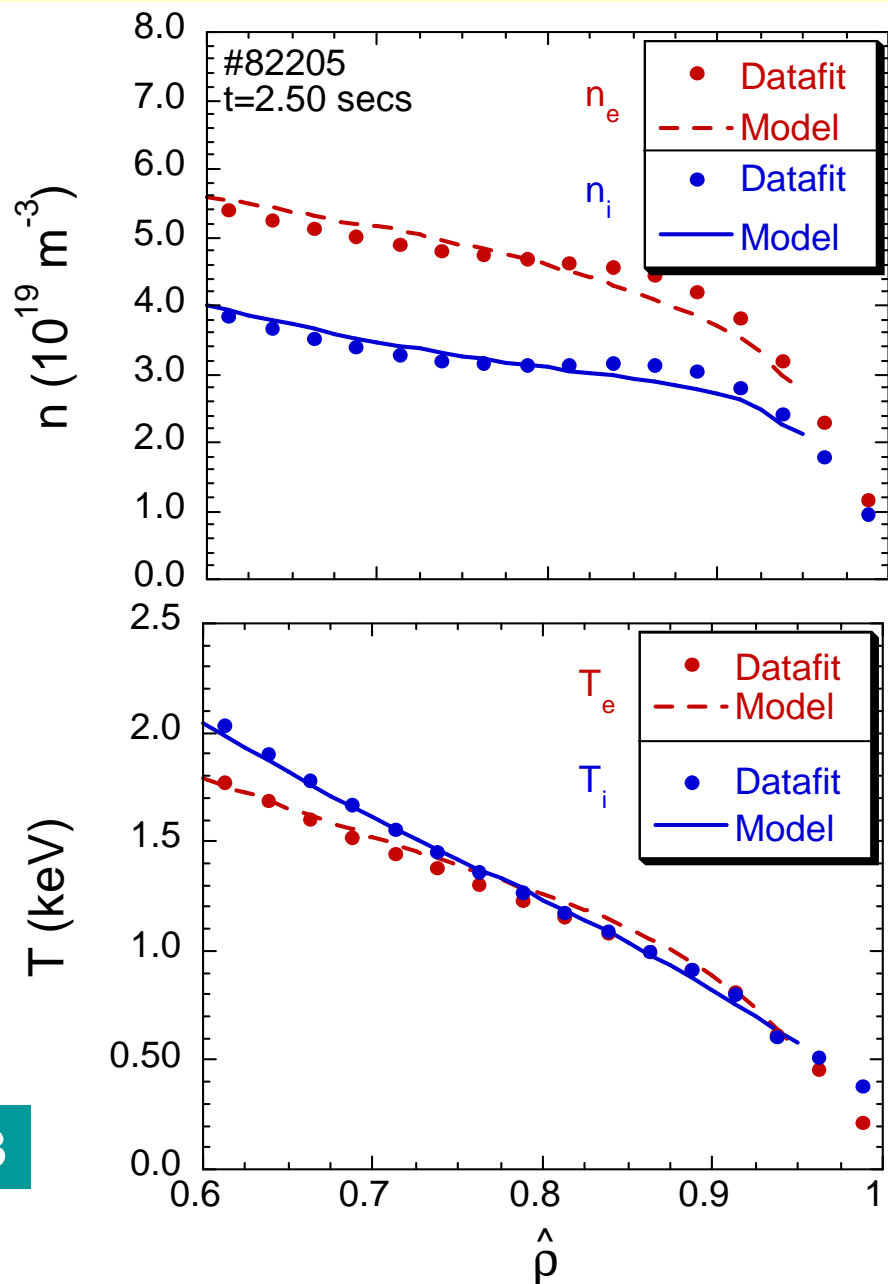
L. Horton – B20



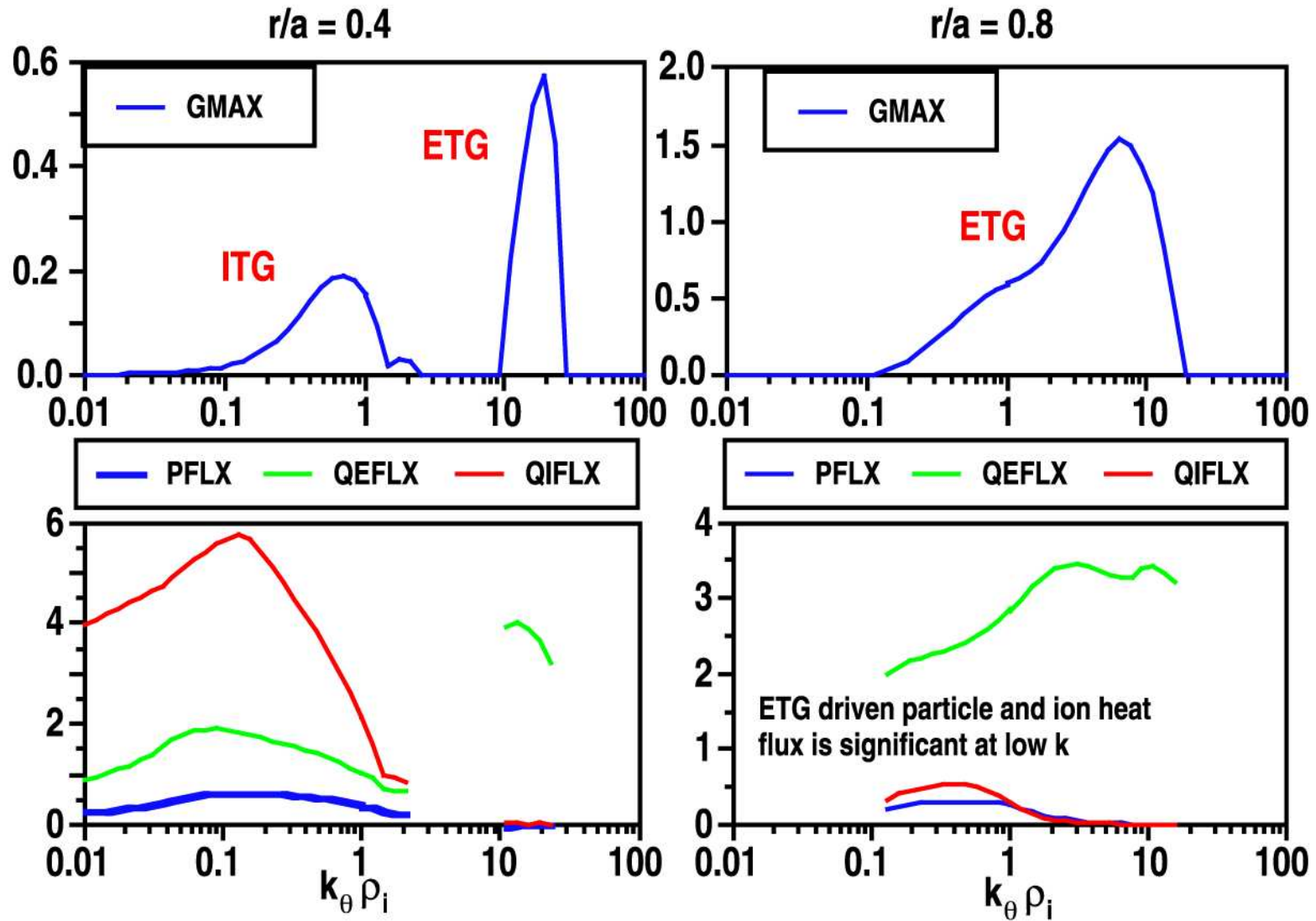
Predictive modeling of H-mode pedestal with GLF23

- GLF23 drift wave + NCLASS neoclassical predicts n_i , T_i , T_e , v_ϕ in DIII-D pedestal
- Experimental values as boundary condition at $\rho=0.95$
- Steady-state solution for single time slice using XPTOR code
- MHD stability not considered
- Magnetic shear in pedestal strongly affects results
- Reasonable agreement with data when ITG/TEM transport marginally unstable (not quite neoclassical)

J. Kinsey – C13



ETG/TEM at low k important for ion and particle flux near edge, will be added to GLF in near future



G. Staebler – C17

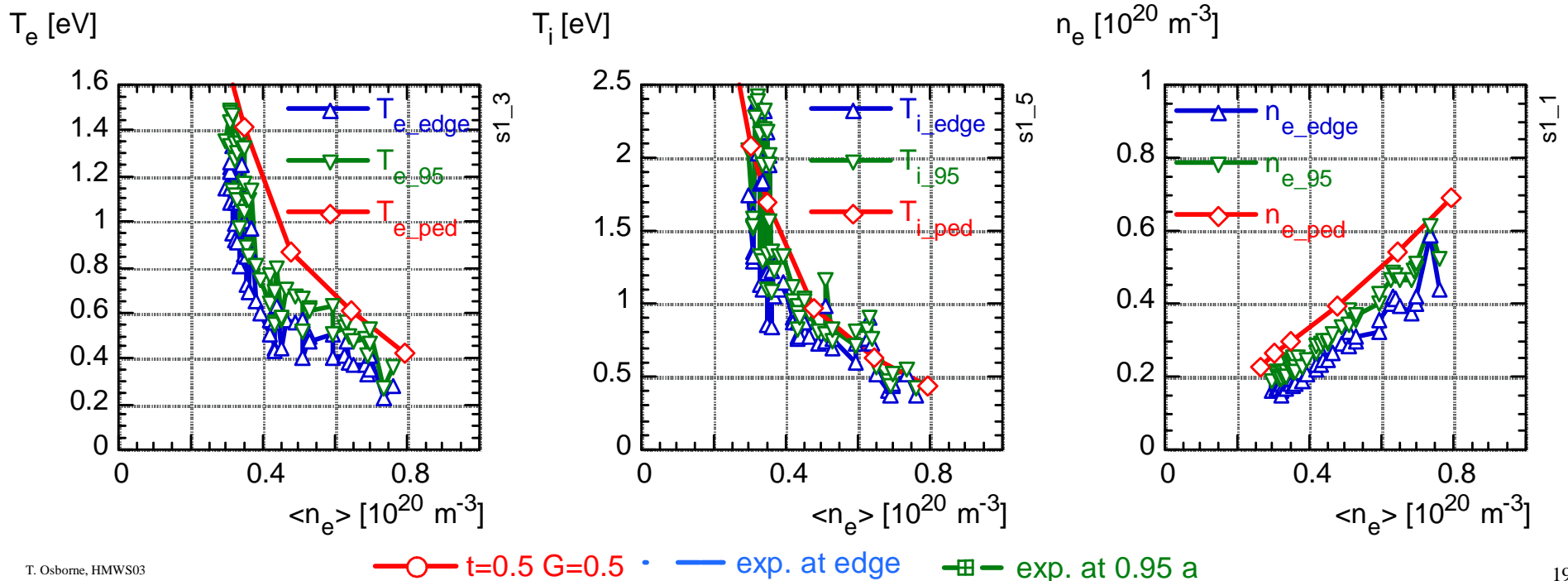
Modeling of entire profile with MMM transport coefficients + additional shear effect in pedestal

- $E \times B$ velocity shear + magnetic shear \Rightarrow pedestal in MMM + B2/Eirene model
 - but appreciably lower than experiment
 - additional magnetic shear stabilization is therefore postulated.
- MMM transport gives good profile shape \Rightarrow threshold for additional shear stabilization.

G. Pacher – C15

$$\chi = \chi_{MMM} / \left\{ \left(1 + \left(\omega_{E \times B} / (G \gamma_0) \right)^2 \right) \cdot \max \left(1, (s - t)^2 \right) \right\}$$

G and t derived from JET predict AUG pedestal values



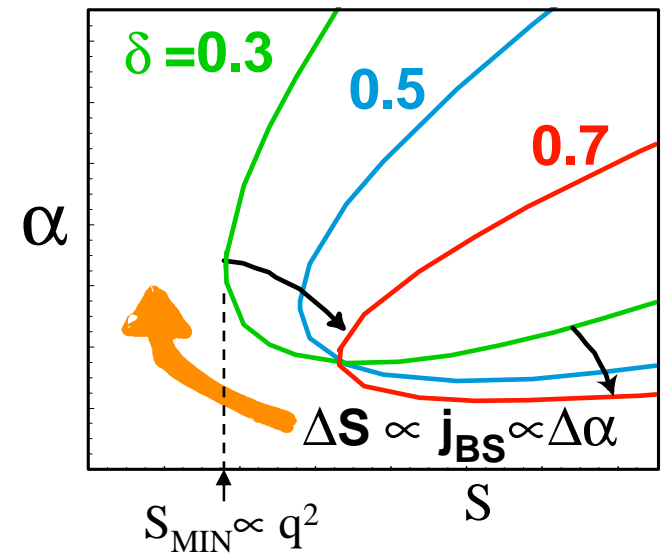
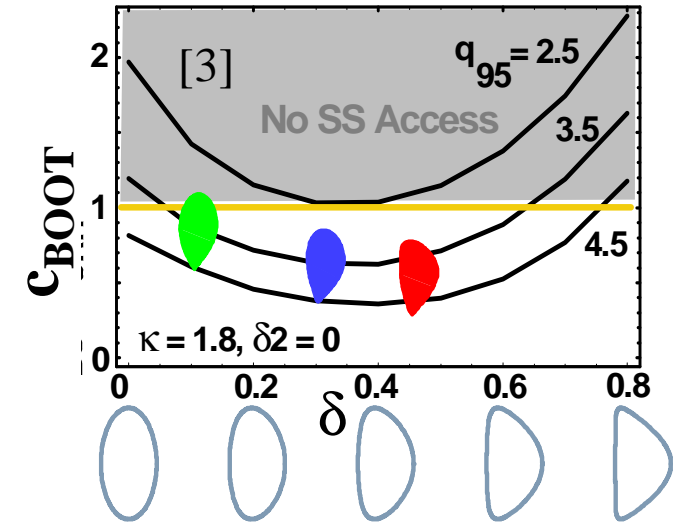
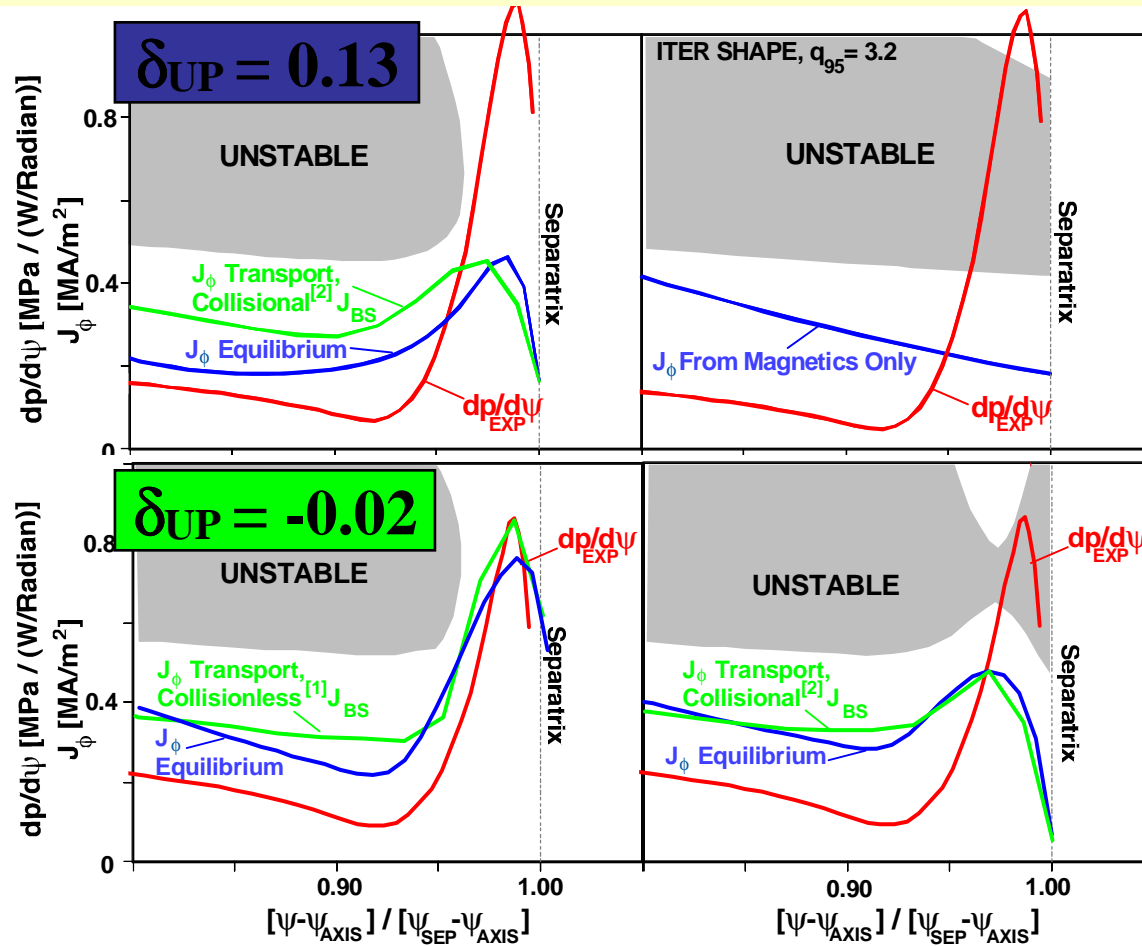
ETB width summary, conclusions

- Attempts to derive an empirical expression for ETB width from scalar databases not successful
 - results might emerge from improved diagnostics
- Significant support for edge neutral source controlling density pedestal
- Role of neutrals in setting ETB width and applicability of dimensionless scaling still unclear
 - 2-D kinetic neutral transport simulations should be applied to inter-machine comparison experiments
 - Need for integrated SOL/CORE modeling
- Extension of turbulent transport models through pedestal in the near future very promising
 - AUG $\eta_e \sim 2$ result suggest ETG
 - Important to produce set of high quality experimental profile and equilibrium time histories.

Edge Stability in Type I ELM regime

- Need for extension of ballooning mode model
- Peeling ballooning mode stability
- Experimental support for PB mode association with ELM
- ELITE code as a tool for understanding edge stability space.

Edge second stable access allows p'_{PED} to exceed $n=\infty$ ballooning mode pressure gradient limit



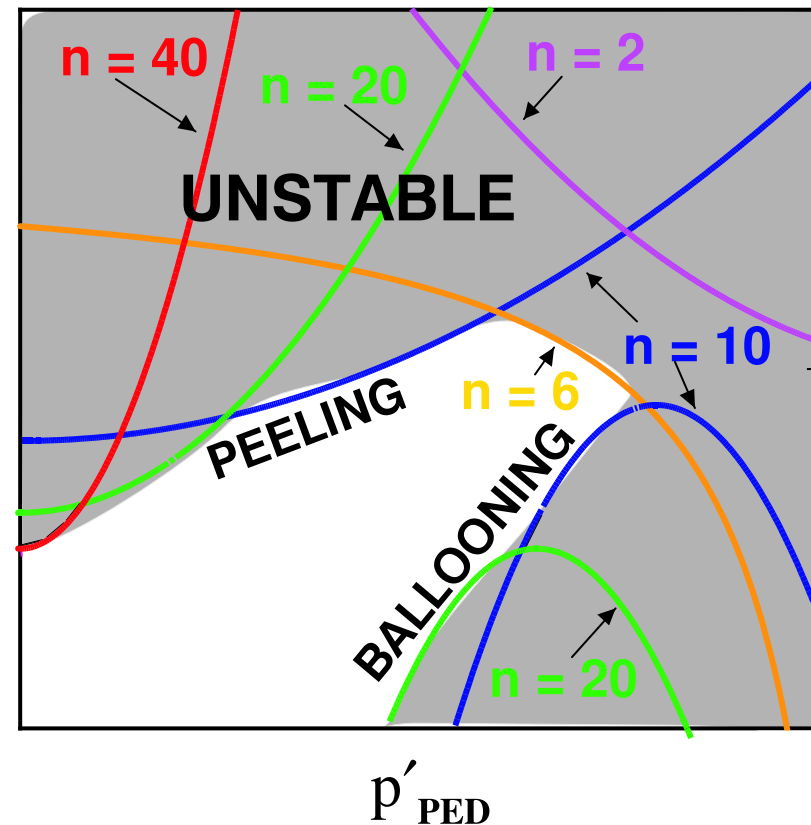
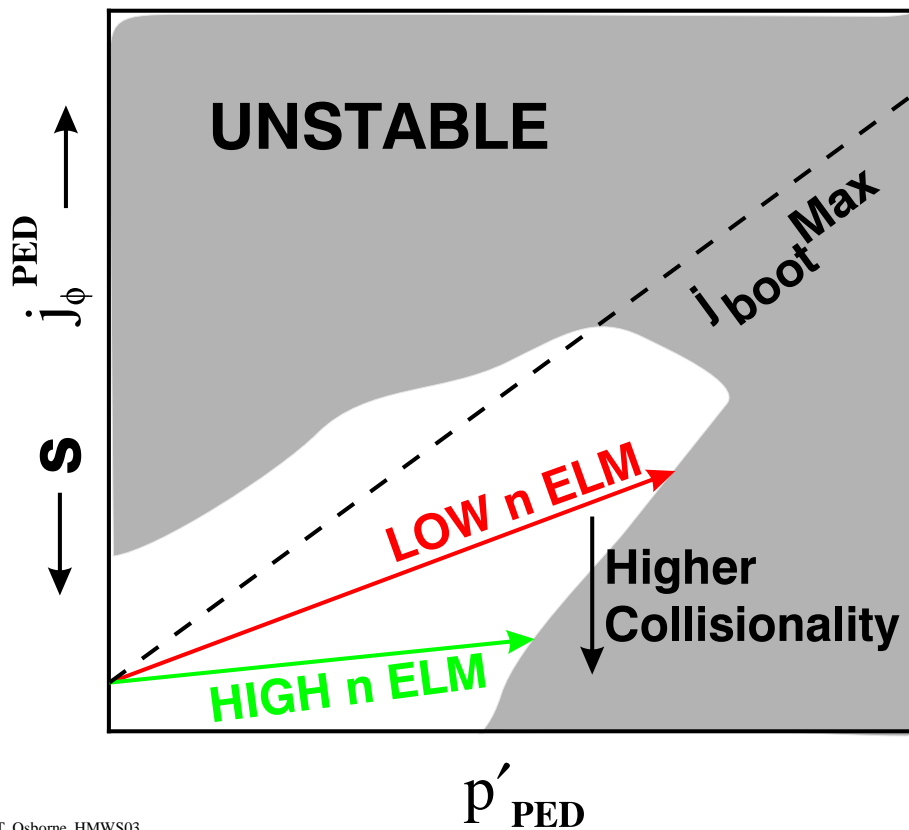
- [1]Hirshman '89
- [2]Houlberg '95
- [3]R.L. Miller, et. al, Plasma Phys. Control. Fusion **40** (1998).

- S_{MIN} rises with δ
- α_{CRIT} decreases with δ
- $f_{TRAPPED}$ decreases with δ

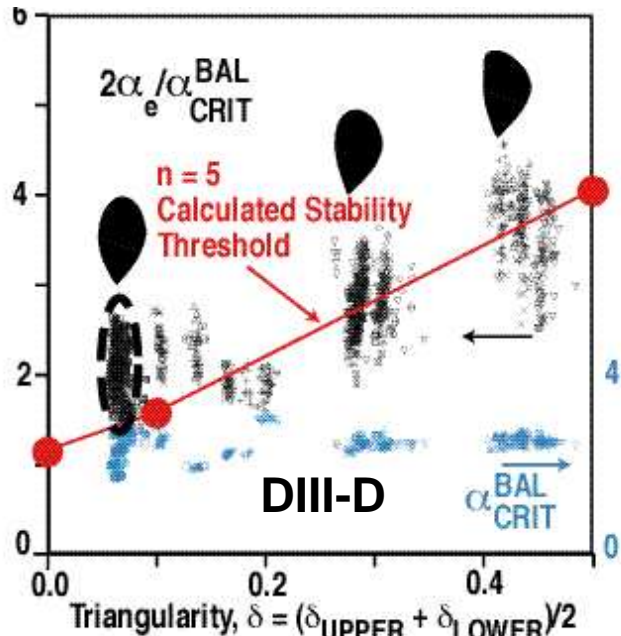
Both P'_{PED} And J_{ϕ}^{PED} Important in Peeling-Ballooning Mode Stability Boundary

- Higher J_{ϕ}^{PED} (reduced shear) stabilizes high n ballooning modes (second stab) but drives intermediate n peeling modes
- P'_{PED} and J_{ϕ}^{PED} interact through J_{BOOT}

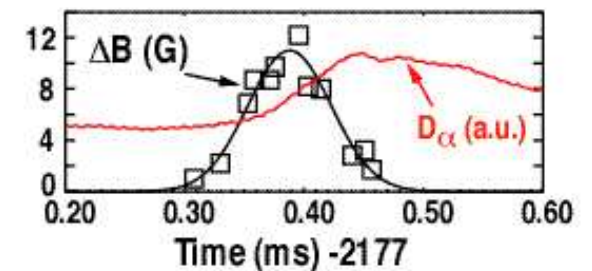
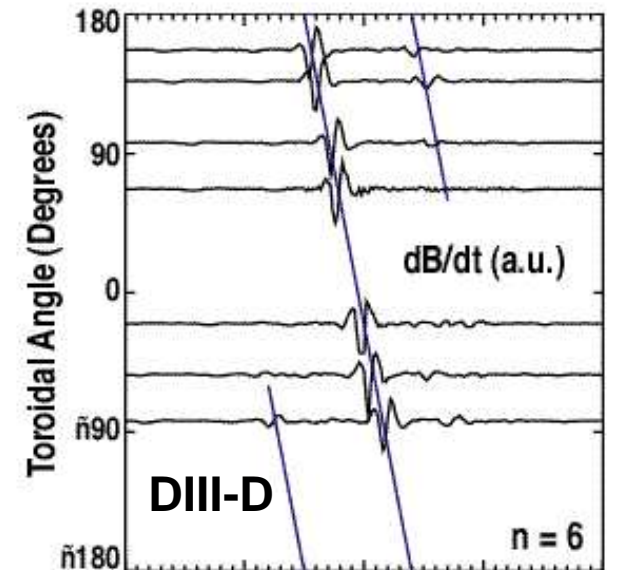
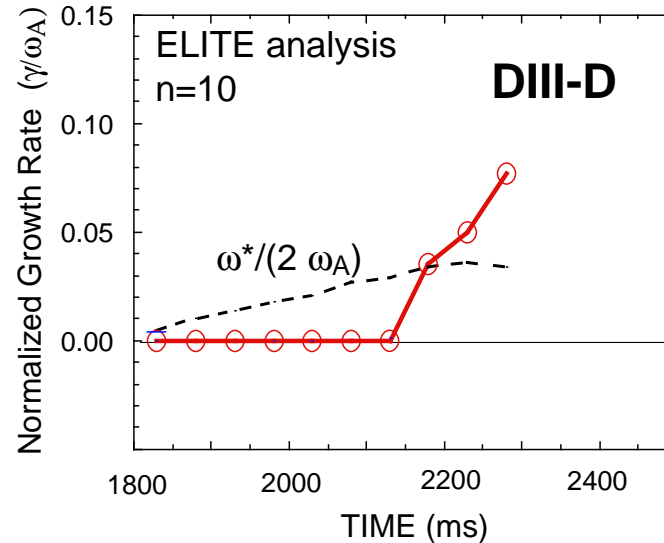
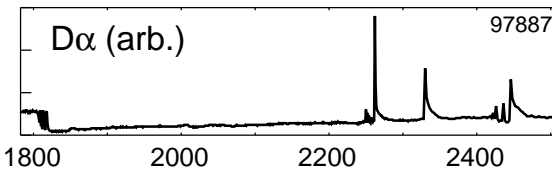
H.R. Wilson, P.B. Snyder



Observations consistent with low n , ideal, edge localized, peeling-ballooning as mode associated with Type I ELM



- P' variation with shape in DIII-D, JT-60U, and AUG consistent with edge peeling-ballooning stability
- ELM time agrees predicted instability onset
- Fast growing $1 < n < 13$ modes are observed



J.R. Ferron,
L.L. Lao,
P.B. Snyder,
E.J. Strait

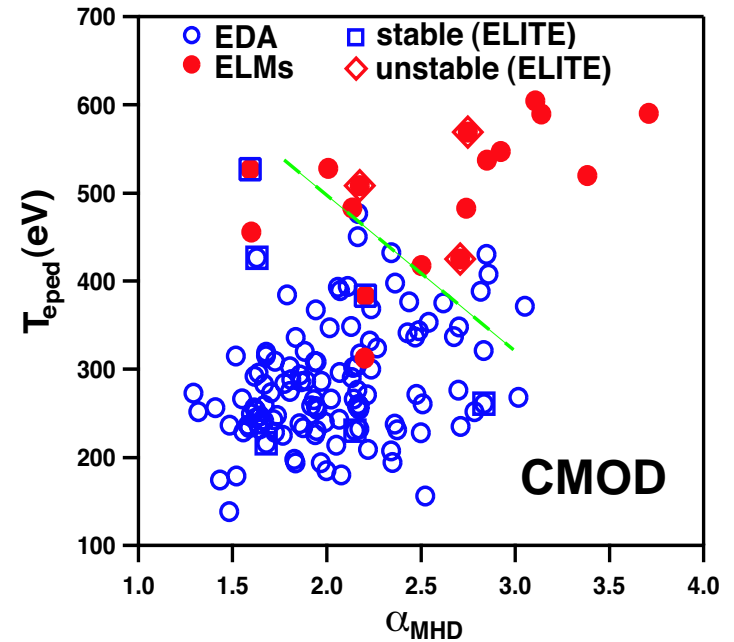
PB mode model consistent with results on other tokamaks

Alcator C-Mod

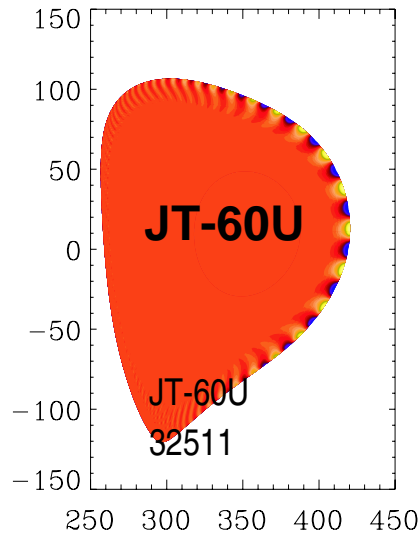
- ELM-free and EDA shots are peeling-ballooning stable
- Peeling-Ballooning modes consistently unstable just before ELMs

JT-60U

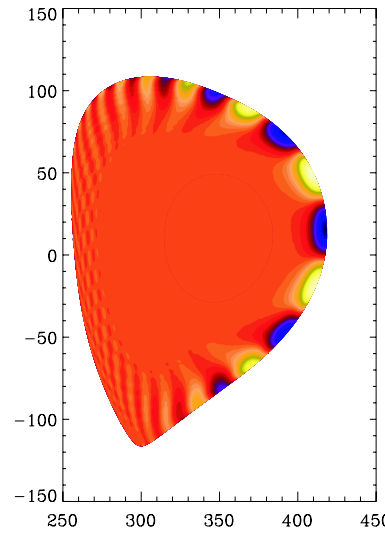
- Peeling ballooning modes unstable before ELMs
- Broader mode structures in "Giant ELM"



Grassy ELMs



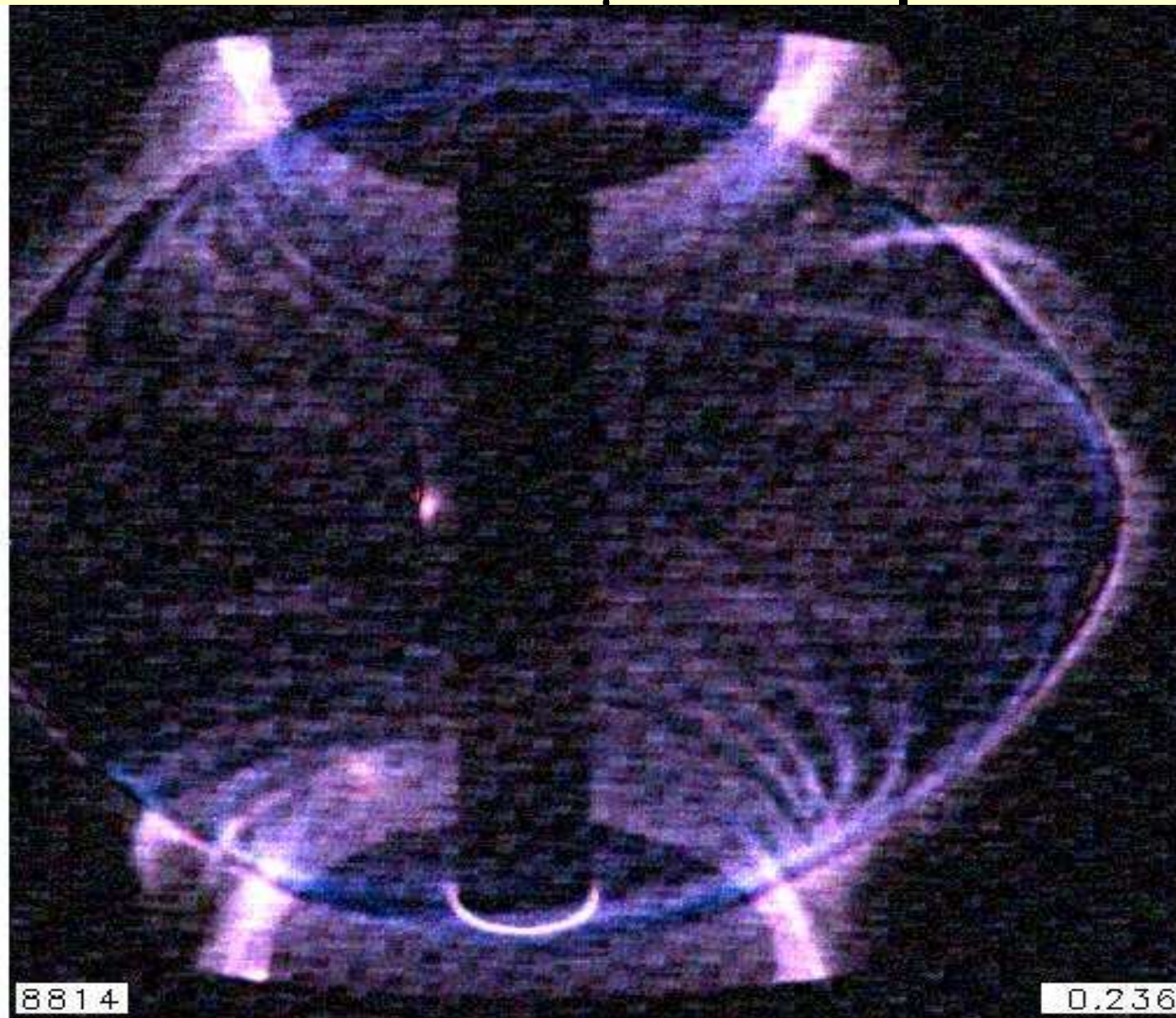
Giant ELMs



D. Mossessian,
P.B. Snyder

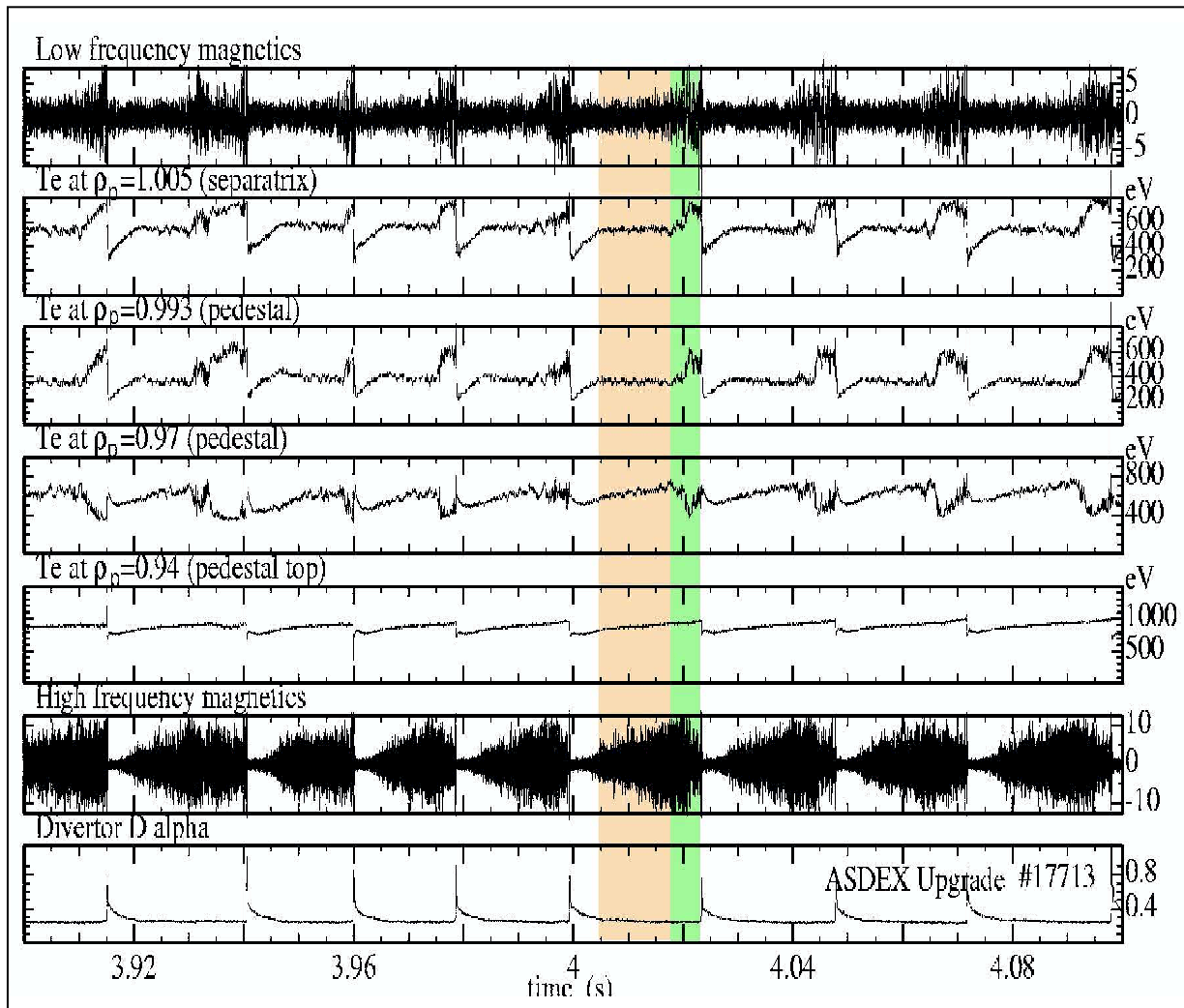
L.Lao, P.B. Snyder-B11

n=8-10 mode at ELM in 25 μ s time exposure on MAST

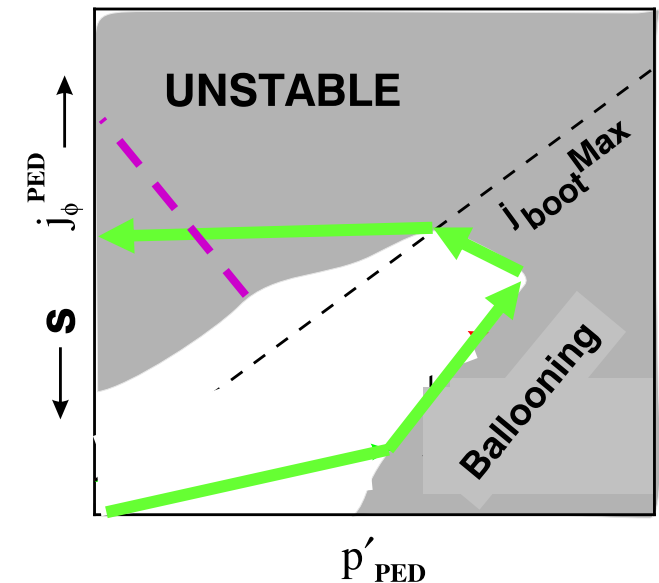


A. Kirk – B18

AUG ELM precursor studies suggest two phases in ELM instability



- HF (300-500kHz, $m=10-15$) clamps T_e^{PED}
- LF Mode at crash
- Conner: p' clamped at ballooning boundary, j increases until peeling mode is triggered



H. Zohm – B12

ELITE is a Highly Efficient 2D MHD Code for $n > \sim 5$

ELITE is a 2D eigenvalue code, based on ideal MHD (amenable to extensions):

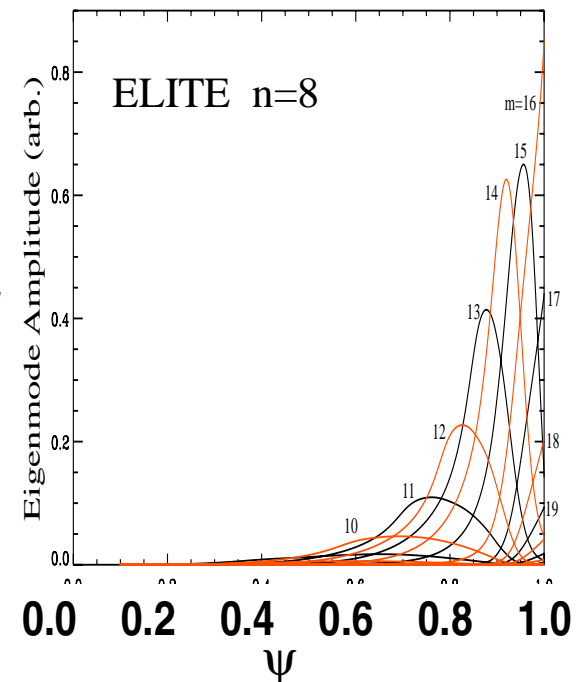
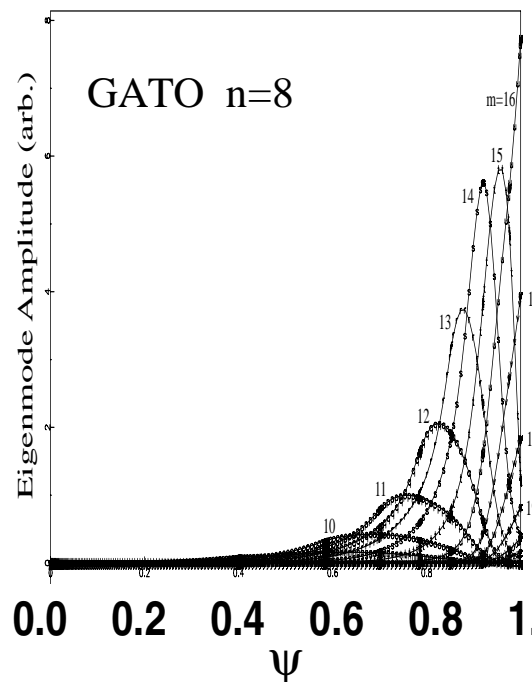
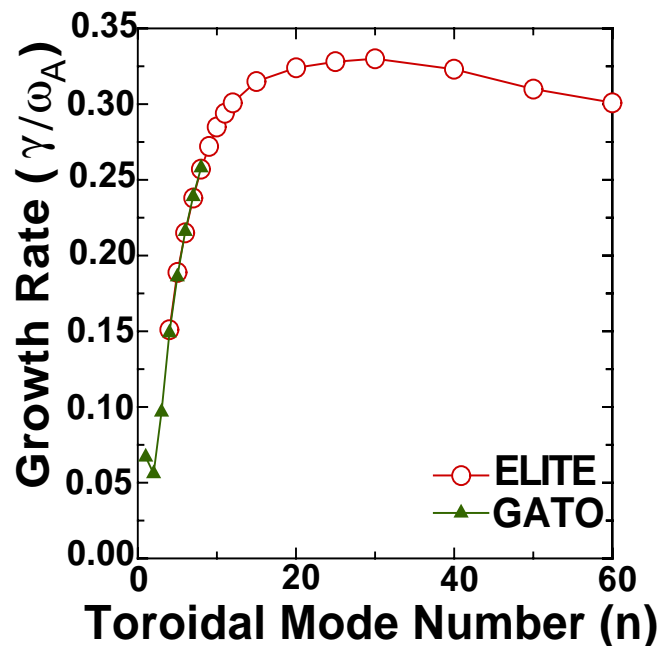
-Generalization of ballooning theory:

- 1) incorporate surface terms which drive peeling modes
- 2) retain first two orders in $1/n$ (treats intermediate $n > \sim 5$)

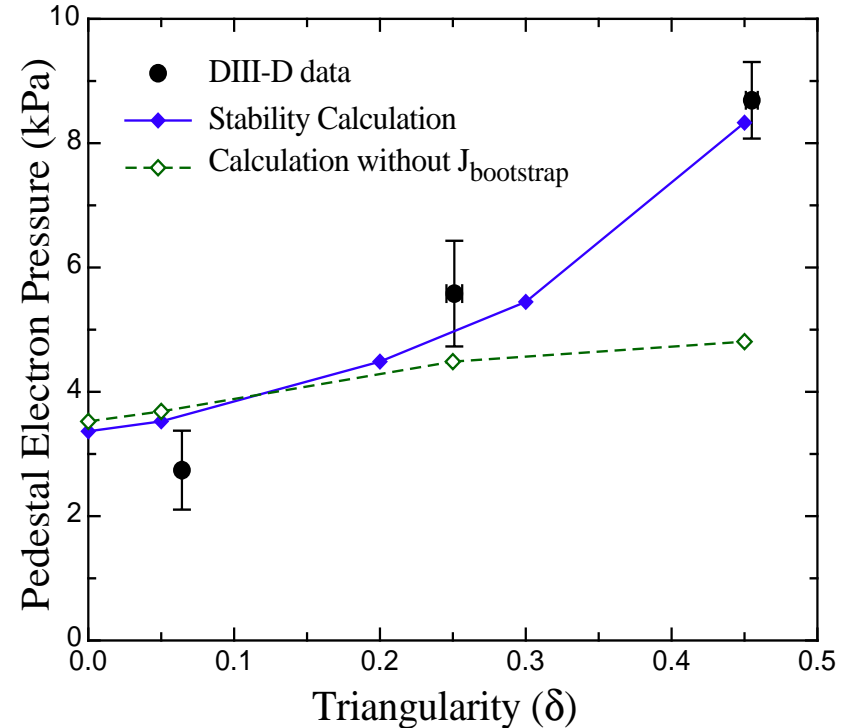
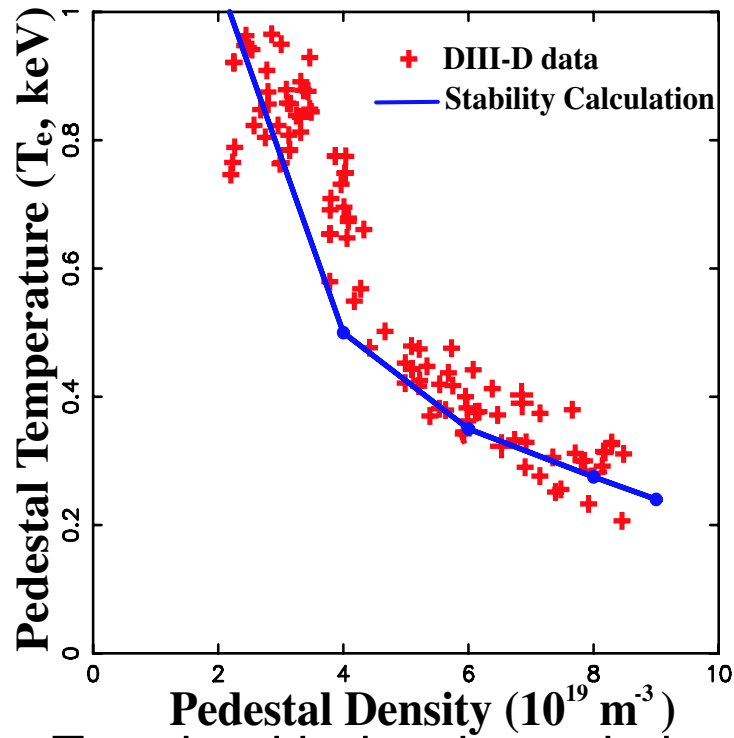
-Makes use of poloidal harmonic localization for efficiency

-Successfully benchmarked against GATO, MISHKA and MARS

[H.R. Wilson, P.B. Snyder et al Phys Plas 9 1277 (2002); P.B. Snyder, H.R. Wilson et al Phys Plas 9 2037 (2002).]



Trends in Existing Pedestal Database Can Be Understood Using Stability of Model Equilibria



- Trends with density and triangularity calculated using series of model equilibria, and compared to database
 - Inputs are B_t , I_p , R , a , κ , δ , $\langle n \rangle$, Δ
- Strong increase in pedestal height with triangularity is due to opening of second stability access
 - Bootstrap current plays a key role here. Without it (dashed line) second stability is not accessed at high n and strong δ trend not predicted

P.B. Snyder –B11

Edge Stability in Type I ELM regime: Summary, Conclusions

- Substantial evidence for PB mode setting edge stability limit in Type I regime
- ELITE code provides a efficient tool for computing edge stability
 - Efforts toward building up a database of stability runs under different discharge conditions should provide a better understanding of trends in the data and aid in future tokamak design

Physics based pedestal pressure empirical scaling

- p' set by ballooning mode stability modified by terms to account for stronger shape dependence in PB modes
- Barrier width scaling taken as a fraction of ρ_{POL} .

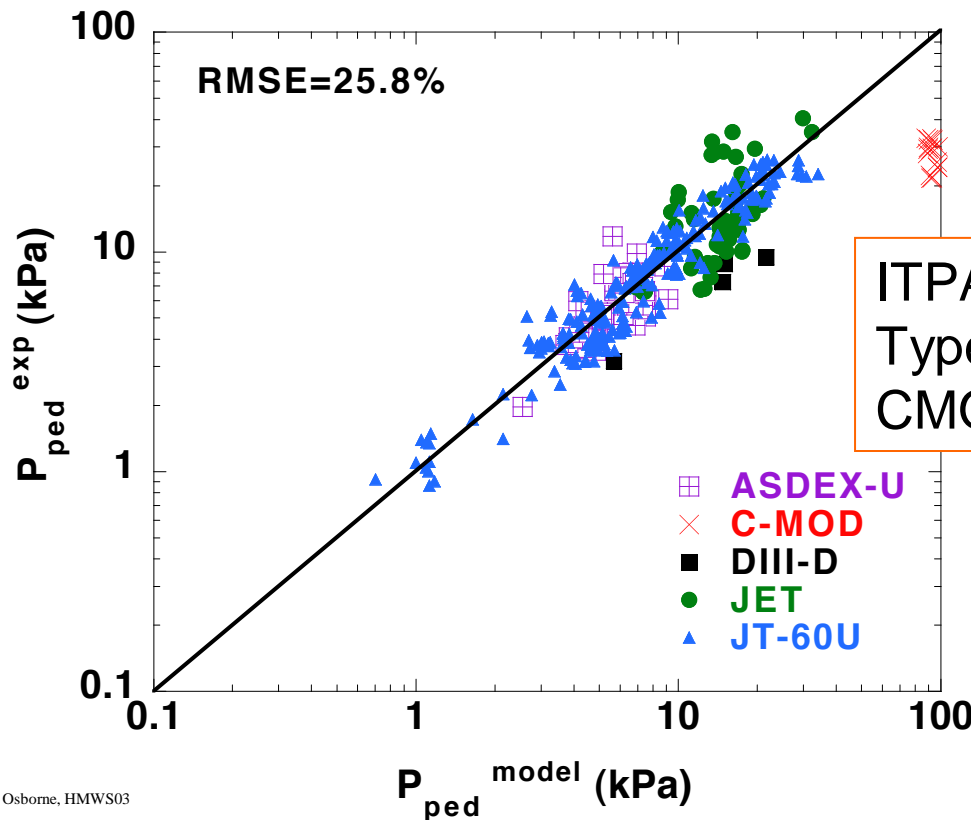
$$P_{ped} = \left(\frac{dP}{dr}\right)_{crit} \Delta_{ped} \quad \Delta_{ped} \propto \sqrt{a \rho_{pol}}$$

$$\left(\frac{dP}{dr}\right)_{crit} \equiv \left(\frac{dP}{dr}\right)_0 F(shape, \beta_p)$$

$$F(shape, \beta_p) \propto \kappa^{C_1} (1 + \delta)^{C_2} A^{C_3} (P_{TOT} / P_{LH})^{C_4}$$

$$P_{LH} = 2.84 M^{-1} B^{0.82} \bar{n}_e^{0.58} Ra^{0.81}$$

$$\left(\frac{dP}{dr}\right)_0 \equiv \frac{1}{2\mu_0} \frac{1}{R} \left(\frac{RB_{pol}}{a}\right)^2 \left(\frac{2}{1 + \kappa^2}\right)$$



ITPA Database of Type I ELM Discharges + CMOD Type III

⇒ ITER = 5.3keV @ 0.7x10¹⁰m⁻³

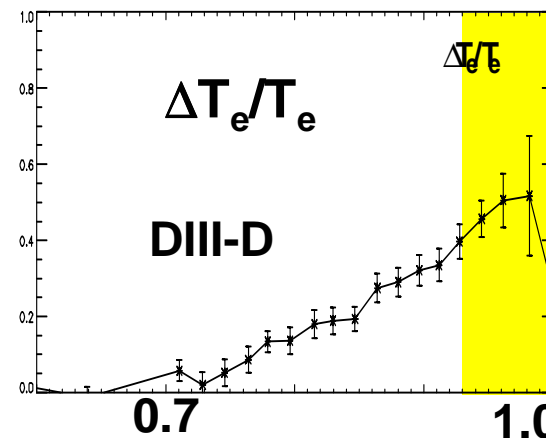
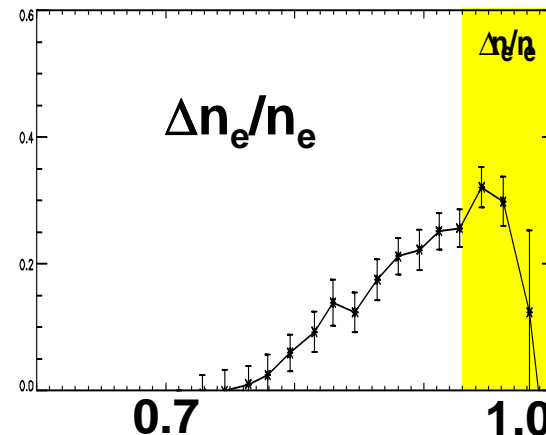
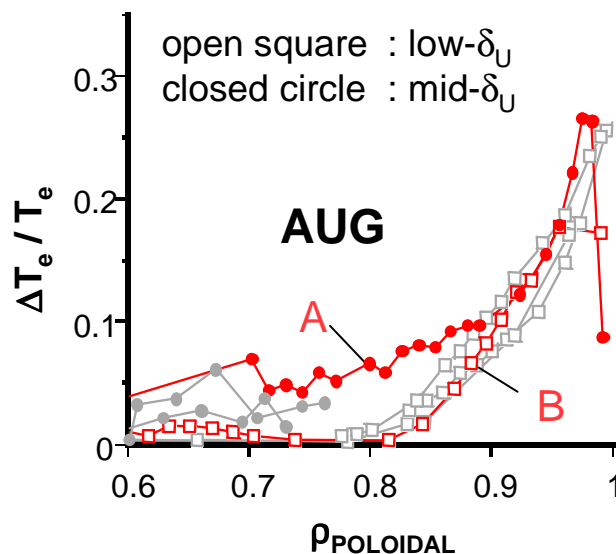
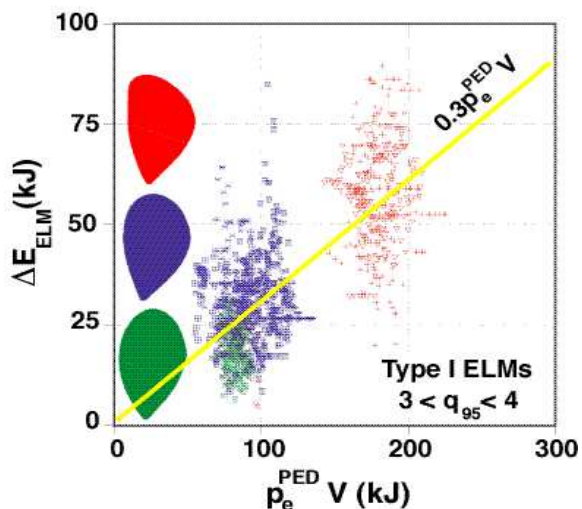
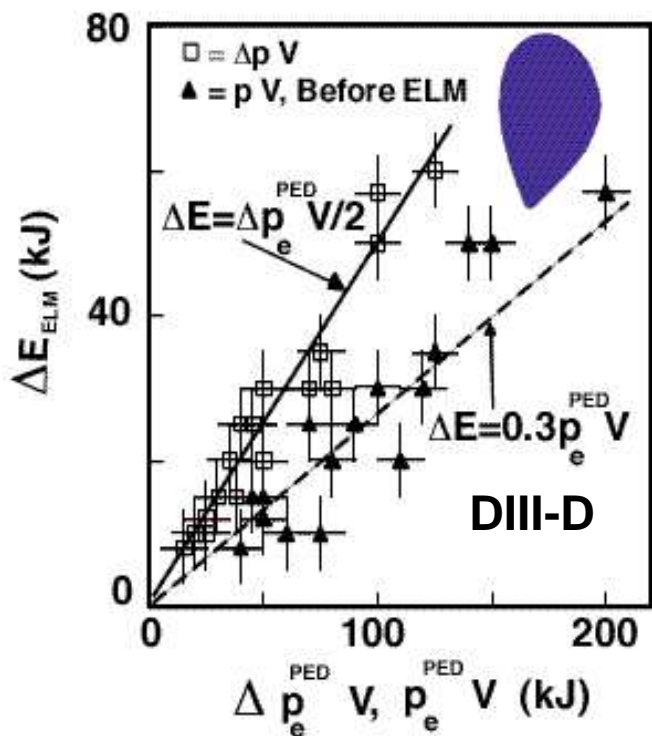
M. Sugihara – C7

Understanding Type I ELM Affects

- Scaling of ELM energy loss
- Extent of ELM-affected region
- Connection to PB linear eigenmode
- Nonlinear stability physics
- Transport simulation including ELM dynamics

ΔW_{ELM} is proportional to W_{PED} . ELM effect extends well beyond ETB. Extent of ELM relatively fixed as ΔW_{ELM} varies.

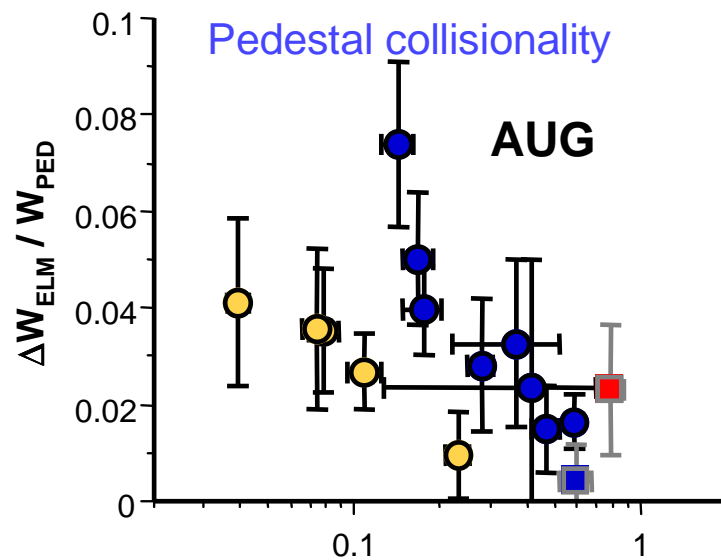
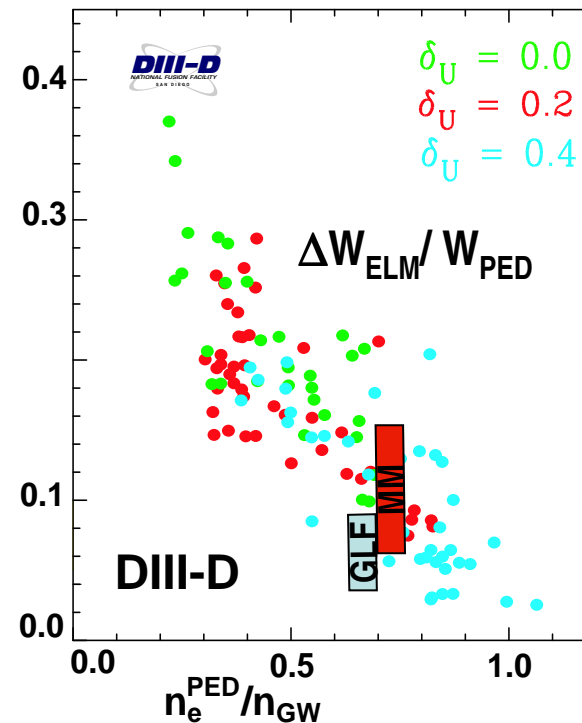
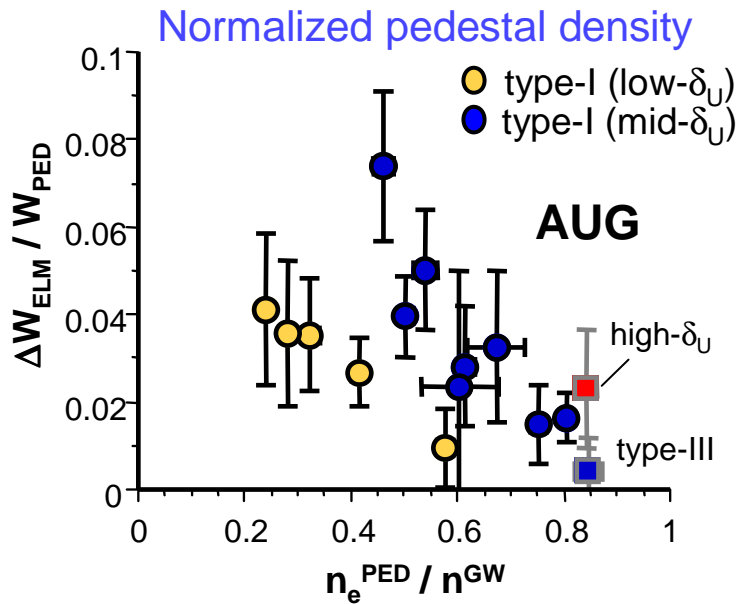
- ELM effect to $\rho \sim 0.75$ in $< 400\mu s$
- ELM-affected region larger with strong shaping (AUG)



H. Urano – D8

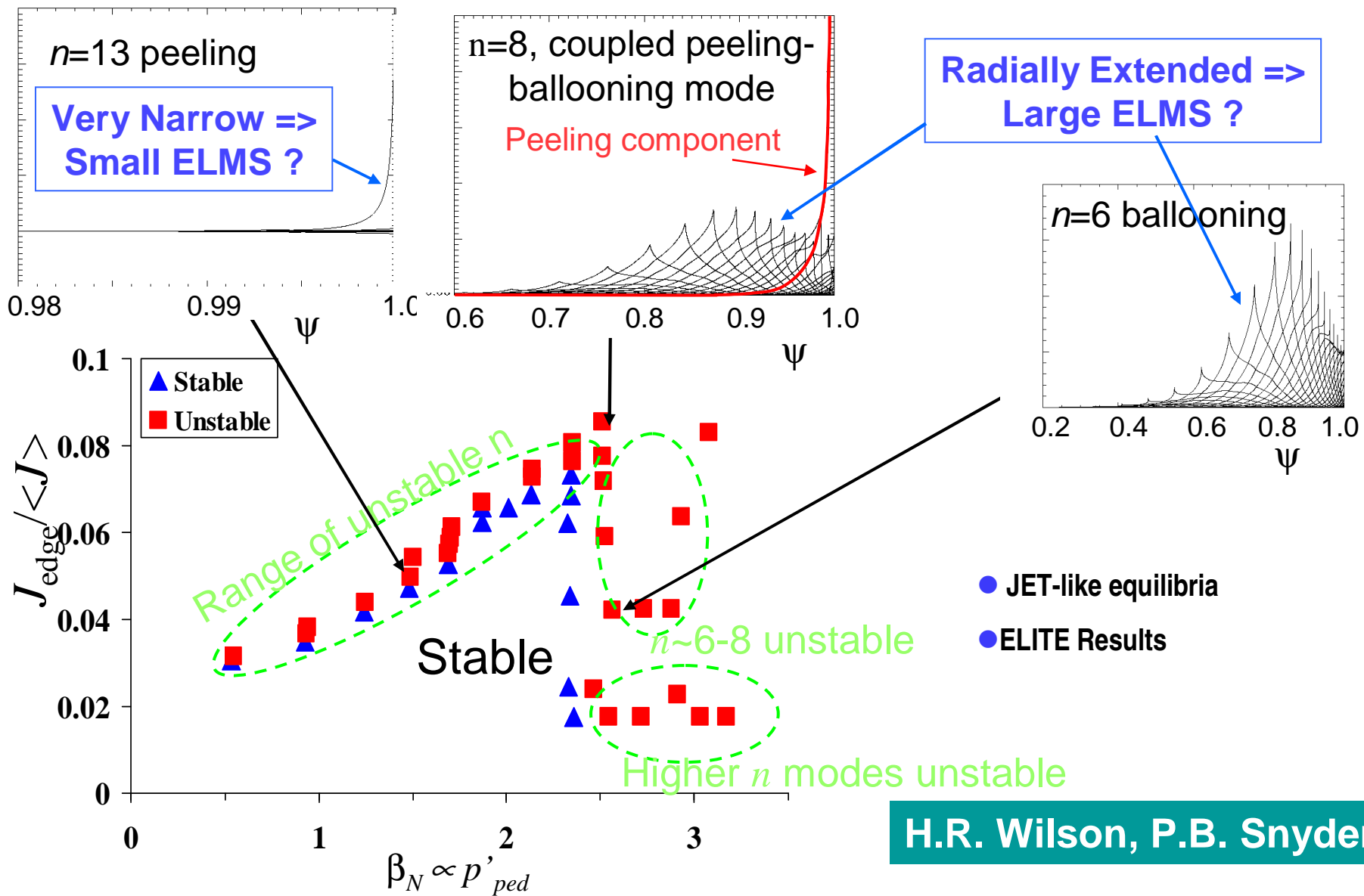
A. Leonard

$\Delta W_{\text{ELM}}/W_{\text{PED}}$ is reduced at high $n_e^{\text{PED}}/n^{\text{GW}}$, v_* , τ_{\parallel} ,



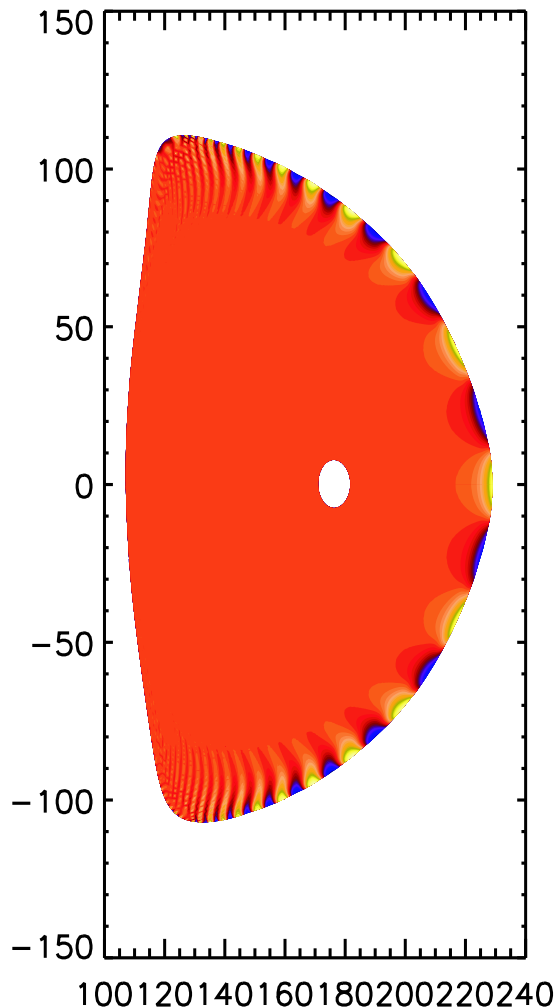
- $\Delta W_{\text{ELM}}/W_{\text{PED}}$ covers a range well beyond what would be tolerable in ITER-FEAT
- $\Delta W_{\text{ELM}}/W_{\text{PED}}$ reduced at high density, increased with shaping on AUG
- Important to understand and possibly exploit the density dependence to produce tolerable ELMs
- Presently no consistent scaling law for $\Delta W_{\text{ELM}}/W_{\text{PED}}$ which covers all tokamaks

Different n's and Mode Structures Predicted in Different Regimes

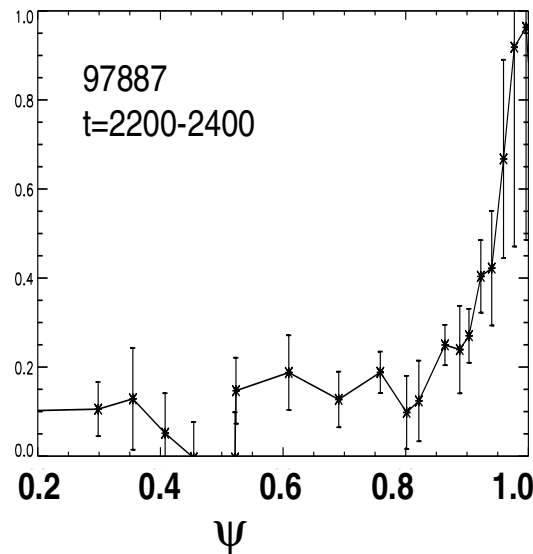


H.R. Wilson, P.B. Snyder

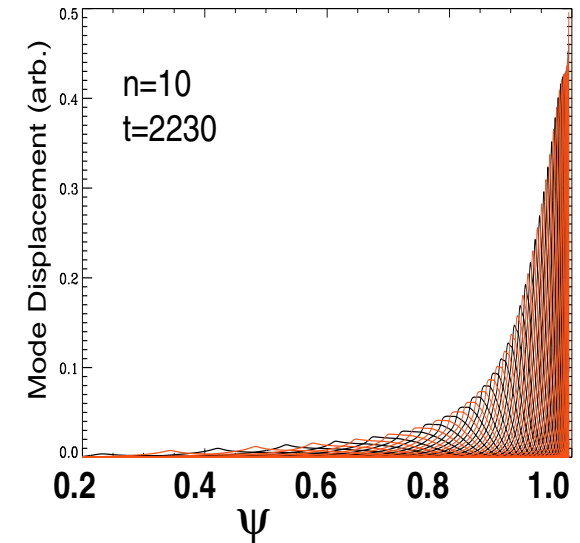
Extent of ELM affected region correlated with PB mode radial eigen function width



Observed $\Delta T_e/T_e$ across ELMs



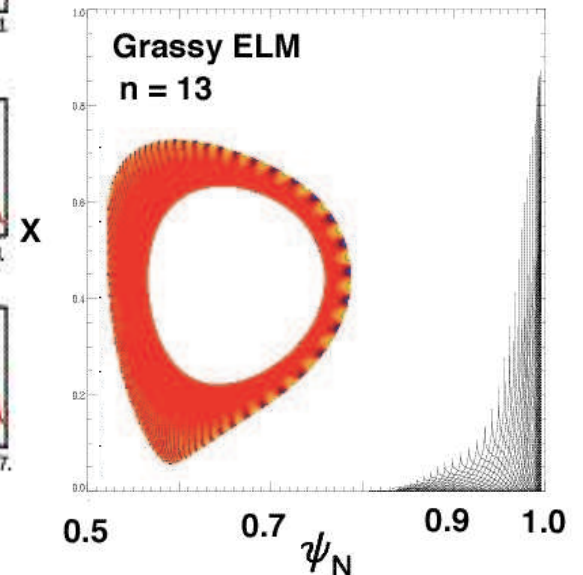
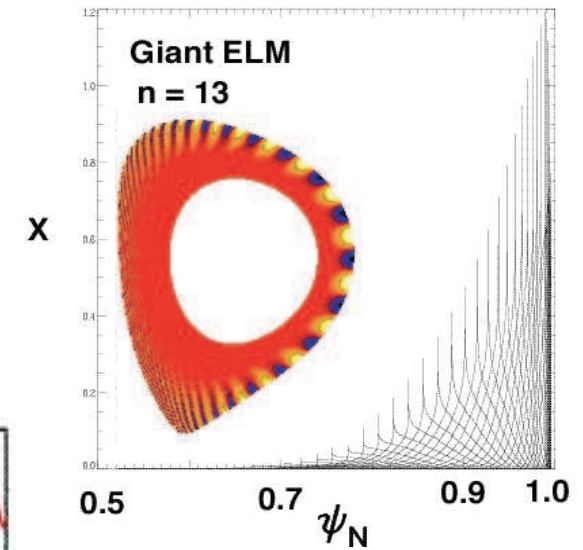
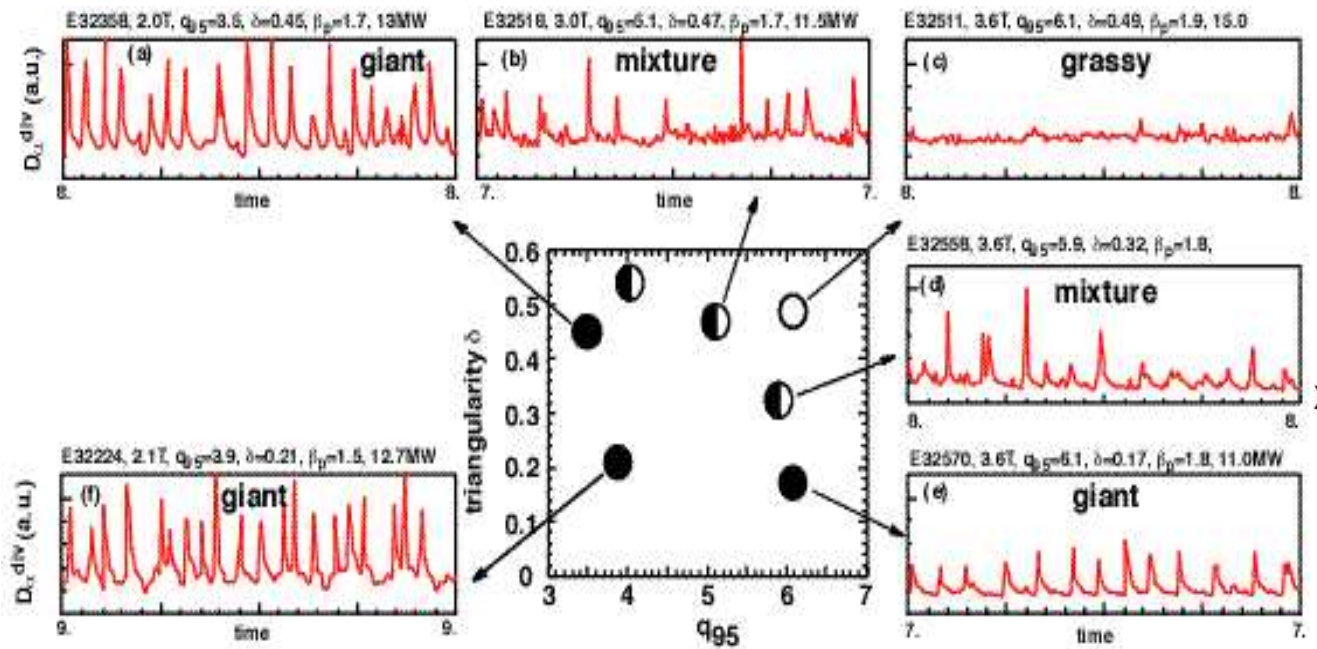
Calculated eigenmode structure



- Predicted radial mode width consistent with ELM affected area, both extend beyond pedestal
- Mode localized on outboard side, consistent with observations in divertor balance experiments
- **Mode width set mainly by extent of high p' region, but also expands at low n , low q , low triangularity, low S .**

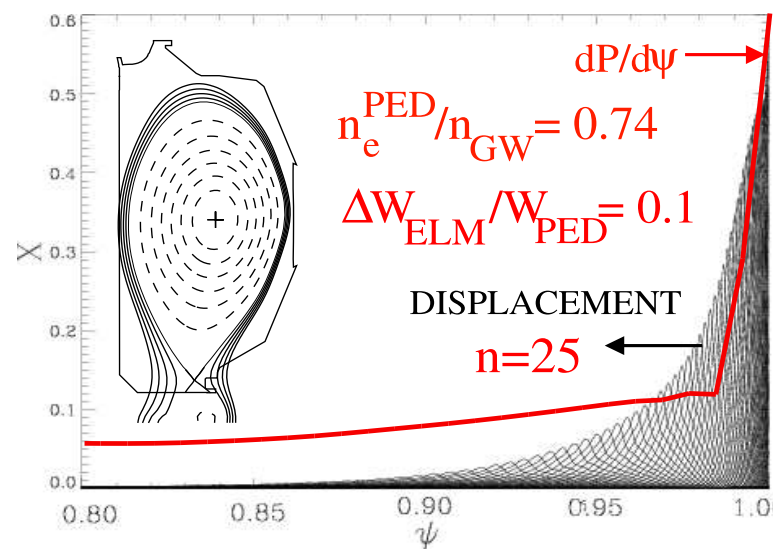
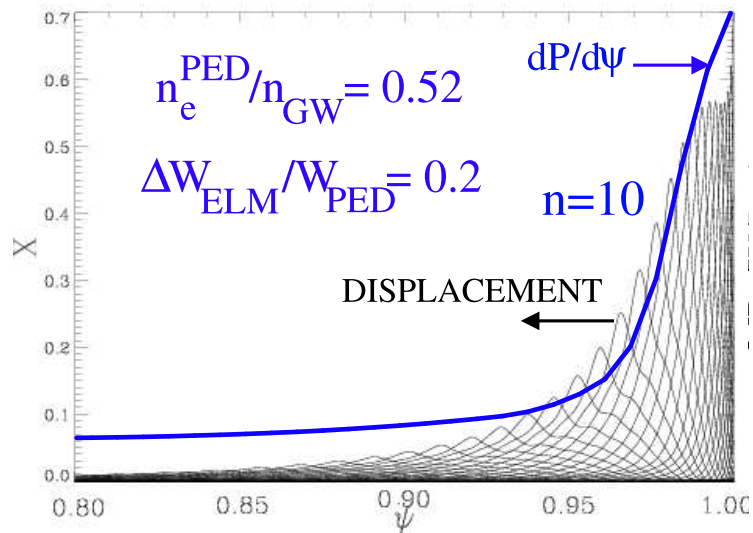
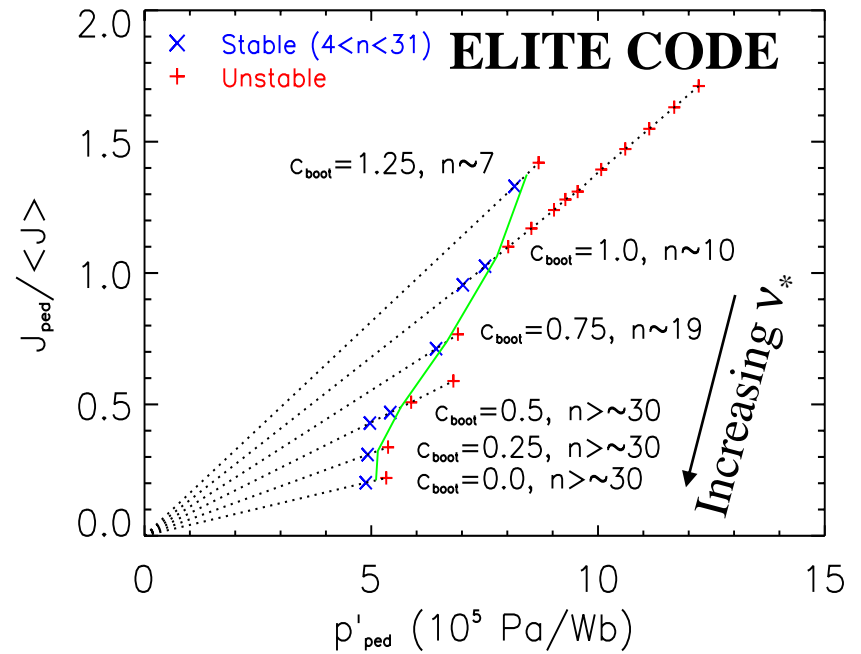
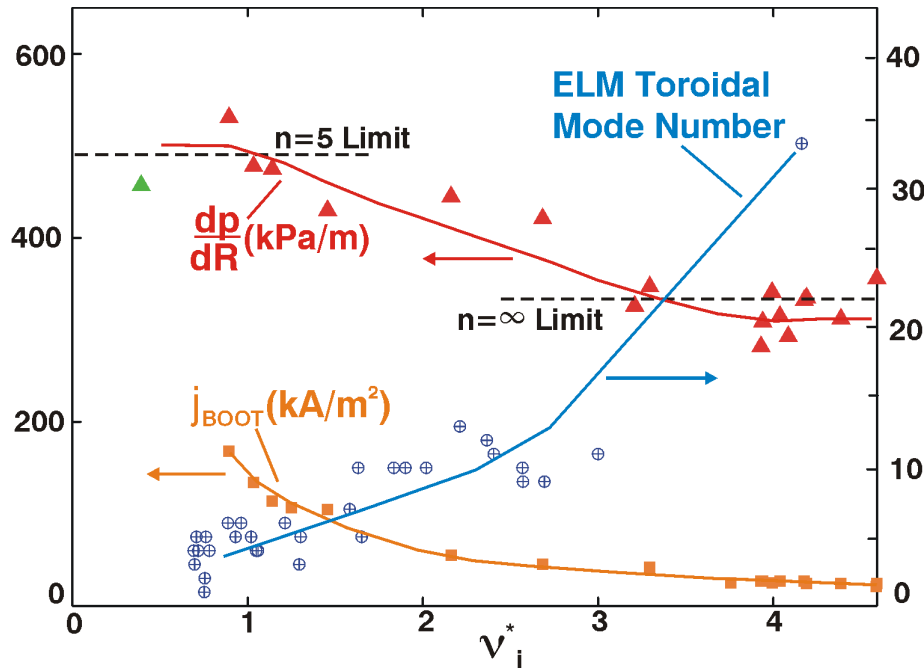
ELM size (energy loss) correlated with peeling-ballooning eigenmode radial in JT-60U high triangularity discharges

- Giant ELMs ~ 100 Hz, small amplitude “grassy” ELMs ~ 500-1000 Hz
- At intermediate δ and q_{95} mixtures of giant and grassy ELMs
- Unstable edge modes in grassy elm discharges have narrow radial mode width (ELITE Code).

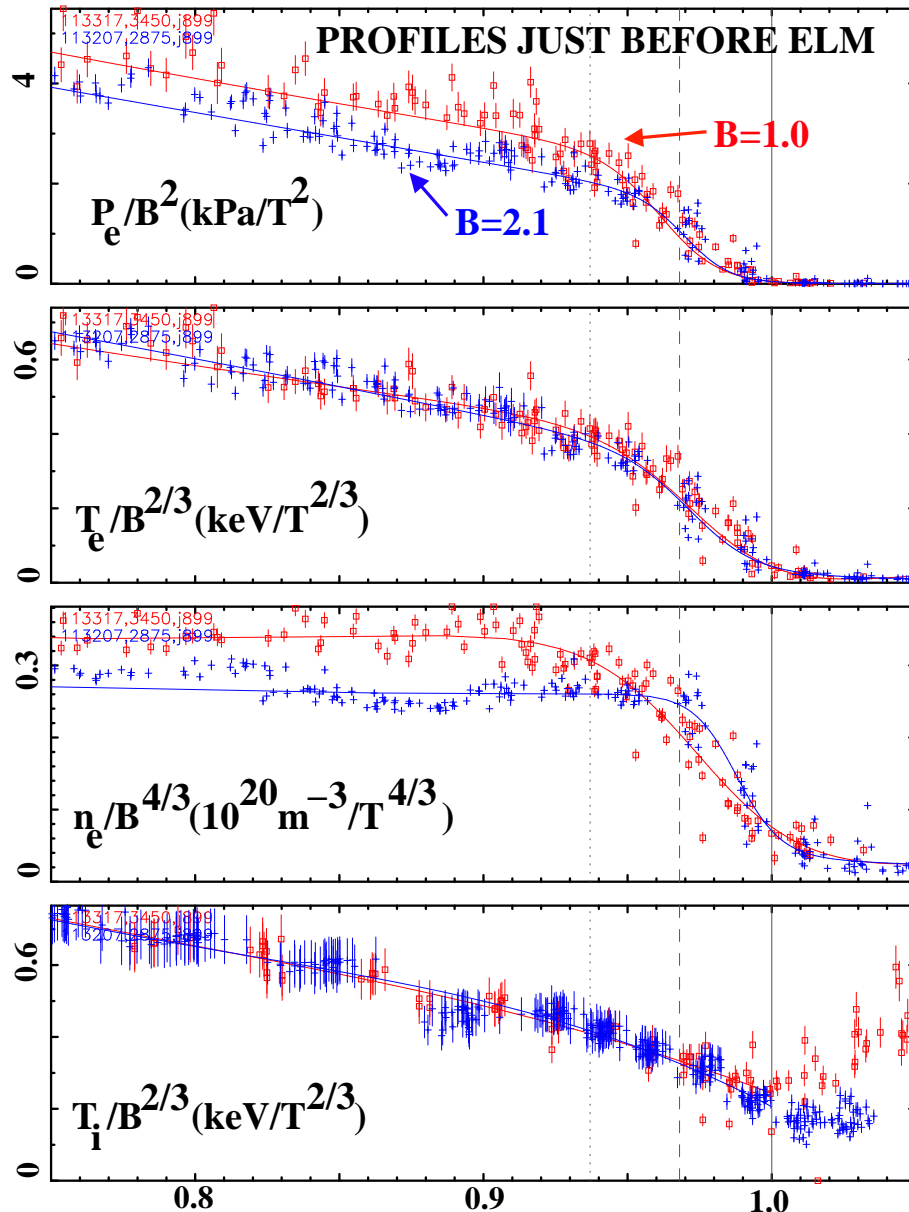


LL. Lao, et. al, Nucl. Fusion, 41 295 (2001).

Reduced $\Delta W_{ELM}/W_{PED}$ at high n_e, v_* correlated with reduced mode width from increased mode number and reduced Δ



Expansion of the Δ_n at low B with increased λ_N may lead to increased Δ_p and ELM size.

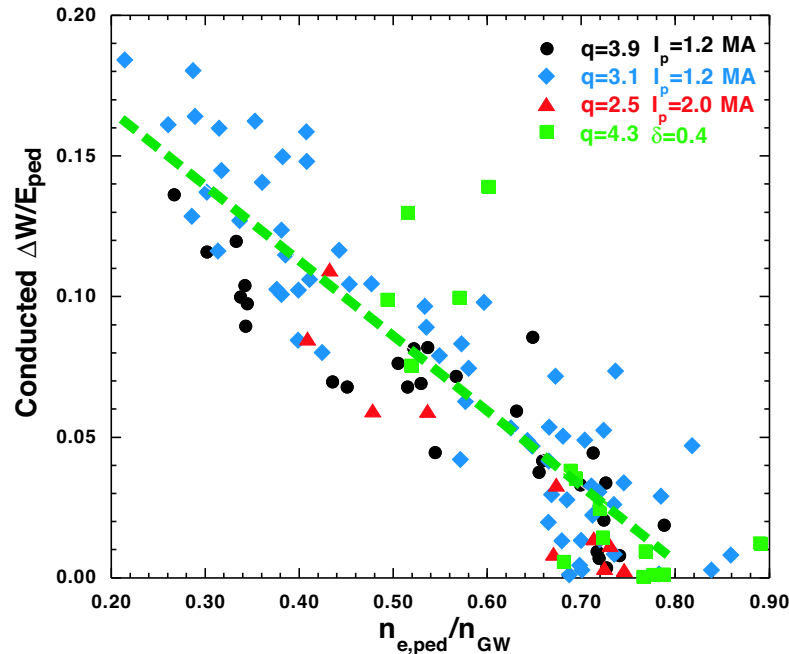


- Eigenmode width of intermediate n PB mode is correlated with ELM size.
- Eigenmode width increases with the extent of the steep gradient region.
- At low field (low density) where neutral penetration is enhanced $\Delta W_{\text{ELM}}/W_{\text{PED}} \approx 30\%$ compared to 12% at high field.

Reduction in $\Delta W_{\text{ELM}}/W_{\text{PED}}$ at high n_e mainly due to reduced conductive loss

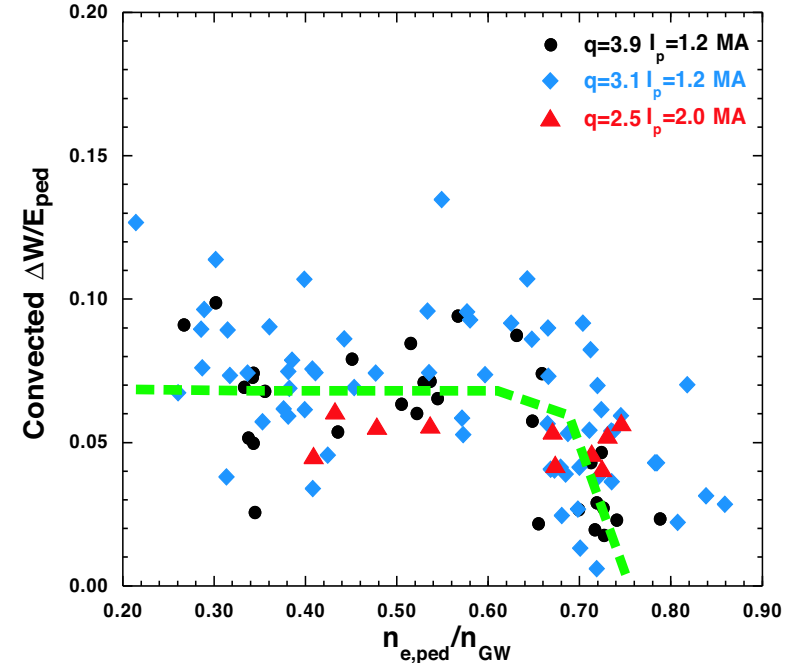
Conducted ELM Energy: $n\Delta T$.

$\Delta T/T$ decreases with increasing n



Convected ELM Energy: $T\Delta n$.

$\Delta n/n$ relatively fixed with n



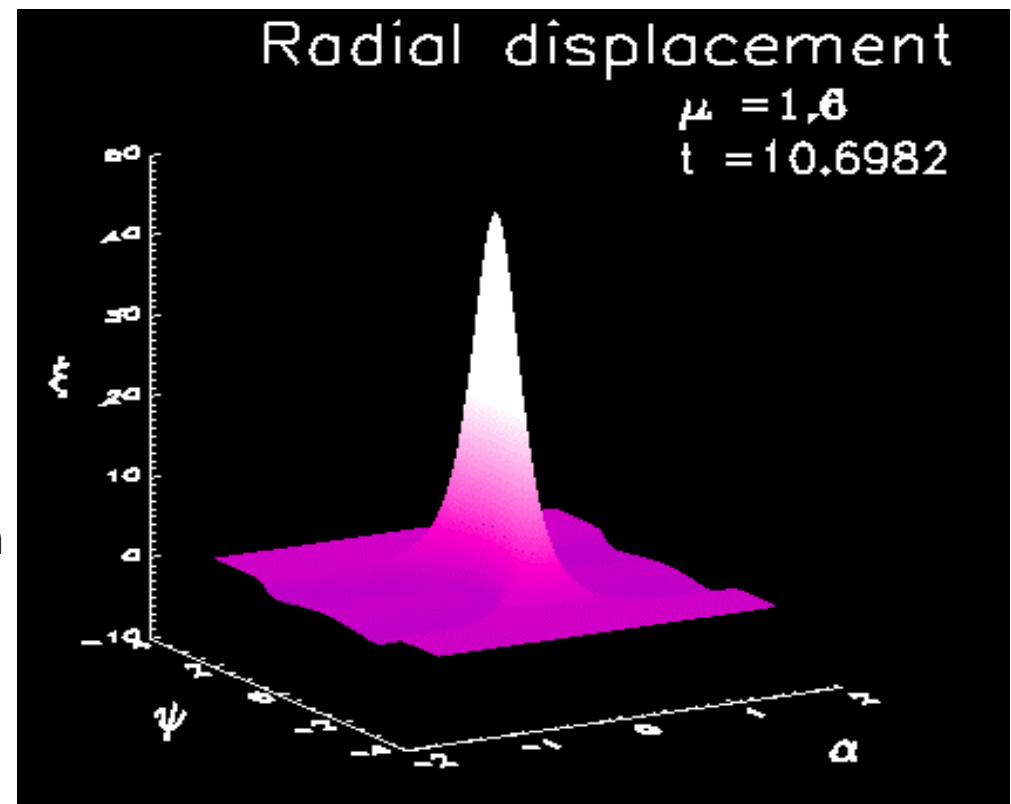
- Do SOL conditions play a role in setting ELM energy loss ?
 - Very high parallel conduction along field lines => energy loss may be limited by conduction through sheath at divertor plate
 $\Delta T/T \sim (\tau_{\text{ELM}} - \tau_{\parallel}) T^{1/2} n_{\text{DIV}}/n_{\text{PED}}, \tau_{\text{ELM}} \approx \tau_{\parallel} = L_{\text{C}}^{\text{DIV}}/c_{\text{S}}$
 - But also particle loss should change $\Delta n/n \sim (\tau_{\text{ELM}} - \tau_{\parallel}) T^{1/2}$

A.W. Leonard

Non-linear ballooning theory: a model for ELMs

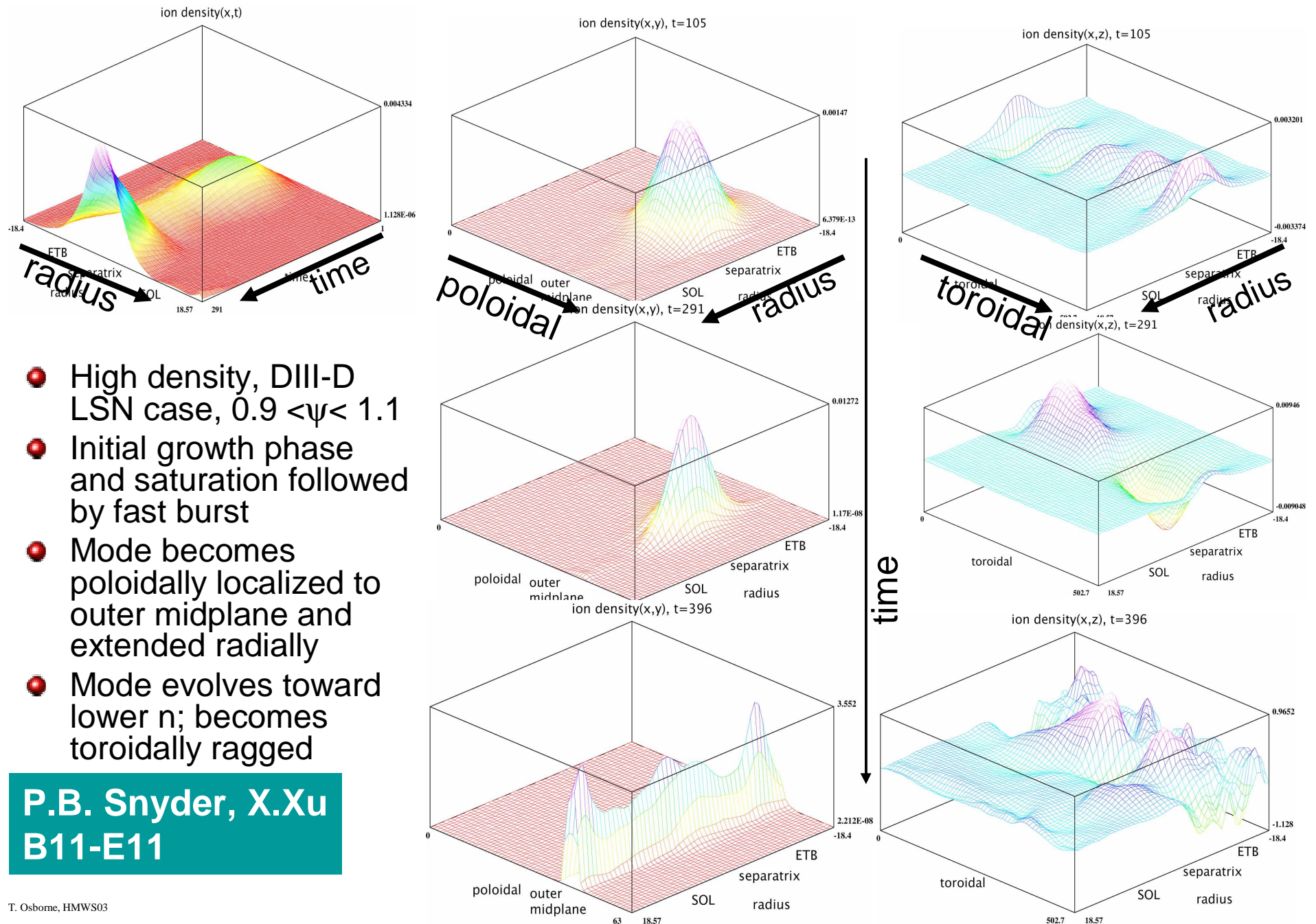
- Non-linear evolution of ballooning modes previously studied in situations with “ends” of the field lines fixed
- In new work field line can wrap many times around (ie is effectively infinitely long)
- Explosive growth of a “finger” is predicted at some time $t=t_0$, but the rate depends on shape through the Mercier stability index, D_M
- A possible model for the ELM is
 - A ballooning mode, destabilised in the pedestal, results in a hot finger of plasma which pushes out into the SOL
 - Heat leaves the finger (eg by diffusion or reconnection), deposited in the SOL
 - The effect of the magnetic shear in the SOL would be to spread the heat load more uniformly onto the targets (toroidally)

H. Wilson



Non-linear mode structure in the two coordinates perpendicular to the field line, the structure is extended along the field line

Preliminary case study of edge instability dynamics with BOUT (I)

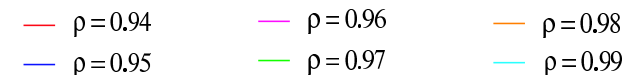
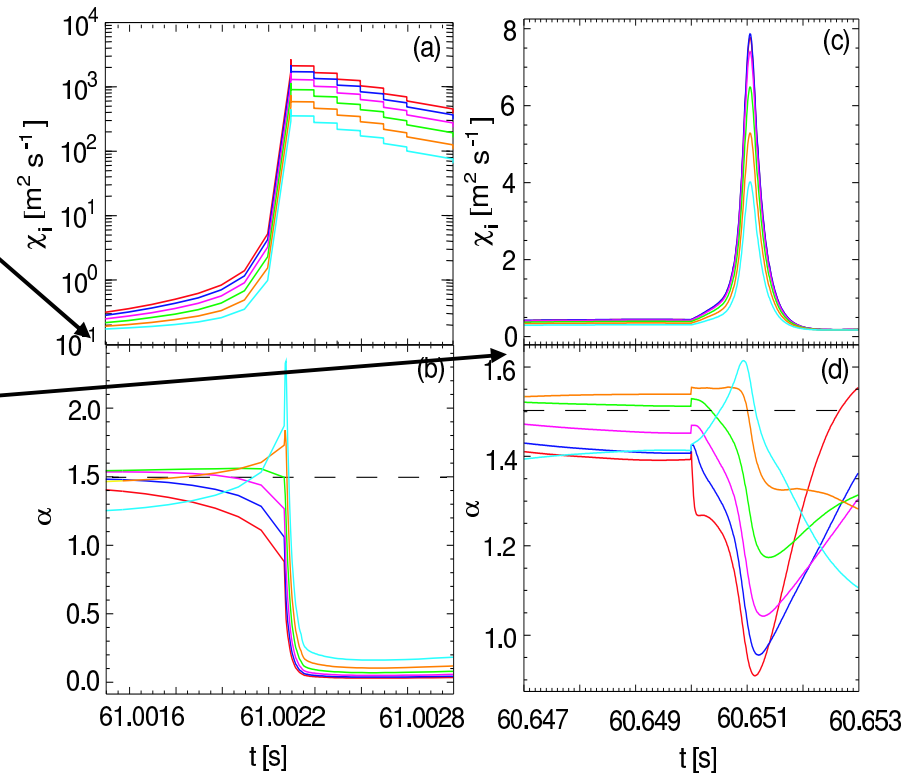
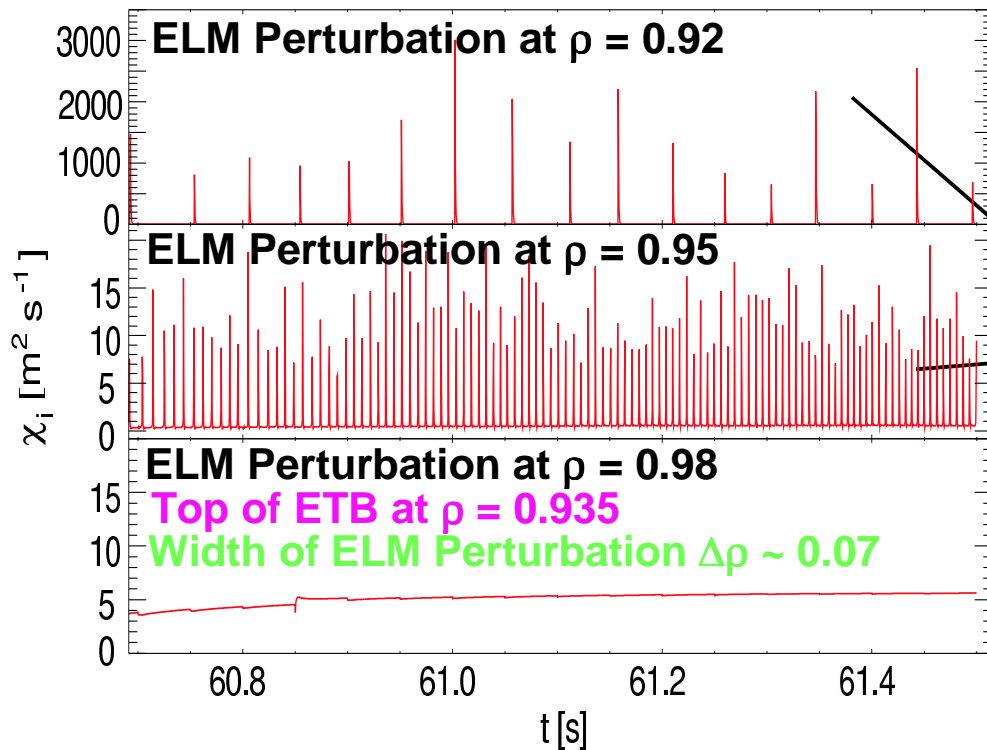


- High density, DIII-D LSN case, $0.9 < \psi < 1.1$
- Initial growth phase and saturation followed by fast burst
- Mode becomes poloidally localized to outer midplane and extended radially
- Mode evolves toward lower n ; becomes toroidally ragged

P.B. Snyder, X.Xu
B11-E11

Transport simulations including ELM show importance of mode radial extent and propagation of the unstable zone

- Gaussian ELM perturbation, $\Delta\rho \approx 0.07 \sim 2 \times \text{ETB width}$ (PB-mode)
- ELM perturbations deeper in the plasma drive larger lower frequency ELMs
 - Transport from inner surfaces drive outer surfaces over the stability limit
 - Unstable outer surfaces keep mode growing on now stable inner surfaces
- ELM perturbations with initial large amplitude close to the separatrix result in continuous transport rather than ELM



J. Lonroth – C14

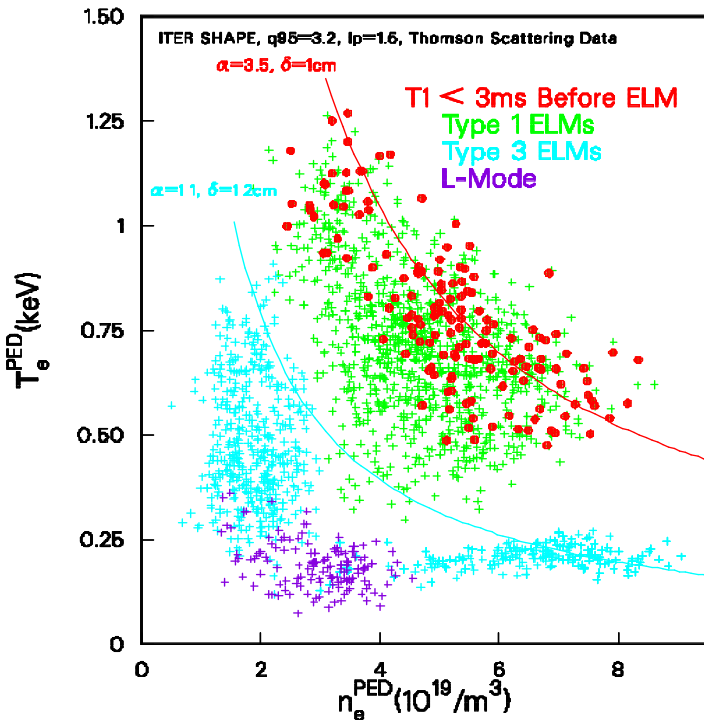
Understanding Type I ELM Effects

- Linear eigenmode width correlated with ELM size but nonlinear simulations show mode becomes radially extended with structure not closely related to linear mode
- SOL physics might also play a role in ELM energy loss
- Transport simulations including ELM models indicate transport during the ELM can spread the region of instability
 - A full understanding of Type I ELM loss will require nonlinear stability physics coupled to a transport simulation

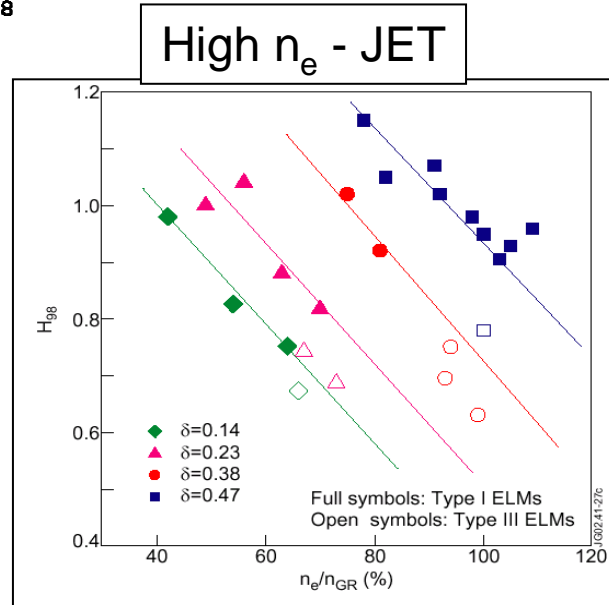
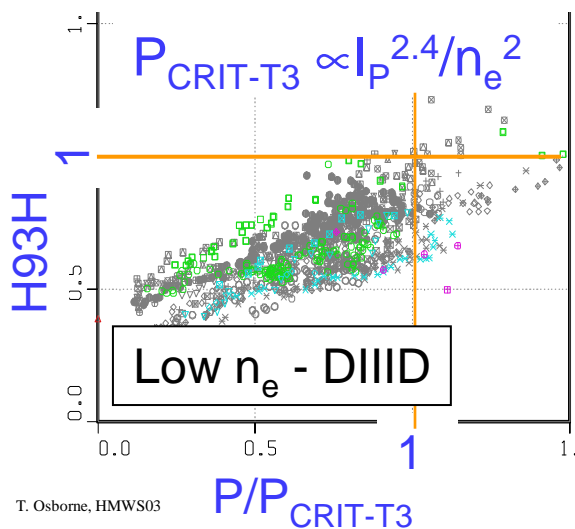
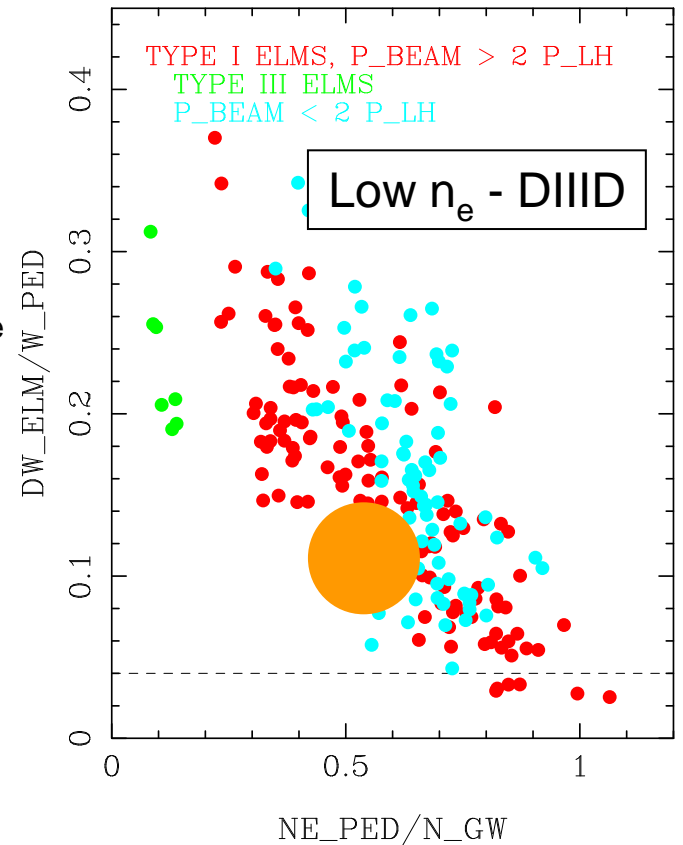
Small ELM Regimes

- Type III ELMs: Most tokamaks
- Type II ELMs: AUG, DIII-D
- Grassy-ELMs: JT-60U

Type III ELMs: Something to avoid ?



- Low and high n_e
- $\Delta W_{\text{ELM}} <$ Type I at same n_e
- $p'_{\text{PED}}, p_{\text{PED}} \Rightarrow H$ reduced on low n_e branch
- H reduced at high n_e consistent with Type I scaling
- Medium n , slowly growing precursors



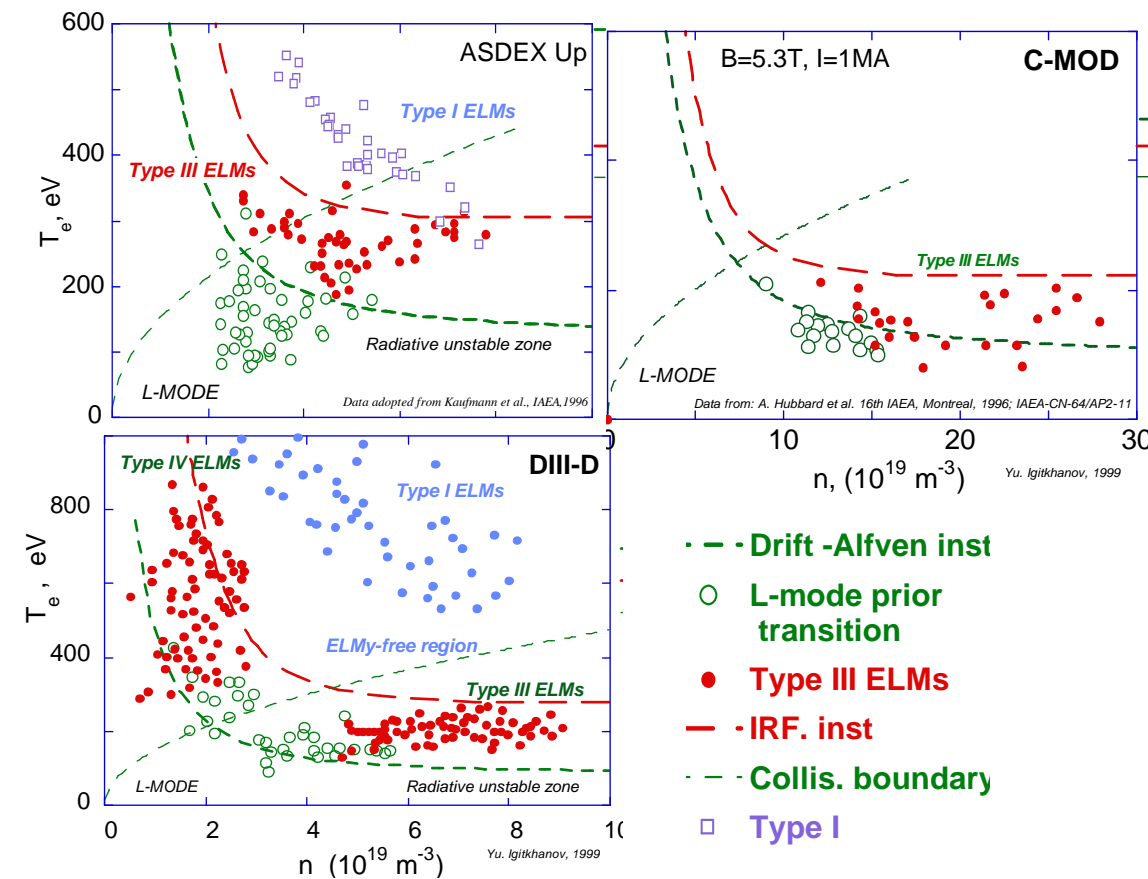
G Saibene – B22
 Phys.Control.Fusion 44,1769
 R. Sartori, submitted to
 PPCF

Transition conditions from Type III to Type I regimes consistent with suppression of RIF instability

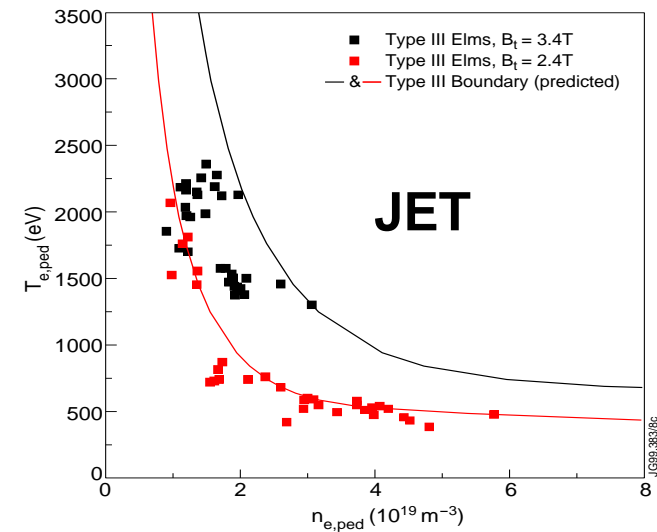
$$T_{0cr} \propto (c_\tau^2 c_F)^{6/5} q^{18/5} R^{-2/5} B_0^2 / A^{8/5} s^{12/5} n_0^{6/5} \quad \text{for } \lambda_e > c_v q R$$

$$T_{0cr} \propto (c_\tau^2 c_F c_v)^{6/17} q^{24/17} R^{4/17} B_0^{10/17} / A^{8/17} s^{12/17} \quad \text{for } \lambda_e < c_v q R$$

- V_{ExB} suppression of resistive interchange instability with magnetic flutter consistent with T3 \leftrightarrow T1 boundary on several tokamaks
- Magnetic shear important

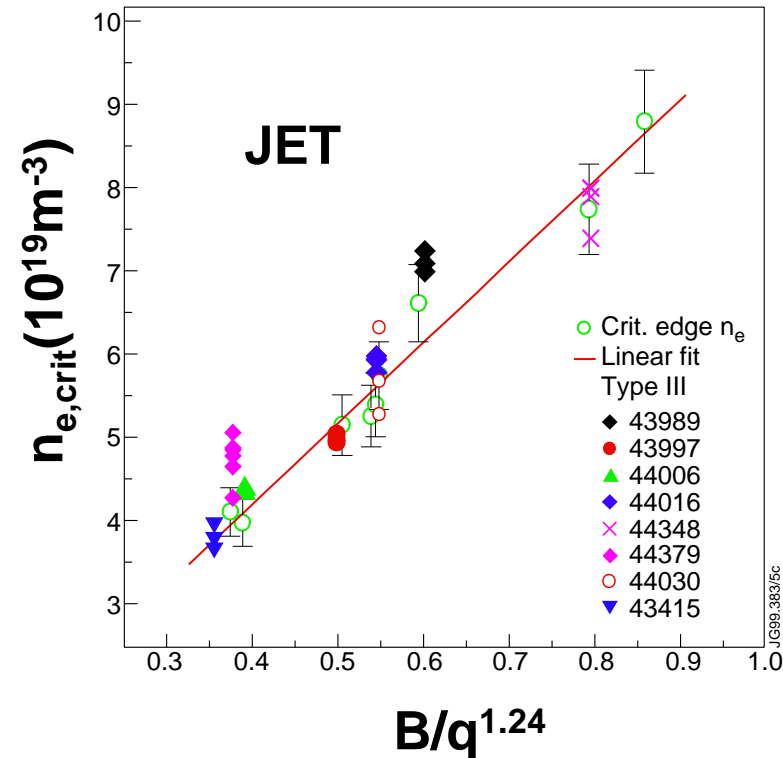
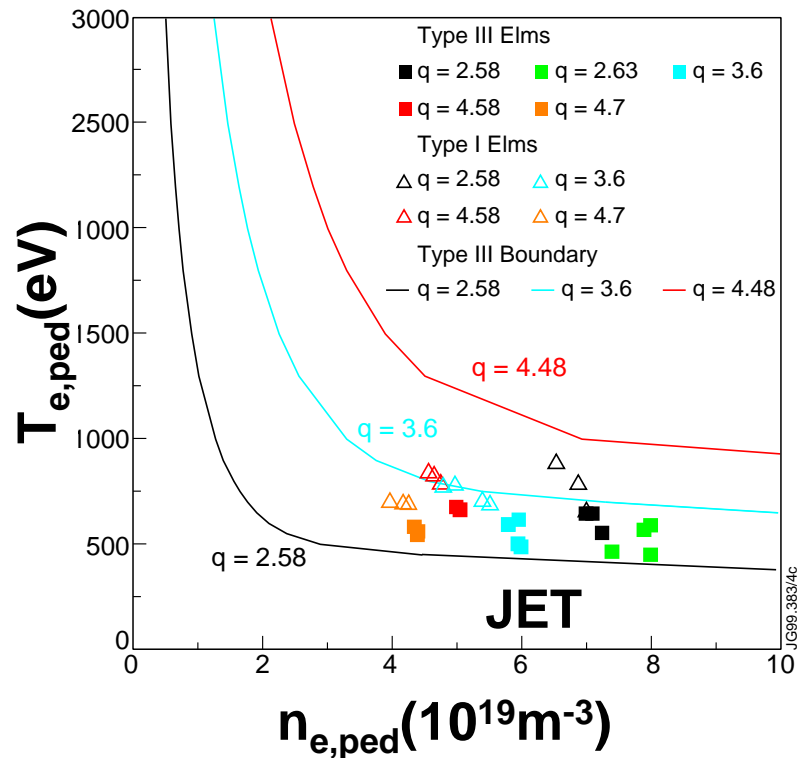


Yu. Igitchanov,
Contrib. Plas. Phys. 40, 368;
R. Sartori, submitted to PPCF



q dependence of high n_e type III boundary is more consistent with resistive ballooning

- T_{CRIT} does not vary with q in a B_T scan on JET while RIF model predicts a significant change
- Data consistent with Chankin, Saibene¹ resistive ballooning mode scaling, $n_{e,\text{crit}} \sim B_T f(s) / q^{5/4} R^{3/4} Z_{\text{eff}}^{1/4}$

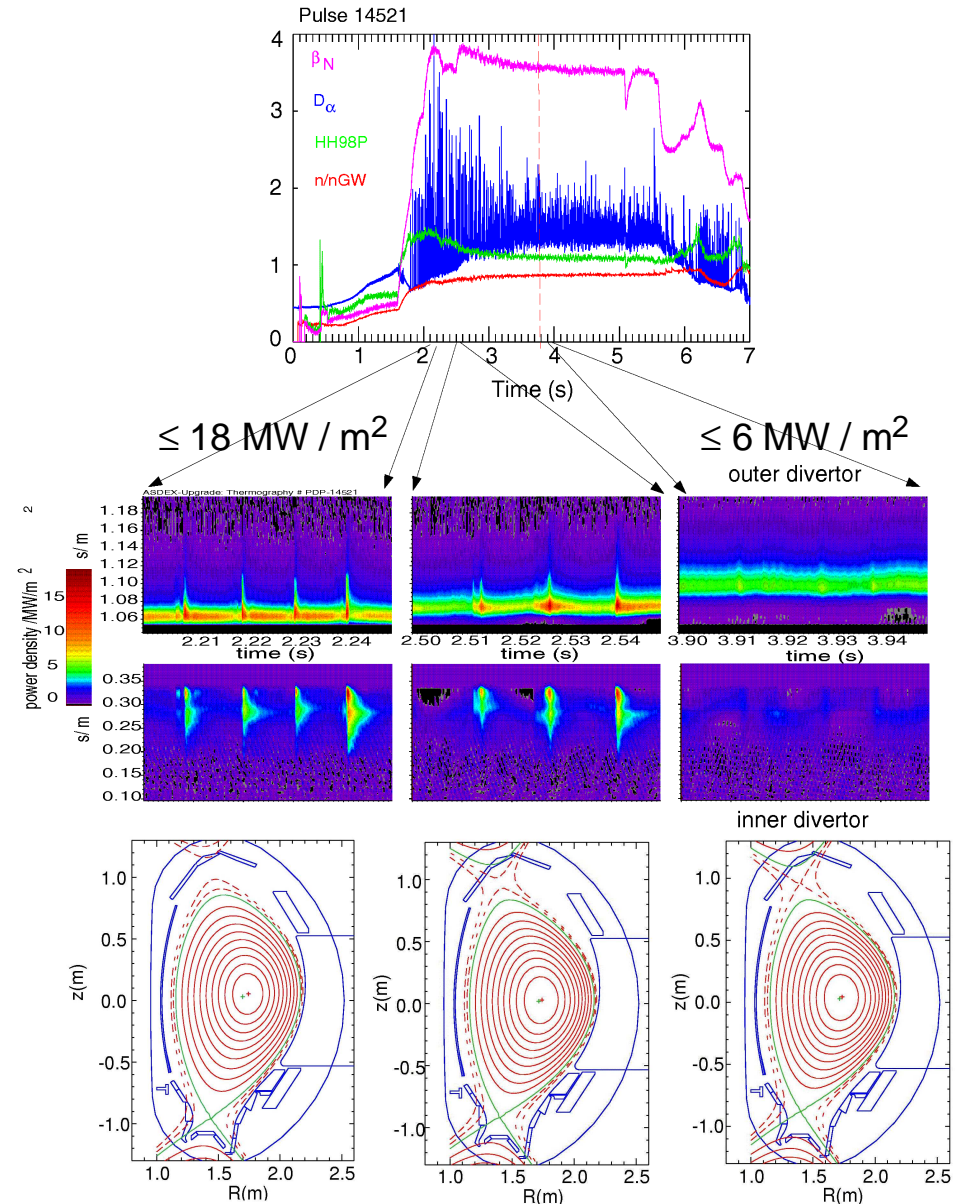


R. Sartori, submitted to PPCF

Type II ELMs (ASDEX-Upgrade)

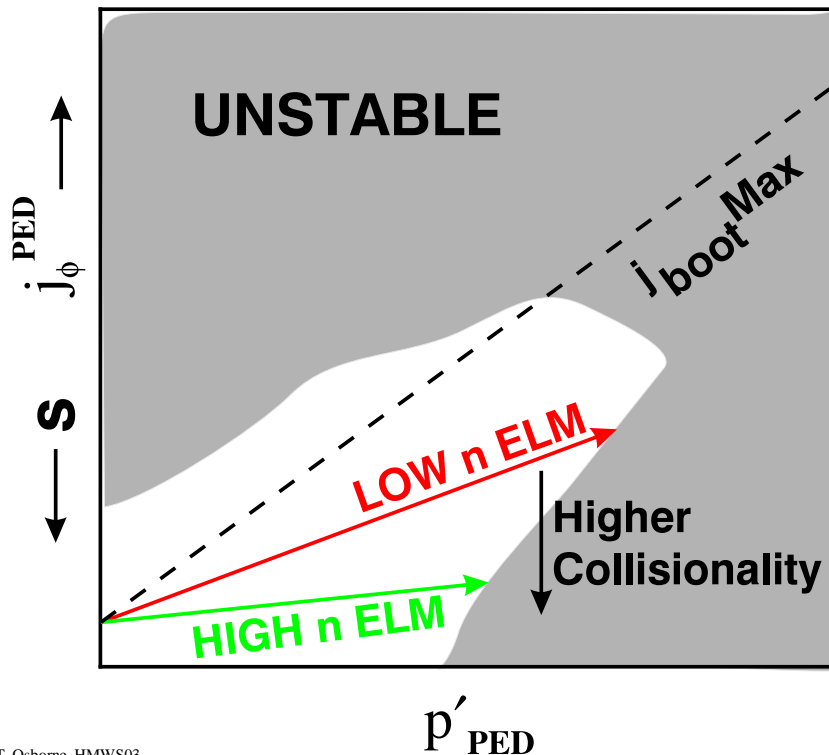
- Peak divertor heat loads significantly reduce compared to Type I ELMs
- Requirements
 - High $\delta > 0.35$
 - Higher $q_{95} > 3.5$
 - Near double null operation, $dr_{sep} < 2.0$
 - Higher density $> 0.5 n_{GW}$

O. Gruber, IAEA 02

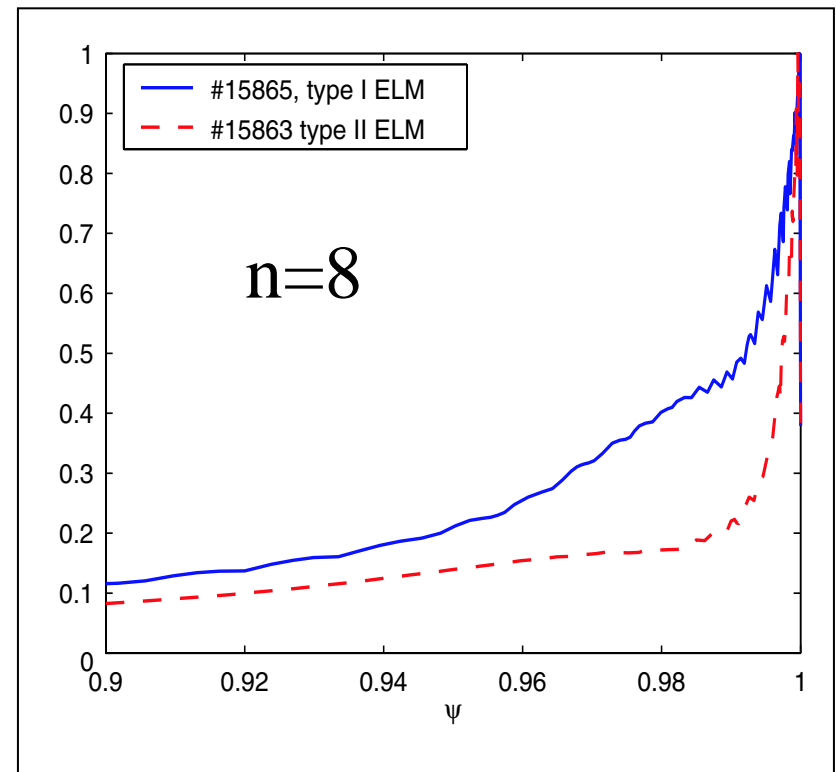


Type II Edge Stability

- High q and closeness to dnull narrows PB eigenmode
- High density moves to higher n also narrowing PB eigenmode.



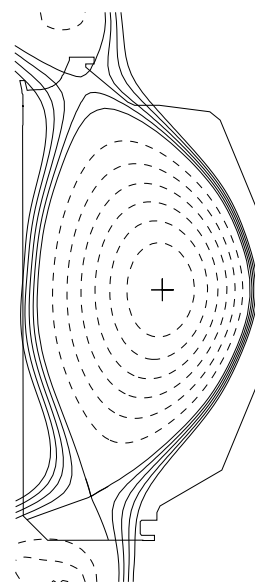
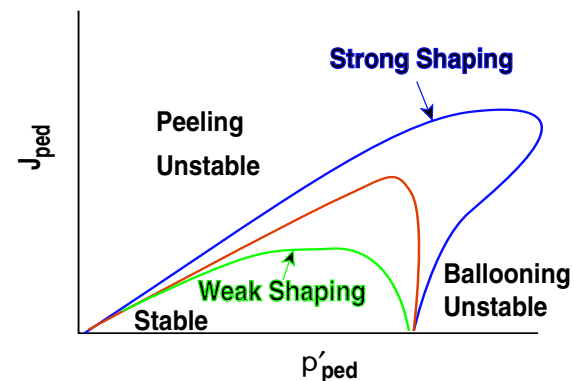
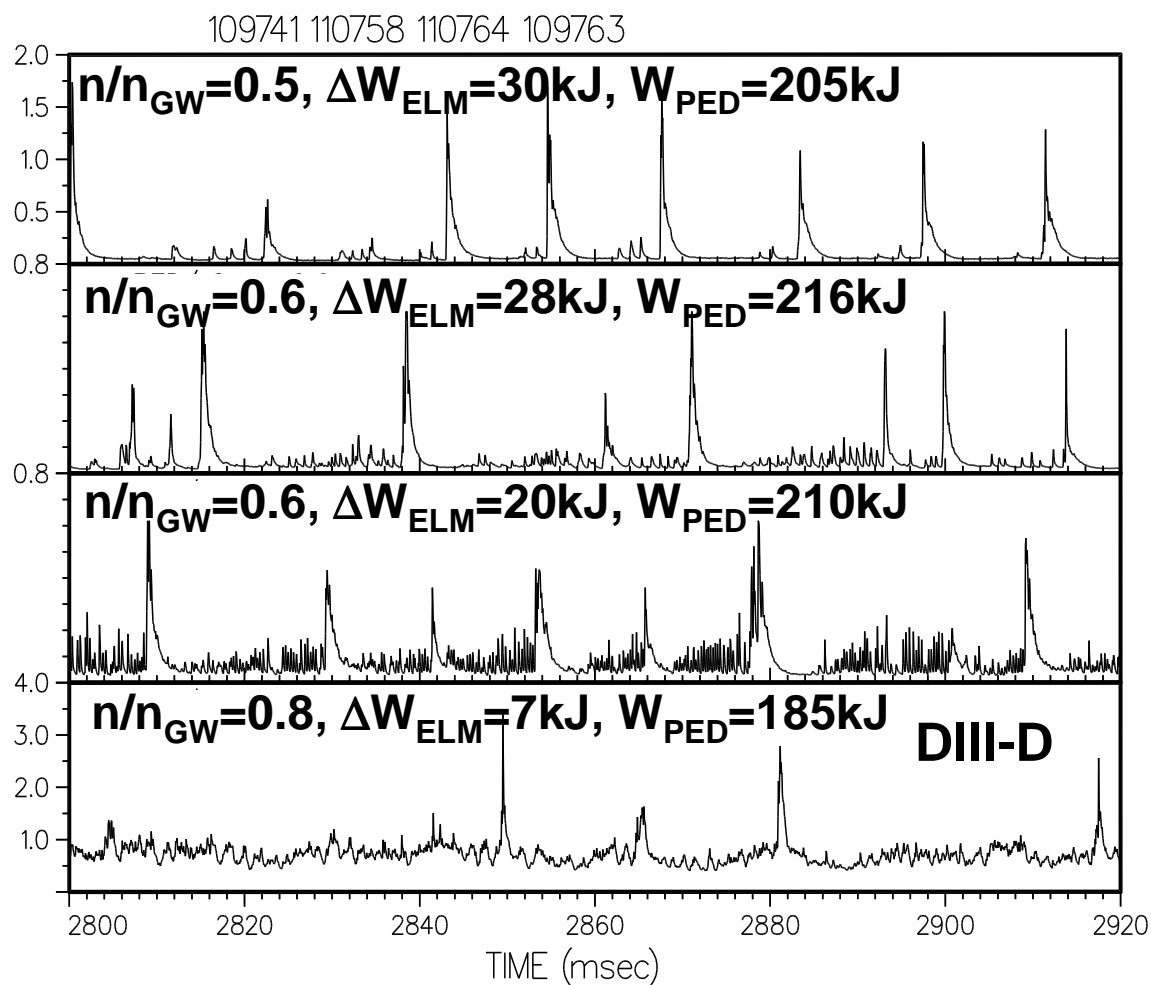
Type II discharge which is closer to Dnull has narrower eigenmode



S. Saarelma, NF 43, 262

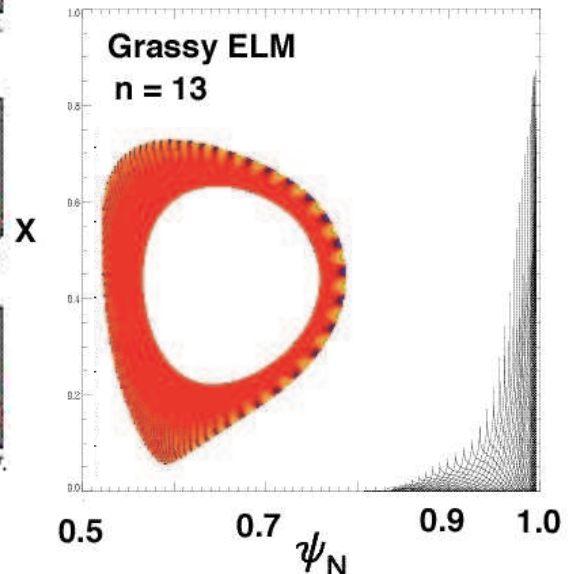
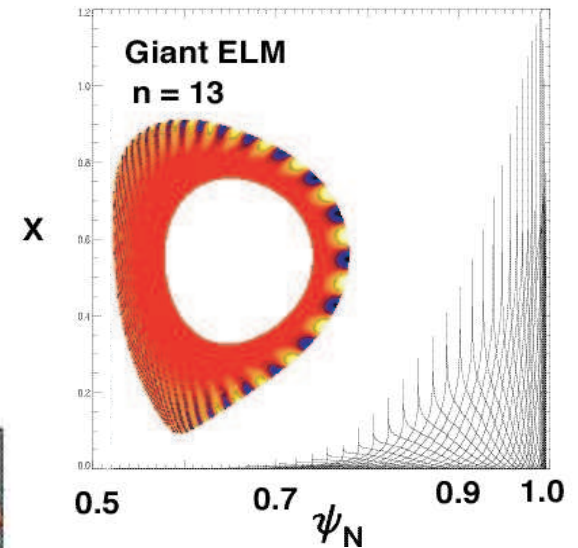
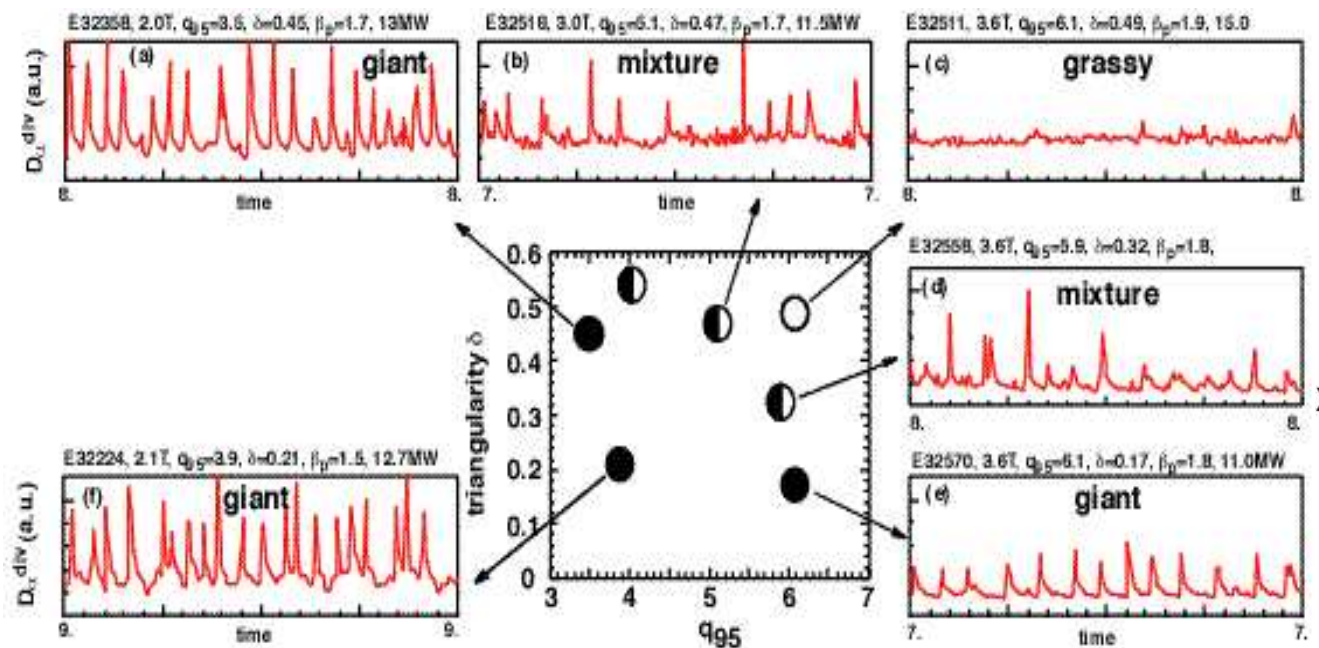
Type II ELMs become more frequent and Type I ELMs more irregular and smaller amplitude as density is raised

- As n_e increases discharge goes through mixed Type I, II phase
- On AUG HF magnetic fluctuations associated with Type II
- Type I and Type II in different regions of pedestal ?



ELM size (energy loss) correlated with peeling-ballooning eigenmode radial in JT-60U high triangularity discharges

- Giant ELMs ~ 100 Hz, small amplitude “grassy” ELMs ~ 500-1000 Hz
- At intermediate δ and q_{95} mixtures of giant and grassy ELMs
- Unstable edge modes in grassy elm discharges have narrow radial mode width (ELITE Code).



LL. Lao, et. al, Nucl. Fusion, 41 295 (2001).

Small ELM Regimes: Summary, Conclusions

- Type II and Grassy ELMs pass through phase where small ELMs are mixed with Type I
 - Unclear how this would fit into PB picture
 - Small ELM more edge localized where J_{BS} is small, shaping is strong and ballooning limit is low ?
 - Perhaps Type II, Grassy another instability as Type III ?
 - Same type of behavior observed in ergodic limiter discharges on DIII-D
- Low density Type III has lower pressure at low q than Type I but perhaps high density Type III may scale to ITER

ELM free regimes without impurity or density accumulation

- EDA-H-mode: CMOD, DIII-D (transient),
- QH-mode: DIII-D ([Burrell – B15](#)), Asdex-Upgrade ([Suttrop – B17](#)), JET ([Suttrop – B17](#)), JT-60U ? ([Sakamoto – D6](#))
- HRS-H-mode: JFT-2M ([Kamiya - B14](#))

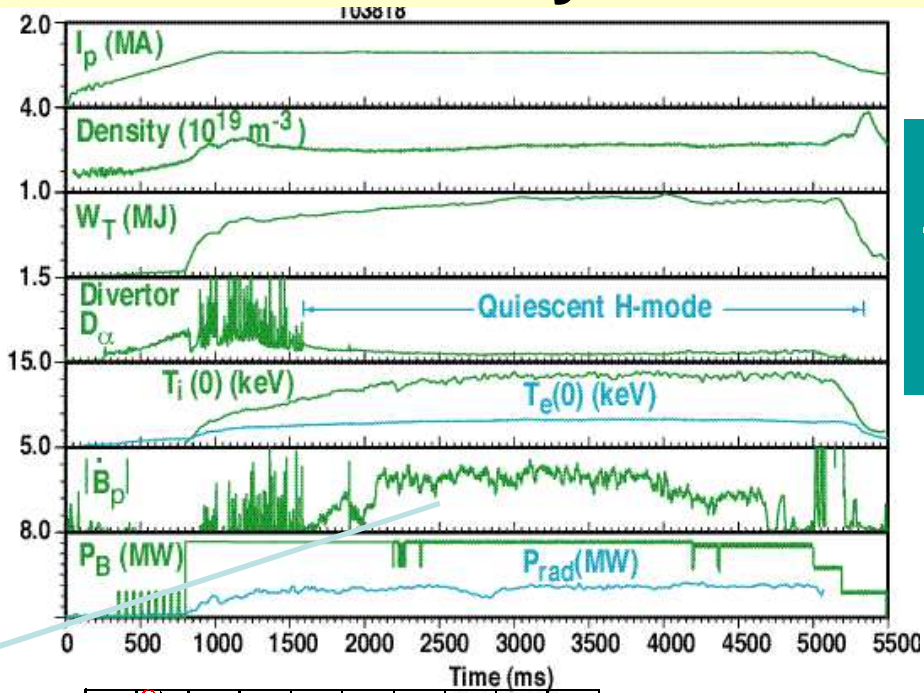
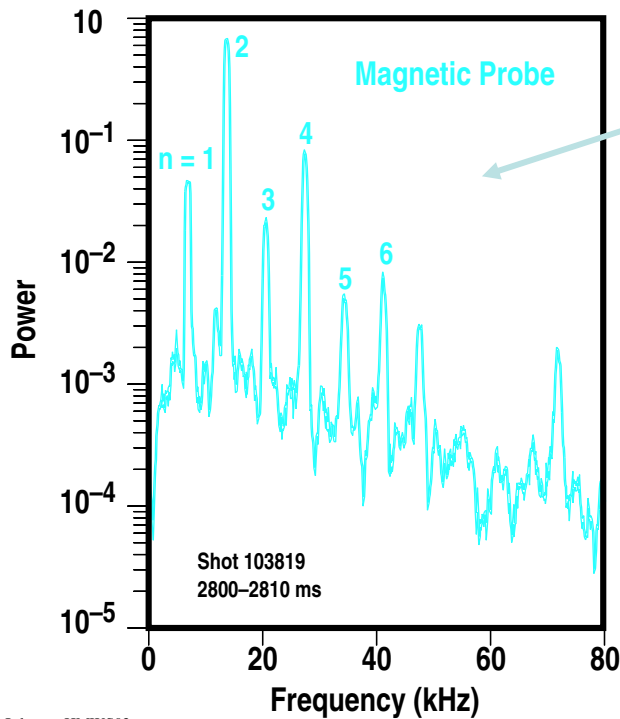
K. Kamiya-B14

| | <i>EDA (C-Mod)</i> | <i>QH (DIII-D)</i> | <i>HRS (JFT-2M)</i> | <i>Grassy (JT-60U)</i> |
|----------------------------------|---|---|---|--|
| Increase D_a level in divertor | Yes | Yes | Yes | No |
| Frequency | 60-200 kHz | 6-10 kHz (n=1) | ~50 kHz (n=1) | No coherent mode |
| Toroidal mode number | n=1 | Multiple variable mix n=1-10 | n=1 for LF-mode n~4-8 for HF-mode | |
| Energy confinement | $H_{89P} \sim 1.9$ | $H_{89P} \sim 2$ | $H_{89P} \leq 1.6$ | $H_{89P} \sim 2$ |
| Particle confinement | $t_{\text{impurity}} \sim 2-3t_E$ | $t_p < t_p^{\text{ELM-free}}$ | $t_p < t_p^{\text{ELM-free}}$ | $t_p \sim t_p^{\text{Type I}}$ |
| Dependence on q_{95} | $q_{95} > 3.7$ | $3.7 \leq q_{95} \leq 5.8$ | Favored at high q_{95} , but even at $2 < q_{95} \leq 3$ | Favored at high q_{95} and δ , q_{95} can reduce (6 to 3.8) with increasing δ (0.35 to 0.55) |
| Dependence on δ | EDA: $0.35 < \delta < 0.55$ ELM-free: $\delta < 0.35$ and $0.55 < d$ | $0.16 \leq \delta \leq 0.75$ | HRS: $0.35 \leq \delta \leq 0.75$ ELMy: $\delta < 0.35$ | |
| Dependence on n_e | Higher target n_e ($> 1-2 \times 10^{20} \text{ m}^{-3}$) | Lower density and neutrals with cryopumping | $n_e/n_{\text{GW}} \geq 0.4$ | $n_e/n_{\text{GW}} \leq 0.6$ |
| Dependence on neutrals | Favored at high neutral pressure | | Favored at high neutral pressure | Low recycling |
| Heating | ICRF/OH | Ctr-NBI (only) | NBI | NBI |
| Compatibility with ITB | Yes | Yes (QDB) | Yes | Yes (high- b_p H) |

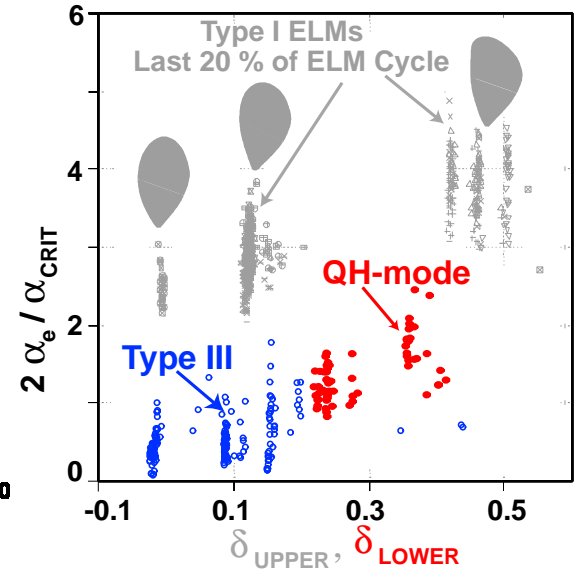
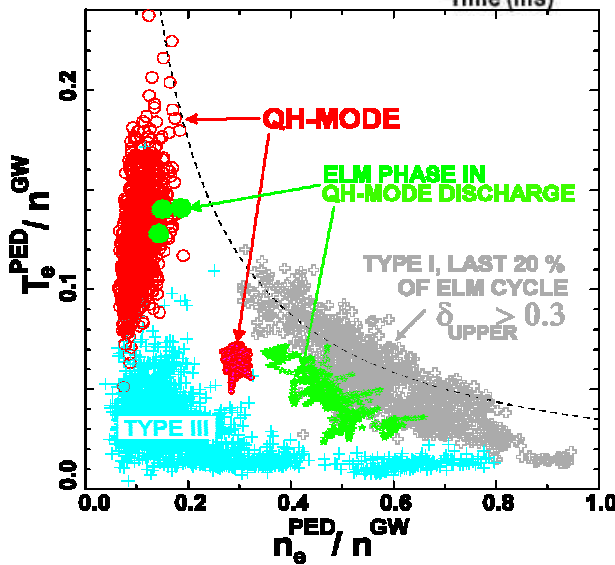
ELM free QH-mode with edge harmonic oscillation (EHO) has high H and no density accumulation.

- Counter Injection
- Low density with divertor pumping
- Large outer gap
- H89P to 2.4
- β_N to 2.9
- $\beta_N H$ to 7

DIII-D

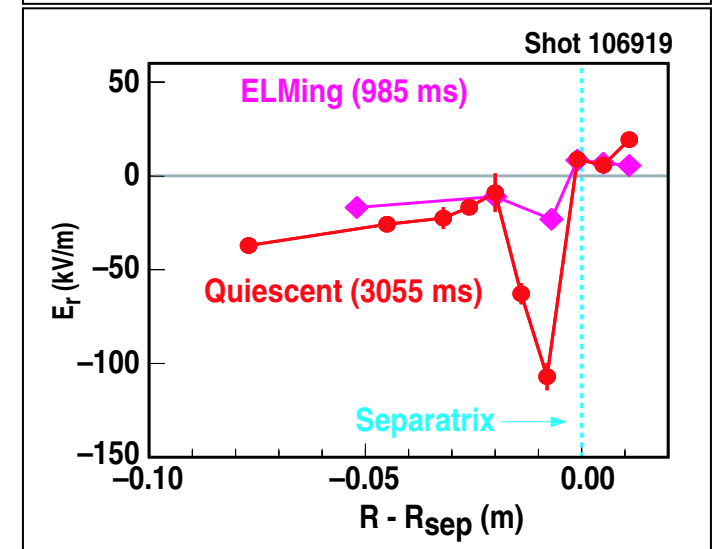
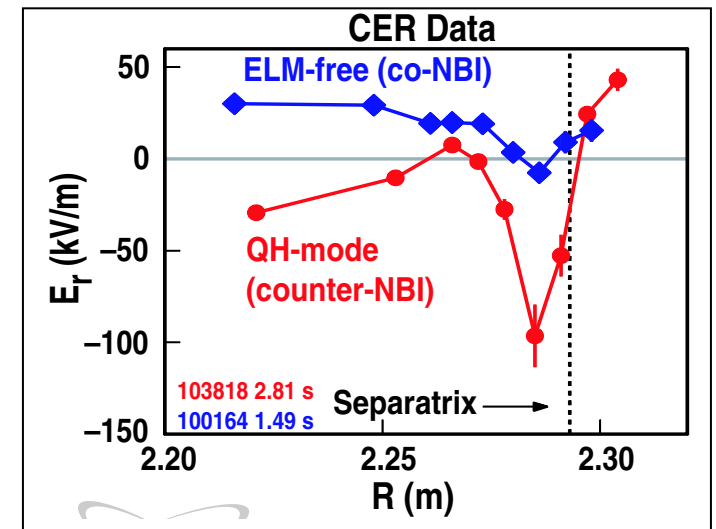
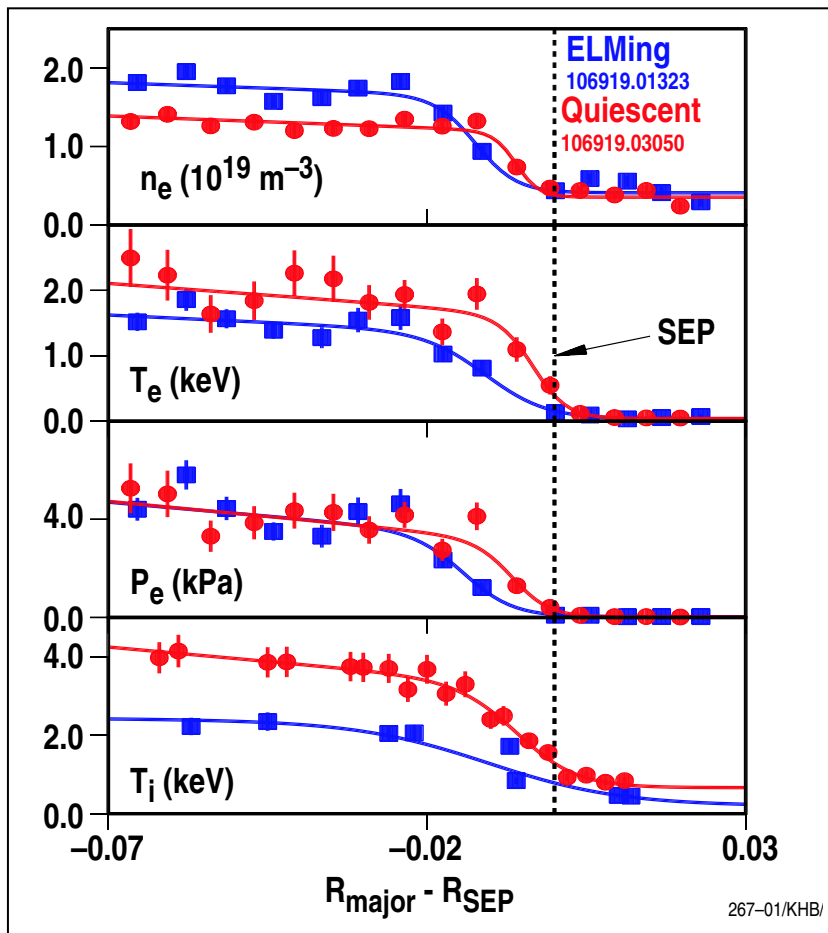


K. Burrell
- B15
W. Suttrop
- B13, B17



QH-mode discharges have large E_r wells

- p' in QH-mode comparable to ELMing H-mode
- E_r well very large in QH-mode
 - Could the larger velocity shear stabilize the ELM ?



K. Burrell – B15

ELM free regimes

- ELM free regimes associated with an edge instability that prevents density and impurity accumulation
- In EDA transport (possibly from the QCM) keeps the pressure gradient below the PB-mode limit
- In QH-mode pressure gradients are similar to ELMing discharges
 - Is the EHO a saturated PB-mode ?
 - Is the high V_{ExB} shear involved in stabilization of the ELMs ?

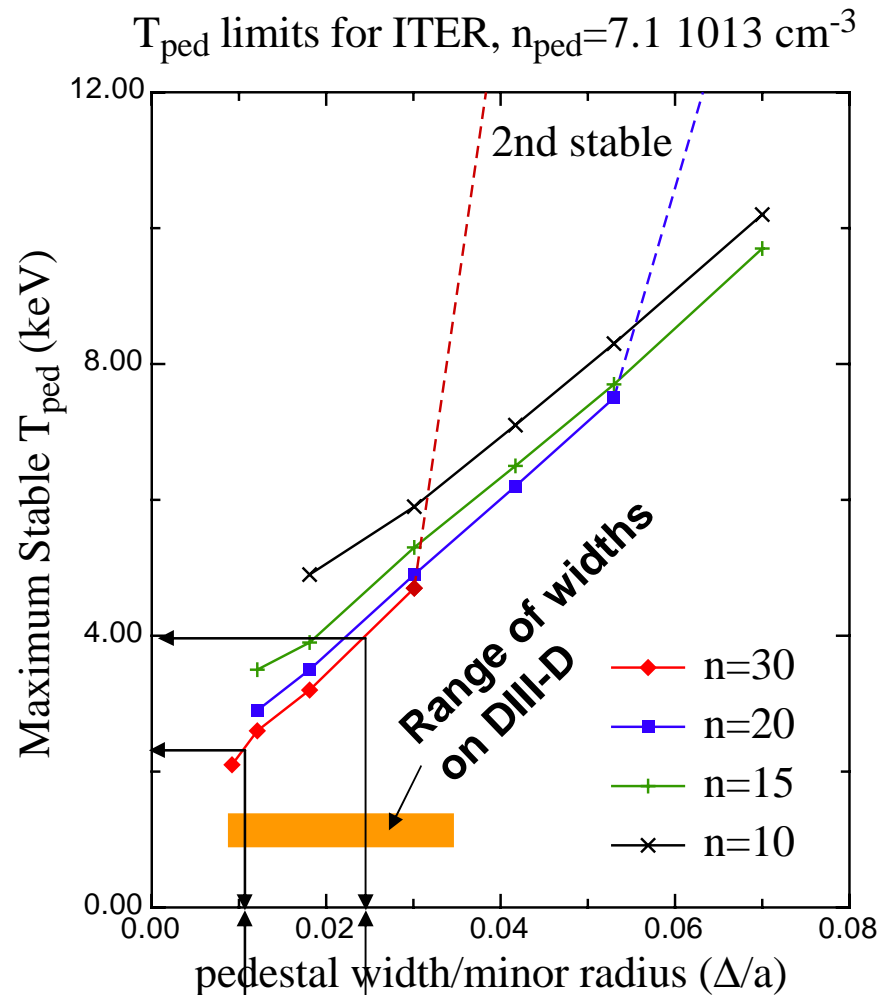
Summary, Topics for Discussion

- Transport barrier width
 - Indications that edge density profile is set by edge neutral source
 - Unclear where ETB is also controlled by edge neutral source
 - Dimensionless scaling experiments and AUG $\eta_e = 2$ suggest neutrals do not control ETB but better neutral modeling or measurements required to resolve this
 - Transport modeling including turbulent transport codes extended to pedestal becoming a reality.
 - Need database of good experimental data through ELM cycle including good estimate or measure of edge current
 - Need to put accurate global MHD constraints into transport codes – or possible fitted expressions from a database of stability calculations
- Edge Stability
 - P-B model for edge stability is consistent with experiments and imposes constraints on pedestal height, which are strong functions of pedestal width, Δ , and plasma shape – MAJOR SUCCESS !

Summary, Topics for Discussion

- Type I ELM size
 - The connection between mode width and ELM size is interesting but nonlinear phase of the instability has much different structure. Presently unclear how the nonlinear development would be tied to the linear structure
 - SOL physics may play a role by limiting the heat flux through sheath formation at the divertor plate
 - More work needs to be done on basic scaling
- Small ELM regimes
 - Type II and Grassy ELMs appear as mixtures with Type I. How does this fit into the stability picture ?
 - Are any of the small ELM regimes scalable to ITER
- ELM free regimes
 - A continuous mode near the separatrix appears to be required for density control.
 - How are these continuous modes related to the ELM instabilities ? Type I precursor \leftrightarrow EHO ?, Type II HF fluctuation \leftrightarrow QCM, modes between Type I on AUG ?

Peeling-Ballooning Stability Plus Core Transport Simulations Sets Minimum Barrier Width



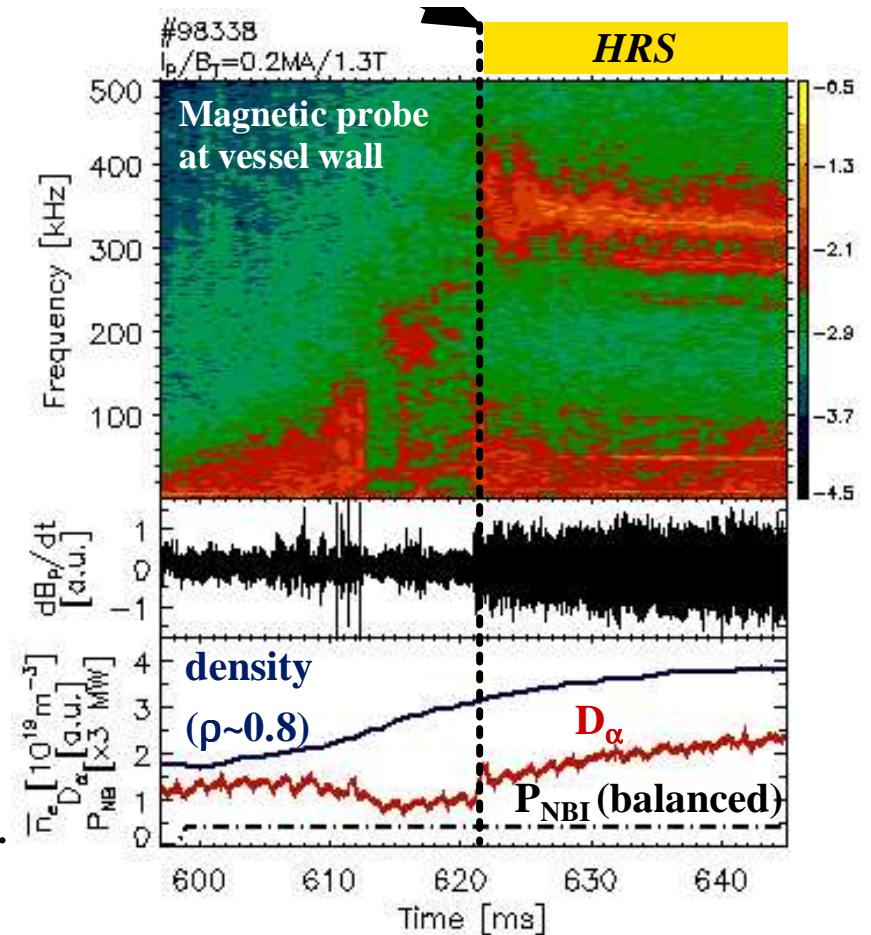
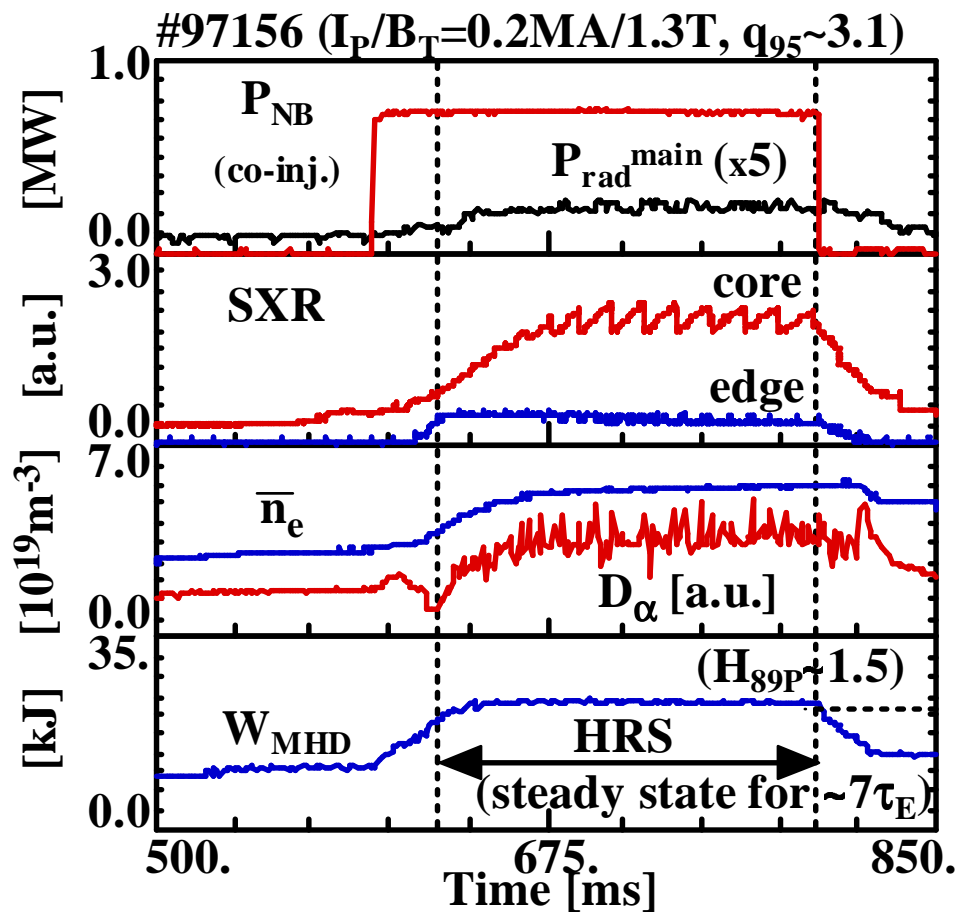
- ELITE code results for simplified equilibrium and Sauter model j_{Boot}
- Stability + temperature requirement for core confinement \Rightarrow minimum transport barrier width
- Existing experiments have widths in the required range

P.B. Snyder
- B11

STABILITY + GLF23 @ $Q=10 \Rightarrow \Delta_{MIDPLANE}/a = 2.5 \%$

STABILITY + MM @ $Q=10 \Rightarrow \Delta_{MIDPLANE}/a = 1 \%$

HRS-H-mode on JFT-2M associated with magnetic fluctuations



K. Kamiya-B14